

# Notes on Atmospheric Physics

Arnaud Czaja<sup>1</sup>

Physics Department &  
Grantham Institute for Climate Change,  
Imperial College, London.

May 5, 2017

<sup>1</sup>Contact details: Huxley Building, Room 726; email: [a.czaja@imperial.ac.uk](mailto:a.czaja@imperial.ac.uk).  
Office Hours: Thursdays, 11.30-12.30; Fridays, 1-2pm.



# Contents

<b>1</b>	<b>An overview of the atmosphere</b>	<b>1</b>
1.1	Atmospheric composition . . . . .	2
1.2	Mass . . . . .	4
1.2.1	Pressure as a measure of mass . . . . .	4
1.2.2	Measures of water in air . . . . .	5
1.3	Main features of the atmosphere . . . . .	8
1.4	What drives atmospheric winds, weather patterns, etc? . . . . .	9
1.5	Further reading . . . . .	18
1.6	Problems . . . . .	18
<b>2</b>	<b>Radiative heating and cooling of the atmosphere</b>	<b>21</b>
2.1	Concepts and definitions . . . . .	21
2.1.1	Intensity of radiation . . . . .	21
2.1.2	Blackbody radiation . . . . .	23
2.1.3	Shortwave and longwave radiation . . . . .	24
2.1.4	Irradiance . . . . .	24
2.1.5	Kirchoff's law . . . . .	26
2.1.6	The "solar constant" . . . . .	27
2.1.7	Radiation balance and emission temperature . . . . .	28
2.2	A simple model of the greenhouse effect . . . . .	30
2.3	Beer's law . . . . .	32
2.4	Schwarzchild's equation . . . . .	33
2.4.1	Derivation . . . . .	33
2.4.2	Physical interpretation . . . . .	34
2.4.3	Final form . . . . .	34
2.5	Some applications of Schwarzchild's equation . . . . .	35
2.5.1	No scattering . . . . .	35
2.5.2	Infrared radiation by an isothermal atmosphere . . . . .	36
2.5.3	Remote sensing of temperature . . . . .	36
2.6	Radiative heating and cooling rates . . . . .	38
2.6.1	Shortwave heating . . . . .	39

2.6.2	Longwave cooling . . . . .	41
2.6.3	Net radiative heating rates . . . . .	49
2.7	Problems . . . . .	50
<b>3</b>	<b>Radiative-convective equilibrium</b>	<b>55</b>
3.1	Radiative equilibrium . . . . .	55
3.2	Convection . . . . .	57
3.2.1	The “parcel’s equation” . . . . .	57
3.2.2	Potential temperature . . . . .	59
3.2.3	Stability of temperature profiles to vertical displacements of air parcels . . . . .	60
3.3	Radiative-convective equilibrium . . . . .	63
3.3.1	Stability of the radiative equilibrium temperature profile	63
3.3.2	The Tropopause . . . . .	63
3.4	Dynamical effects of moisture* . . . . .	64
3.4.1	Dry and moist adiabatic lapse-rates . . . . .	64
3.4.2	Application of “dry and moist adiabats thinking” . . . . .	67
3.5	Radiative-convective equilibrium and the real world . . . . .	69
3.6	Sloping convection . . . . .	71
3.7	Summary . . . . .	75
3.8	Problems . . . . .	76
<b>4</b>	<b>Atmospheric motions</b>	<b>81</b>
4.1	Equations of motions . . . . .	81
4.1.1	Forces acting on a parcel of air . . . . .	82
4.1.2	Material derivative . . . . .	82
4.1.3	Rotating frame of reference . . . . .	84
4.1.4	Coriolis and centrifugal forces . . . . .	86
4.1.5	Mass conservation . . . . .	88
4.2	Scale analysis of the equation of motions . . . . .	89
4.2.1	Vertical momentum equation . . . . .	89
4.2.2	Horizontal momentum equation . . . . .	91
4.2.3	The thermal wind relation . . . . .	92
4.3	The vorticity view . . . . .	95
4.3.1	The geostrophic flow, vorticity and divergence . . . . .	95
4.3.2	Predicting the vorticity of the flow: the vorticity equation	97
4.3.3	Rossby waves . . . . .	100
4.4	References . . . . .	104
4.5	Problems . . . . .	104

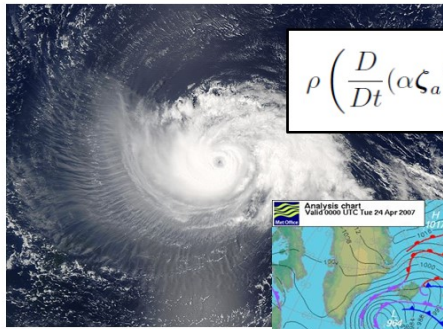
<b>5</b>	<b>Climate change</b>	<b>111</b>
5.1	Anthropogenic radiative forcing . . . . .	112
5.2	Response of the atmosphere to a sudden doubling of $CO_2$ . . .	112
5.2.1	Fast response: atmospheric processes only . . . . .	114
5.2.2	Slow response: the atmosphere interacts with the up- per ocean . . . . .	118
5.2.3	Very slow response: the atmosphere interacts with the ocean circulation . . . . .	121
5.3	Climate change in realistic models and observations . . . . .	123
5.4	References . . . . .	124
5.5	Problems . . . . .	125
<b>6</b>	<b>Appendices</b>	<b>129</b>
6.1	Radiative transfer . . . . .	129
6.1.1	Radiation pencils vs. photon showers . . . . .	129
6.1.2	Conservation of intensity . . . . .	131
6.1.3	Application to blackbody radiation . . . . .	131
6.2	Thermodynamics of moist air . . . . .	131
6.2.1	Entropy of cloudy air . . . . .	131
6.2.2	A general formula for the Brunt-Vaisala frequency* . .	132
6.3	Dynamics of rotating fluids . . . . .	133
6.3.1	Formula for $D/Dt$ in a change of frame of reference . .	133
6.3.2	Kelvin's identity . . . . .	134
6.3.3	The vorticity equation* . . . . .	135

## Welcome to Atmospheric Physics!

I used to live in the US and I remember watching a Brian Green's episode of "The Elegant Universe" about quantum mechanics. He entered the "Quantum café", asked for an orange juice and the waiter answered: "yes, maybe".

The more I work on the physics of the oceans and the atmosphere, the more I realise that climate is like the Quantum café. Take the winds. You think it's straightforward. Well, winds on Earth are governed by the Taylor-Proudman theorem: "there can be no variations of the steady state winds in the direction of the axis of rotation". A lab demo of this is just spectacular.

And this is the world we live in, the atmosphere whose composition we are altering, the climate whose heat balance we are perturbing. Within the current state of understanding, we can only make a few scientific predictions: "The radiative forcing due to human activities is large", "Sea level will keep rising" are two examples. Not very satisfactory isn't it? To say more with confidence, we need to use our senses –build new senses (instruments)– to collect observations of the climate as it is now with future generations in mind; and, for our own pleasure and maybe a chance to see the future more clearly, to use our intelligence to unravel how the atmosphere, the oceans, the cryosphere and the biosphere work and interact. Please join in.



$$\rho \left( \frac{D}{Dt} (\alpha \zeta_a) \right)_R = (\zeta_a \cdot \nabla) \mathbf{u}_R - \nabla \alpha \times \nabla P + \nabla \times \mathbf{F}_{fric}$$

$$\theta = T \left( \frac{P}{P_{ref}} \right)^{-R_d/c_{p,d}}$$

$$I_\lambda(s) = I_\lambda(s_o) e^{-\tau_\lambda(s_o, s)} + \int_0^{\tau_\lambda(s_o, s)} T_\lambda(s', s) J_\lambda(\tau') d\tau'$$



## Practical things

These notes contain only the basic information discussed in the lectures (the latter are where emphasis is on the physical interpretation and schematics). My aim in writing them is to provide you with a support and a clear knowledge of what is examinable (=what is in the notes). The formal “Aims and objectives” for the course follows next page. In terms of reading:

- I recommend the excellent textbook by Wallace and Hobbs (“Atmospheric Sciences: an introductory survey”) as a companion for the course (the library has many copies).
- You might also enjoy reading “Clouds in a glass of beer: simple experiments in atmospheric physics” by Craig Bohren (cheap paperback Dover edition), as well as the textbook by John Marshall and Alan Plumb entitled “Atmosphere, Ocean and Climate Dynamics: An introductory text” and the older but concise and clear “The Physics of Atmospheres” by John Houghton. I have also included further references in some chapters.

Each chapter contains a set of problems, whose solutions will be provided as we go along. Some sections in the notes are highlighted with a ★ which indicates that they are a little more challenging.

There are a couple websites which I would like to emphasize:

- <https://earth.nullschool.net> This is a wonderful website depicting the state of the atmosphere and the (surface) ocean in nearly real time. The data comes from a global operational forecast system from the US (which is constrained by many observations) and satellite observations for the ocean. The graphics are stunning and there is so much to learn and wonder spending time on it (believe me it beats Youtube).
- [http://www.ecmwf.int/s/ERA-40\\_Atlas/docs/](http://www.ecmwf.int/s/ERA-40_Atlas/docs/) An excellent source of quick plots for the mean atmospheric state. This climatology has been developed at a big European centre for weather forecast and climate in Reading (ECMWF).

- [http://www.sp.ph.ic.ac.uk/aczaja/EP\\_ClimateModel.html](http://www.sp.ph.ic.ac.uk/aczaja/EP_ClimateModel.html) This is a simple climate model which I will at times use during the lectures. It is well documented and cheap to run (either in Matlab or in Python, thanks to the hard work of an undergraduate student Joe Marsh Rossney).

Please do not hesitate to come to Office Hours (Thursdays, 11.30-12.30; Fridays, 1-2pm) for further help or to give me feedback on the course. You are also welcome to make any suggestions by email at [a.czaja@imperial.ac.uk](mailto:a.czaja@imperial.ac.uk).

## Aims and Objectives for the Course

**Aims** To provide students with an understanding of the physics behind the structure, the dynamics and the energetics (radiative transfer, thermodynamics) of the Earth's atmosphere (emphasis on troposphere and stratosphere).

**Objectives** By attending the course, the students should:

- be able to describe the basic structure of the Earth's atmosphere and the climate system
- be able to use fundamental thermodynamics to derive expressions for the variation of temperature, pressure, and density with height
- understand the concept of potential temperature and how it relates to stability, buoyancy frequency and temperature lapse rate
- understand the concept of radiative-convective equilibrium
- know the components of the Earth radiation balance
- understand the concepts of optical depth, radiation intensity, irradiance, and transmission of radiation
- be familiar with Schwarzschild's equation of radiative transfer and be able to solve it for both solar and thermal radiation streams under simple conditions
- be able to derive a simple model of the greenhouse effect
- be able to compute radiative heating rates given irradiances
- know the forces acting on a parcel of air and apply Newton's 2nd Law to deduce the equations of motion for a compressible gas on a rotating planet
- know how to apply scale approximations to the equations of motion (e.g., hydrostatic and geostrophic approximations, Rossby number)
- understand why vorticity is a useful concept for the study of atmospheric motions
- understand the effect of water on the radiative, thermodynamic and dynamical aspects of Atmospheric Physics
- understand the concept of radiative anthropogenic forcing and the basic response of the atmosphere to this forcing



# Chapter 1

## An overview of the atmosphere

**key concepts:** well mixed gases, “dry” and “moist” air, measures of water vapour in air, top-of-the-atmosphere (TOA), global budgets of mass, heat and angular momentum.

Before we dive into quantitative analysis of the atmosphere it is important not to lose sight of some of the big questions. Here are a few which I mentioned in the introduction lecture (ppt slides on Blackboard):

- *The atmosphere is our common environment.* It is the fluid we all breathe. We say that we are connected with the internet but we are actually physically connected because we constantly share and recycle air molecules through our lungs. When the surface winds come from the South, I am breathing air which was a day or two before breathed in and out by someone in Spain or maybe Africa. This is because typical north-south velocities in a weather system are on the order of  $10\text{ms}^{-1}$  so an air parcel covers approximately  $10^\circ$  of latitude in one day ( $\approx 10^5\text{s}$ ).
- *Randomness.* The tropical Pacific ocean is one area of the globe with the most observations (ocean and atmosphere) because it is the site of a major reorganisation of the wind, temperature and precipitation patterns known as El Nino. Every few years, heat builds up in the western Pacific ocean and is suddenly released eastward and poleward, shifting entirely the tropical precipitation pattern. The atmosphere is “rung” by this shift and generates waves propagating towards the Northern and Southern Hemispheres, perturbing the weather systems there. El Nino is also the climate phenomenon with the best theories. Or so we thought. In the summer of 2014, all El Nino experts

predicted that the largest event ever recorded will develop during the following winter. It simply did not happen! No El Nino event at all (see McPhaden, 2015). Imagine telling your friends you're an expert at something, predicting the largest anomaly ever seen...and things go on perfectly normally. This shows that there is a lot more to understand. Maybe, fundamentally, deterministic predictions of the coupled atmosphere - ocean system are impossible. Maybe this system is a bit like a quantum mechanics system, with only probabilistic statements possible.

- *Observations.* In fifty or a hundred years, we will still need to check that our numerical models of the climate are accurate. The ones we have and use now have been only tested over a short period of time (true global observations of the atmosphere only started with the satellites launched in the 1970s –in the ocean this type of coverage simply does not exist below about a 1000m) and one should not be overconfident regarding their accuracy (see point above). People in fifty or a hundred years will not be able to travel back in time and make these observations. It is our duty to do so. Even if like me, you are not someone developing instruments, you can help those who do by finding the most useful quantity to observe. And by using the data in your own way, you help maintain the observational network.

## 1.1 Atmospheric composition

The most abundant substance in the atmosphere is diatomic nitrogen ( $N_2$ ), which accounts for 78% of the air molecules we breath. Most of the nitrogen on Earth is actually stored in the atmosphere ( $3.9 \times 10^{18}kg$ ), with the Lithosphere (Earth's crust) coming second ( $\approx 2 \times 10^{18}kg$ ) The large atmospheric reservoir of nitrogen reflects the outgassing from the Earth's interior in the earliest stage of its history and the great stability of the  $N_2$  molecule.

Next in abundance comes “free” oxygen ( $O_2$ ), which represents 21% of atmospheric molecules. The Earth is unique in having so much of its atmosphere made up of diatomic oxygen, and there is little doubt that this reflects the presence of life early in its history (it is believed that oxygen started to accumulate in the atmosphere about 2Gyr ago, when the production of  $O_2$  by bacteria exceeded the consumption of  $O_2$  by iron ions dissolved in the oceans).

The percentages given above assume that any given sample of air has the same composition. In practice, this is only true for gases whose residence time in the atmosphere is long compared to the time it takes for atmospheric

motions to mix (from a few days to a few months). This is for example the case for  $N_2$ ,  $O_2$  as well as argon ( $Ar$ ,  $\approx 0.9\%$  of air molecules) and carbon dioxide ( $CO_2$ ,  $\approx 0.04\%$  of air molecules), the next two most abundant species after  $N_2$  and  $O_2$ . Water vapour has a highly variable distribution (with concentrations which can be greater than that of  $Ar$  locally) depending on time and location because it can be quickly removed from the atmosphere through rainfall. The height at which mixing by motions is not vigorous enough to maintain a uniform composition is about  $100km$  (the turbopause).

For the troposphere (the lowest layer of atmosphere where temperature decreases with height, roughly from the Earth's surface to a height  $z = 10km$ ) and stratosphere (the layer above the troposphere where temperature increases with height, from about  $z = 10km$  to  $z = 50km$ ), which will be the focus of the course, it is convenient to simplify atmospheric composition by considering “dry air”, a mixture of  $N_2$ ,  $O_2$ ,  $Ar$ ,  $CO_2$  and other trace gases, and “moist air” (water vapour). The primary reason for this is phase change: as we'll see in Section 1.5, there is a net heat gain by the atmosphere through the hydrological cycle (latent heat) whereas this does not occur for other species ( $N_2$ ,  $O_2$ , etc, although they are also exchanged between the atmosphere and the Earth's surface). It is thus important to keep track of local concentrations of water vapour. A useful measure of the “distance to equilibrium of phases” is given by relative humidity (RH), the ratio of the vapour pressure  $e$  of a sample to the vapour pressure in thermodynamic equilibrium of phases ( $e_{eq}(T)$ , a sole function of temperature  $T$  from the Thermodynamic year 2 course):

$$RH \equiv \frac{e}{e_{eq}} \quad (1.1)$$

*NB: This is just a definition. In thermodynamic equilibrium  $RH = 1$  but this condition is rarely met in the atmosphere (for example, it is in the core of deep clouds but not in the accompanying downdrafts which are too dry for  $e$  to match  $e_{eq}(T)$  and thus are air masses with  $RH < 1$ ).*

At a given temperature  $T$  and volume  $V$ , the pressure of “dry air”  $P_d$  obeys the ideal gas law to an excellent approximation,

$$P_d V = N_d k_B T \quad (1.2)$$

as does water vapour,

$$eV = N_v k_B T \quad (1.3)$$

In these two equations,  $k_B$  is Boltzmann's constant while  $N$  denotes the number of molecules (the subscripts  $d$  and  $v$  will be used throughout the course for dry air and water vapour, respectively). Note that the total pressure  $P$

of a given sample of air is simply the sum of  $P_d$  (the partial pressure of dry air) and  $e$  (the partial pressure of water vapour), as result known as Dalton's law,

$$P = P_d + e \quad (\text{Dalton's law}) \quad (1.4)$$

Atmospheric pressures are usually expressed in  $hPa$  where  $1hPa = 100Pa$  (you might also find pressures expressed as millibar ( $1mb = 10^{-3}bar$ ), in which  $1bar = 10^5Pa$ ).

Because of the very large number of molecules in the atmosphere, it is convenient to rewrite the ideal gas law as,

$$\frac{P_d V}{N_d \mu_d} = \frac{k_B}{\mu_d} T \quad (1.5)$$

in which  $\mu_d$  is the mass of a "dry air molecule" ( $\mu_d = \sum N_i \mu_i / \sum N_i$  where  $\mu_i$  is the mass of molecule  $i$  of which there are  $N_i$  in the sample considered –the sum is carried over  $i = N_2, O_2, Ar, CO_2, etc$ ). Introducing the specific volume of dry air  $\alpha_d$ , and the gas constant for dry air  $R_d = k_B / \mu_d = 287 J kg^{-1} K^{-1}$ , this becomes,

$$P_d \alpha_d = R_d T \quad (1.6)$$

Likewise, for water vapour,

$$e \alpha_v = R_v T \quad (1.7)$$

with  $R_v = k_B / \mu_{H_2O} = 461 J kg^{-1} K^{-1}$ .

## 1.2 Mass

### 1.2.1 Pressure as a measure of mass

In layers of air of large horizontal extent, and in particular for the global horizontal average, there is an approximate balance between gravity and the vertical pressure gradient force,

$$\rho g = -\frac{\partial P}{\partial z} \quad (\text{hydrostatic equation}) \quad (1.8)$$

Note the minus sign, which expresses that pressure must decrease with height to be able to oppose the downward acceleration due to gravity.

One interesting use of this equation is to integrate it in the vertical as,

$$P(z) = \int_z^{+\infty} \rho g dz \quad (1.9)$$

in which we have used the fact that pressure vanishes at sufficiently large heights. The discussion in section 1 showed that this is a good approximation for  $z \gg 8km$  and this loosely defines the “top-of-the-atmosphere” (TOA throughout the course). The corresponding layer of air is still very thin compared to the Earth radius so that one can approximate  $g$  in the integral by its surface value  $g = 9.81ms^{-2}$ ,

$$P(z)/g = \int_z^{+\infty} \rho dz \quad (1.10)$$

This shows that atmospheric pressure can be thought of as a mass measurement since  $\rho dz$  is simply the mass per unit area sandwiched between heights  $z$  and  $z + dz$ . A couple of straightforward applications of this equation are worth mentioning. An order of magnitude for the surface pressure is  $P_s = 1000hPa$  while for the tropopause it is  $100hPa$ . This shows that the troposphere contains about  $\simeq (1000 - 100)/1000 = 90\%$  of the mass of the atmosphere. Conversely, since the pressure  $P$  in (1.10) is the total pressure ( $P = P_d + e$ ), and that  $e$  at the Earth’s surface is typically  $10hPa$  in the global and annual mean, water vapour contributes to  $\simeq 10/1000 = 1\%$  of atmospheric mass.

*Technical sidenote: units of pressure. Pressure is usually expressed in  $hPa = 100Pa$  in atmospheric sciences. You might also find the use of millibars ( $mb$ ,  $1mb = 10^{-3}bar$  where  $1bar = 10^5Pa$ ).*

### 1.2.2 Measures of water in air

A given sample of air is described, besides its temperature and pressure, by its mass of dry air  $m_d$  (see previous section), water vapour  $m_v$ , liquid water  $m_l$  and ice water  $m_i$ . It is common practice to introduce ratios of these quantities:

$$q_v \equiv \frac{m_v}{m_d + m_v + m_l + m_i} \quad (\text{specific humidity}) \quad (1.11)$$

$$q_l \equiv \frac{m_l}{m_d + m_v + m_l + m_i} \quad (\text{specific liquid water content}) \quad (1.12)$$

$$q_i \equiv \frac{m_i}{m_d + m_v + m_l + m_i} \quad (\text{specific ice water content}) \quad (1.13)$$

$$q_d \equiv \frac{m_d}{m_d + m_v + m_l + m_i} \quad (\text{specific mass of dry air}) \quad (1.14)$$

In terms of size, because there is so little amount of water in the air,  $q_d \gg q_v$ , and typically  $q_v \gg (q_l, q_i)$ . Note that  $q_d = 1 - (q_v + q_l + q_i)$ . The total specific amount of water is denoted by  $q_t \equiv q_v + q_l + q_i$ .

Sometimes, mass mixing ratio, rather than specific humidity is used. The difference is that, for example for water vapour (mixing ratio  $r_v$ ), mixing ratio involves taking the ratio of  $m_v$  to  $m_d$  rather than  $m_v$  to  $m_v + m_d + m_l + m_i$ , i.e.,

$$r_v \equiv \frac{m_v}{m_d} \quad (\text{mass mixing ratio}) \quad (1.15)$$

The air density  $\rho$  is defined according to,

$$\rho = \frac{m_d + m_v + m_l + m_i}{V} \quad (1.16)$$

in which  $V$  is the total volume occupied by the sample (the sum of the volumes occupied by the gas, liquid and solid phases). As a result, the density of dry air  $\rho_d = m_d/V = (m/V)(m_d/m) = \rho q_d$ , and, likewise, the density of water is  $\rho_t = (m_v + m_l + m_i)/V = (m/V)(m_v + m_l + m_i)/m = \rho q_t$ .

The total amount of water vapour in an atmospheric column, or total precipitable water (TPW), is

$$TPW = \int_0^\infty \rho q_v dz \quad (1.17)$$

To get a feel for the surprising result to come below, let's use the simple model  $\rho = \rho_s e^{-z/H_s}$  and  $q_v = q_s e^{-z/H_q}$  in which  $H_s$  is the scale height,  $H_q$  a scale height for moisture (Fig. 1.1) and  $\rho_s, q_s$  refer to surface density and specific humidity, respectively. One can then estimate that,

$$TPW \approx \rho_s q_s H \quad \text{with } H = \frac{H_s H_q}{H_s + H_q} \quad (1.18)$$

Expressed in  $mm$  of water per unit area by dividing this quantity by the density of water, we find typically that the atmosphere holds something like  $20mm$  of precipitable water in vapour form (for  $\rho_s = 1.2kgm^{-3}$ ,  $q_s = 10g/kg$ ,  $H_s = 7km$ ,  $H_q = 3km$ ). Observed values (Fig. 1.2) are indeed within that range. This is somewhat surprising since it can rain much more than that in a matter of a few hours but it can be rationalized by thinking of storms (the cyclones at our latitudes and even more so hurricanes) as very efficient machines collecting water vapour over very large distances, condensing it, and “dumping” it as rain: this is the “dehumidifier view” of cyclones.

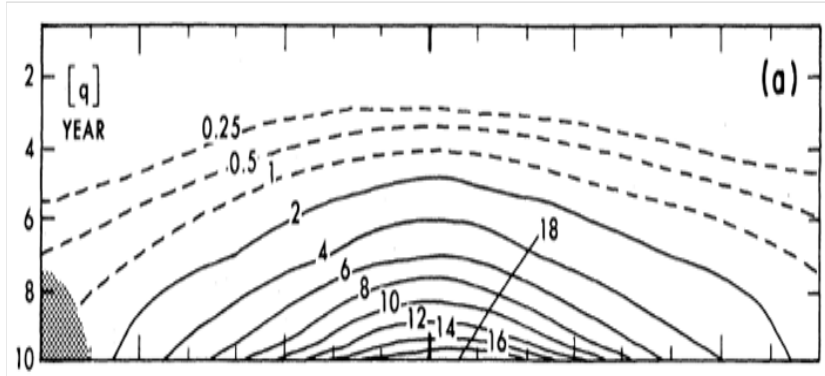


Figure 1.1: Annual mean specific humidity ( $q_v$ , in  $g/kg$ ) as a function of latitude and pressure (here expressed in  $dbar$ ,  $1bar = 10^5 Pa$ ). Note the sharp decrease with decreasing pressure so that the scale height for moisture is much less than it is for pressure. This is because of condensation and rain which removes moisture from the atmosphere.

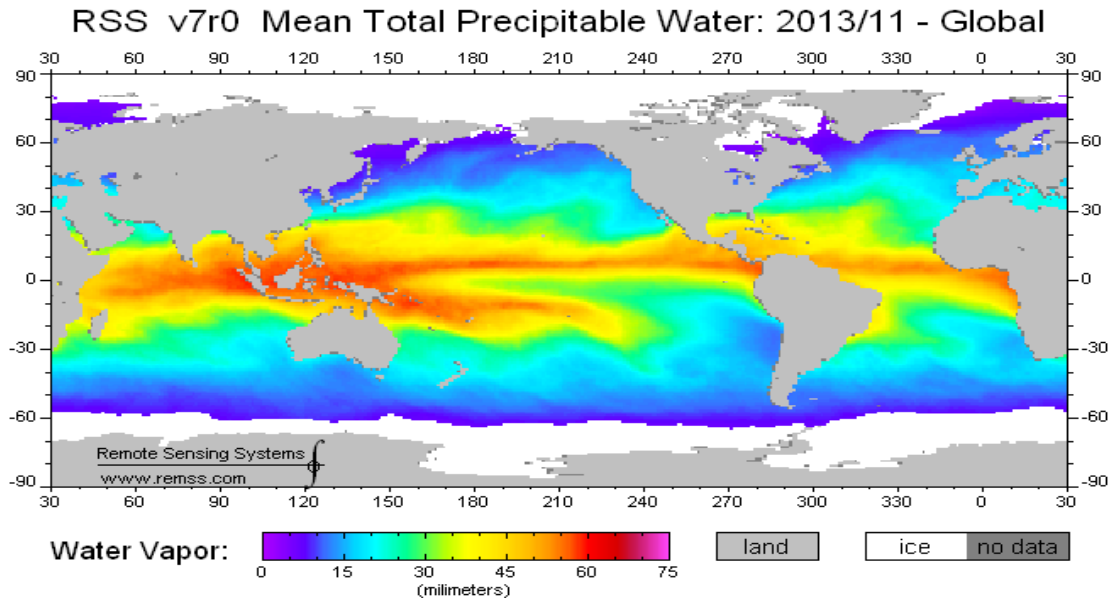


Figure 1.2: Mean total precipitable water (in  $mm$ ) averaged over the oceans for November 2013. This map was produced using passive microwave measurement from satellites.

### 1.3 Main features of the atmosphere

Based on the ppt slides for this chapter (to which you are referred to for illustrations), the main features of the atmosphere are:

- a well mixed structure up to  $\approx 100km$  in terms of constituents, with a near exponential decay of pressure and number densities with height. The associated scale is on the order of  $8km$  for the well mixed layer<sup>1</sup>.
- a rich temperature structure, with, in some regions, temperature decreasing with height and poleward, but in some regions temperature increasing upward and poleward (Fig. 1.3, top panel). The simplest view (global average as a function of height) is schematized in Fig. 1.4, introducing the troposphere, the stratosphere and the mesosphere. The course will focus on the first two of these where 99.9 % of the mass of the atmosphere resides.
- the presence of strong zonal (=along a latitude circle) time mean jets with windspeeds in excess of  $30m/s$ . These are mostly found going from west to east (e.g., the tropospheric Jet Stream) but also exists seasonally from east to west (mesospheric jets) –see Fig. 1.3, bottom panel. At the Earth’s surface, westerlies are found poleward of  $30^\circ$  of latitude, and easterlies (“Trade winds”) are found equatorward of that latitude. The atmosphere is in a state of “superrotation”, an air parcel in the tropospheric Jet Stream coming back to its initial position in about  $23h$ , not  $24h$ ! We’ll prove in Chapter 4 that these jets are in “thermal wind balance”, meaning that their variations with height are constrained by the horizontal temperature gradients.
- the presence of smaller time mean velocities in the North-South direction (a few  $ms^{-1}$ ). These are predominantly seen in the Hadley cell at low latitudes, with rising motions near the equator and descending motion along  $\approx 30^\circ$ . Such “meridional cells” (in the latitude-height plane) also exist in the stratosphere and mesosphere but the associated mass transport is much weaker than that of the Hadley cell.
- its convective nature (Fig. 1.5) on scales ranging from a few  $km$  to thousands of  $km$  (planetary scale). Updraft motions are associated

---

<sup>1</sup>From Boltzmann’s principle we would expect the ratio of distribution of a molecule of mass  $m$  at height  $z_1$  and  $z_2$  to obey  $n_1/n_2 = e^{mg(z_1-z_2)/k_B T}$  where  $g$  is gravity and  $T$  temperature. This provides a different scale height for each molecule according their mass ( $k_B T/mg$ ), which is not observed below  $100km$  (the “turbopause”). It is observed above  $100km$ .

#### 1.4. WHAT DRIVES ATMOSPHERIC WINDS, WEATHER PATTERNS, ETC?9

with phase change and the formation of rain, snow and other hydrometeors. The convection involves mostly upward/downward motions in the Tropics, but sloping (i.e., upward and poleward, downward and equatorward) motions at higher latitudes as we'll discuss in Chapter 3.

- The fundamental role of water vapour. Not only does it affect atmospheric motions through its effect on buoyancy (condensational heating, evaporative cooling add or remove buoyancy to air parcels, as we'll see in Chapter 3), but water vapour is also the main greenhouse gas (as we'll see in Chapter 2). Because the oceans occupy 70% of the Earth's surface and because surface evaporation depends on surface temperature, water vapour couples the state of the oceans to that of the atmosphere.
- The atmosphere is only one component among many (oceans, cryosphere, biosphere, the deep Earth, etc) setting the Earth's climate.
- The atmosphere has a mind of its own. The "butterfly effect" was introduced by MIT's meteorologist Ed Lorenz to illustrate the sensitivity of the atmospheric state to initial conditions. Predictability beyond a week or so arises from slower changes in boundary conditions (sea surface temperature, sea ice, vegetation cover, etc). In addition, the atmosphere is turbulent, with energy transfers towards small scale but also, more surprisingly, towards large scales. This makes the standard definition of weather (=state of the atmosphere at a given time) and climate (=statistics over a long enough time period) a bit ambiguous. One should really add a "grey zone", the low frequency variability of the atmosphere, i.e., fluctuations which can persist for longer than a week (e.g., blocking conditions associated with long lived cold spells in the UK like occurred in 2009-2010). These are not "weather", nor are they "climate".

### 1.4 What drives atmospheric winds, weather patterns, etc?

A few simple ideas are worth mentioning:

- There is an asymmetry between the radiation received from the Sun and that emitted by the Earth (surface + atmosphere). Photons emitted by the Sun have wavelengths smaller than a few microns while photons

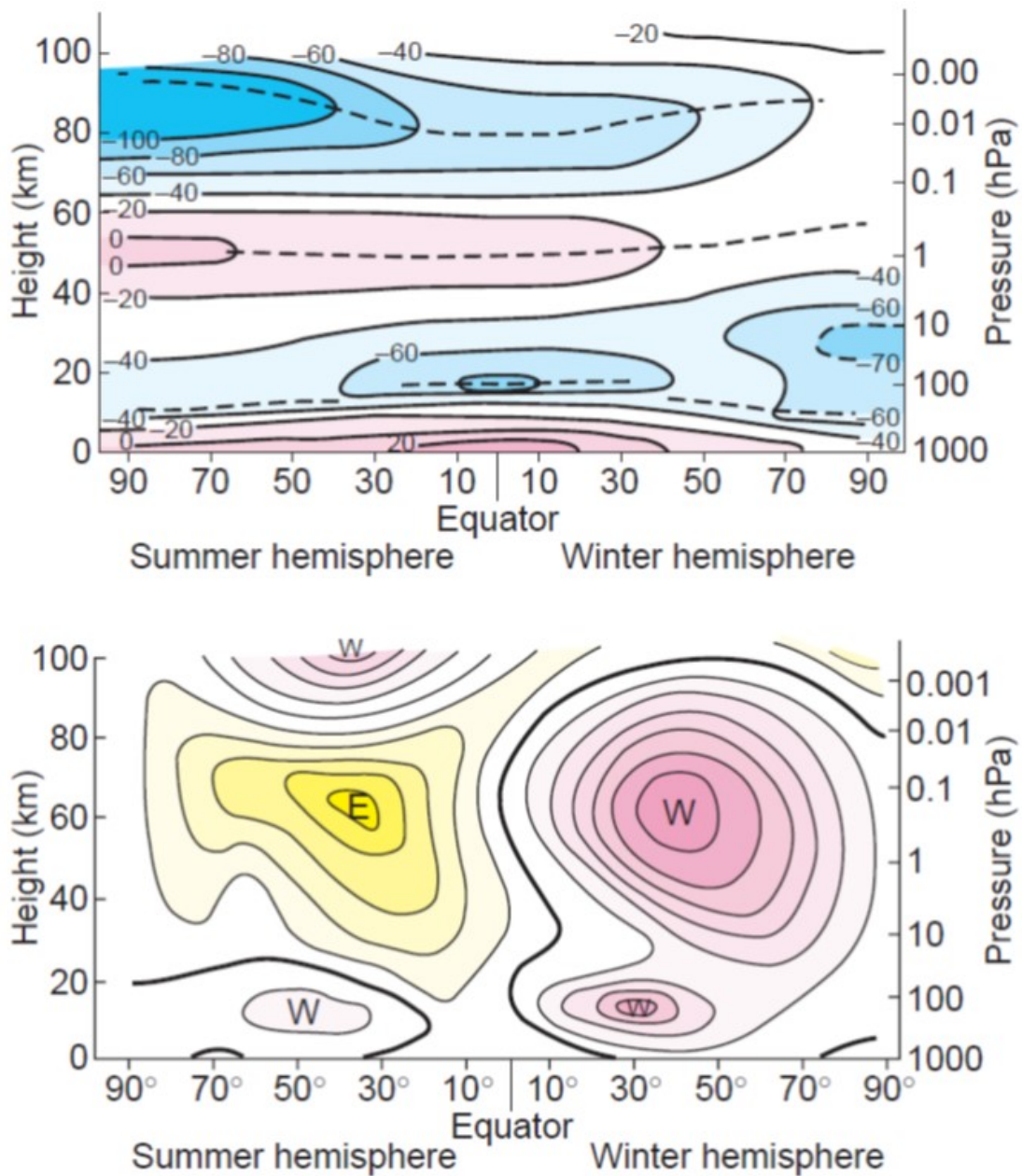


Figure 1.3: Seasonal and zonal (i.e., averaged along a latitude circle) mean atmospheric temperature (top panel, in degree Celcius) and zonal wind (bottom panel, in  $ms^{-1}$  with a contour interval of  $10ms^{-1}$ , W indicating west to east winds and E east to west winds) as a function of height/pressure (vertical axis) and latitude (horizontal axis). Figure taken from Wallace and Hobbs' textbook.

1.4. WHAT DRIVES ATMOSPHERIC WINDS, WEATHER PATTERNS, ETC?11

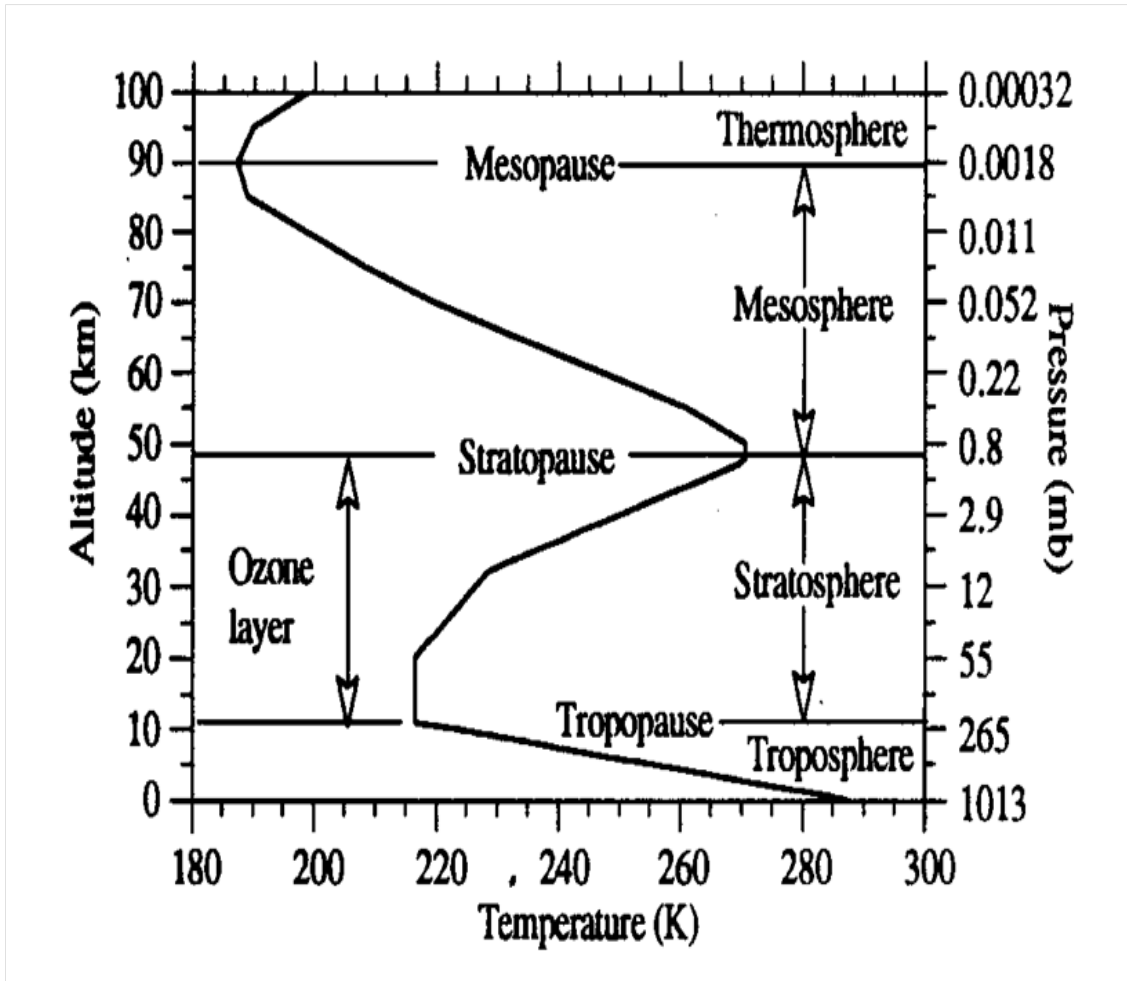


Figure 1.4: Global, annual mean atmospheric temperature as a function of height/pressure.

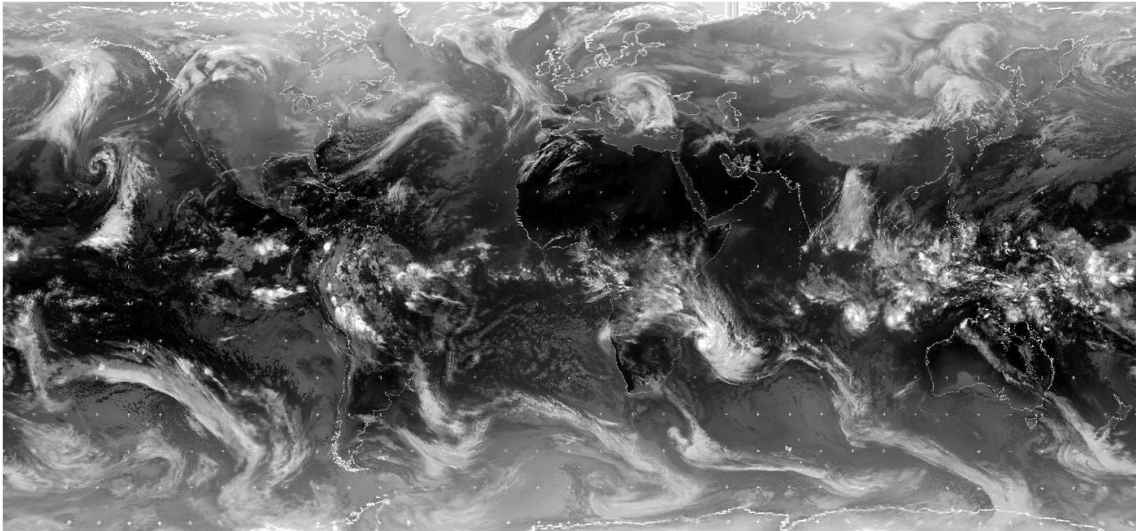


Figure 1.5: Global composite infrared map on 9 March 2004. White is cold on this map and, in most regions, indicates the presence of upper level clouds. Notice the “spotty” nature of the convection in the Tropics and the “wavi-ness” in middle and high latitudes. You can find many of those maps (as well as animations) on the MetOffice website.

emitted by the Earth have wavelength larger than a few microns (Fig. 1.6). As a consequence, an atmospheric layer exchanges radiation with other atmospheric layers and the Earth’s surface (and these exchanges tend to cancel out), but there is no two-way exchange with Space and the atmosphere cools radiatively in the infrared (Fig. 1.7)

- In addition, solar photons are in comparison much less absorbed by the atmosphere than terrestrial photons. This means that, to zero order, the atmosphere can be thought of as transparent to solar radiation, the latter being primarily absorbed by the Earth surface. So the atmosphere is heated from below by the Earth’s surface, and it cools radiatively to Space (previous point). This is a very unstable situation, a bit like a pan of water boiling on a cooker: the atmosphere is in a state of global convection.
- The radiative cooling to space is relatively uniform spatially but incoming solar radiation peaks at low latitudes as a result of the spherical shape of the Earth and the large Earth-Sun distance. This means that in addition to the heating from below and cooling aloft, there is also a net cooling at high latitudes and net heating at low latitudes (Fig.

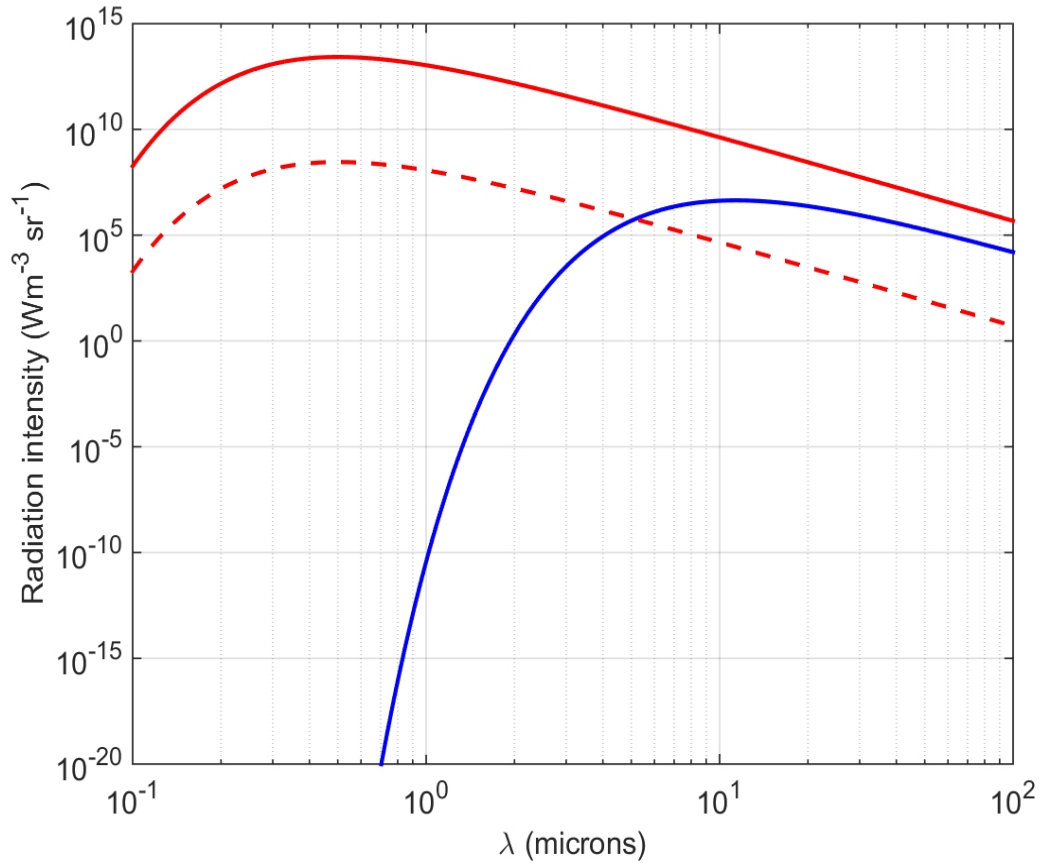


Figure 1.6: Planck function  $B_\lambda$  (see Chapter 2) for a body at  $T = 5780K$  (red) and  $T = 255K$  (blue) in a log-log scale. The red dashed curve rescales the red one by a factor  $\pi(R_{sun}/1AU)^2/2\pi$  where  $R_{sun}$  is the Sun's radius, to account for the different solid angles associated with solar ( $\pi(R_{sun}/1AU)^2$ ) and terrestrial ( $2\pi$ ) radiation.

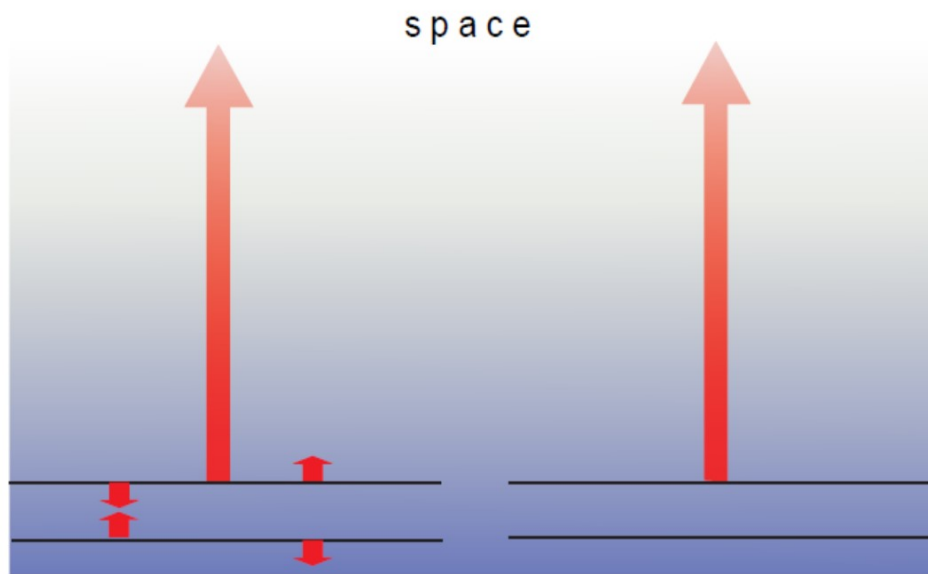


Figure 1.7: A schematic of the radiative exchanges for an atmospheric layer. (Left) All exchanges are represented: the layer absorbs radiation from above and below (including the Earth's surface), and it emits to other layers above and below (small arrows). In addition it also emits radiation to Space (large arrow) but does not absorb solar radiation. (Right) Assuming the inter-layers and surface exchanges nearly cancel, which is not a bad approximation if temperature variations are sufficiently weak and the atmosphere is sufficiently opaque, this leaves a net loss of energy to Space. Picture taken from Wallace and Hobbs' textbook.

1.8). Laboratory experiments with rotating tanks cooled at the outside and heated at the inside, to mimic the equator-to-pole contrast in heating, indicate that the resulting motion can be irregular with clear qualitative similarities with the atmosphere.

The above arguments are rough but they give a feel for the key role of radiation as a driver of atmospheric motions and weather systems (a full estimate of the various energy fluxes is given in Fig. 1.9). The laboratory experiments mentioned in the last bullet point also indicate the very strong constraint imposed by the rotation of the Earth (rotation rate  $\Omega$ ). It is only when the latter is fast enough that the simulated flows bear a qualitative resemblance to the atmosphere. This is because the flow not only transports heat from the equator to the pole, to balance the deficit highlighted in Fig. 1.8, but also transports atmospheric angular momentum ( $L$ ). The latter is simply the azimuthal velocity ( $u + \Omega R \cos \phi$ ),  $R$  being the Earth radius,  $\phi$  latitude and  $u$  the west-to-east velocity relative to the rotating Earth, times the distance to the axis of rotation ( $R \cos \phi$ ):

$$L = R \cos \phi (u + \Omega R \cos \phi) \quad (1.19)$$

Atmospheric angular momentum has thus a contribution from the Earth's solid body rotation, or planetary contribution ( $\Omega R^2 \cos^2 \phi$ ), and a contribution from relative motions ( $u R \cos \phi$ ). In practice, the former dominates over the latter. For example at the latitude of the subtropical Jet Stream ( $\approx 30^\circ$ ), one has  $u \approx 30 \text{ms}^{-1}$  while  $\Omega R \cos(30^\circ) \approx 400 \text{ms}^{-1}$ . Note that in this derivation,  $L$  is angular momentum per unit mass, and that I have used throughout  $R + z \approx R$  where  $z$  is the height of an atmospheric ring above the Earth's surface.

Integrated over the whole mass of the atmosphere  $L$  is approximatively constant, i.e.,

$$\frac{\partial}{\partial t} \iiint \rho L dV \approx 0 \quad (1.20)$$

This implies an intriguing compensation between the Tropics, in which the surface winds are westward (Trade winds) and thus where the atmosphere is gaining angular momentum (friction accelerates low levels in the sense of the Earth's rotation), and higher latitudes, where the surface winds are eastward and thus where the atmosphere is losing angular momentum. As we shall see in Chapter 4, the Tropics and extra-tropics are coupled through the propagation of a certain type of waves called Rossby waves. The latter are excited mostly from midlatitudes by the storm we experience daily and as they propagate equatorward they transport angular momentum poleward.

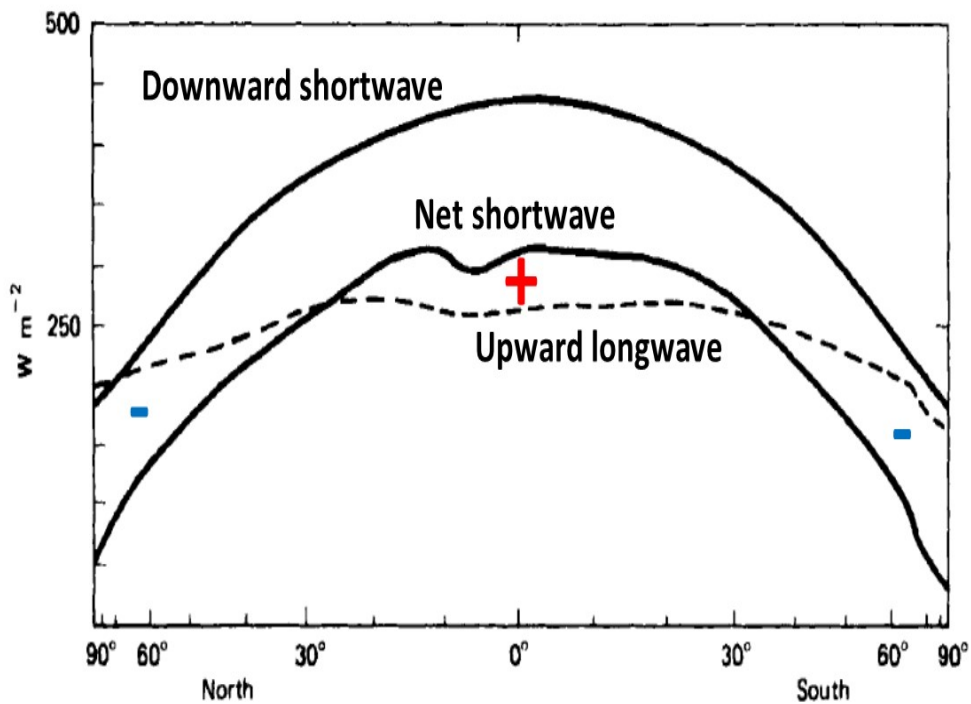


Figure 1.8: Global mean radiative fluxes as seen from satellites, in  $W m^{-2}$ , as a function of the  $\sin$  of latitude. The top continuous curve is the incoming solar radiation, while the lower continuous curve also includes the amount being reflected by the Earth and is thus lower. The dashed line is the infrared energy emitted by the atmosphere (plus a contribution from the Earth's surface). The red + sign indicates net energy gain and the blue - sign indicates net energy loss.

#### 1.4. WHAT DRIVES ATMOSPHERIC WINDS, WEATHER PATTERNS, ETC?17

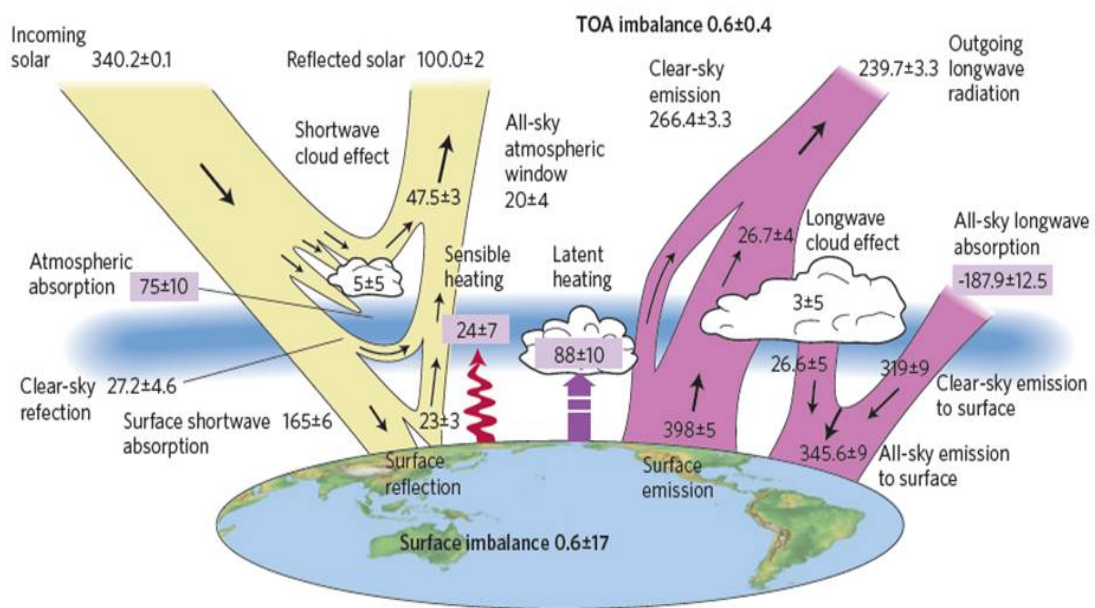


Figure 1.9: Recent observations of the Earth's energy budget. All quoted numbers represent  $Wm^{-2}$ . Solar fluxes are in beige and infrared fluxes in pink. From Stephens et al. (2012).

Thus, the storms we experience daily across the UK provide the mechanical coupling between vastly distant parts of the Earth.

Finally, note that this compensation between surface easterlies and westerlies can only be approximate since torques are also exerted as a result of the pressure contrast across the major mountains of the Earth like the Himalayas and the Rockies.

## 1.5 Further reading

-Stephens et al., 2012: An update on Earth's energy balance in light of the latest global observations, *Nature Geosciences*, 5, 691-696.

-Lovelock, 1979: *Gaia, a new look at life on Earth*, Oxford University Press. This book (and the many sequels) offers a fascinating discussion of atmospheric composition and demonstrates the broadness of the subject.

-McPhaden, M., 2015: Playing hide and seek with El Nino, *Nature Climate Change*, 5, 791-795.

## 1.6 Problems

**Q1** In the (zonal mean) stratosphere and mesosphere, where (latitude, altitude, season) are found: (i) the coldest temperature (ii) the warmest temperature (iii) the strongest westerly wind? You might find useful to refer to the slides for Lecture 1.

**Q2** Why are deserts more likely to be present in the sub-tropics than in either the tropics or mid-latitudes?

**Q3** These two subquestions are independent of each other.

- (i) At 25 km altitude, where atmospheric pressure is  $P_o \approx 25hPa$  and temperature is  $T_o \approx 220K$ , the mass mixing ratio of ozone is 10 parts per million. Compute (a) density and (b) partial pressure of ozone stating any assumptions made. Data:  $R_d = 287JK^{-1}kg^{-1}$ .
- (ii) Express the fraction of water vapour molecules in *ppm* (part per million) in a sample of air where the partial pressure of water vapour is  $e = 10hPa$  and that of dry air  $P_d = 1000hPa$ . Compare the number obtained with the current fraction of carbon dioxide molecules (400*ppm*).

**Q4**

Table 1.1: Data for Q5. The number in parentheses refer to the molecular mass of the main atmospheric constituents.

Planet	Major atmospheric component	Mean lower temperature (K)	Mass kg	Radius km
Venus	CO <sub>2</sub> (44)	750	$4.87 \times 10^{24}$	6,051
Earth	N <sub>2</sub> , O <sub>2</sub> (29)	280	$5.97 \times 10^{24}$	6,371
Mars	CO <sub>2</sub> (44)	250	$6.42 \times 10^{23}$	3,397
Jupiter	H <sub>2</sub> (2)	123	$1.90 \times 10^{27}$	71,490

- (i) One  $kg$  of air of specific humidity  $q_1 = 10g/kg$  is mixed with one  $kg$  of air of specific humidity  $q_2 = 5g/kg$ . What is the specific humidity  $q_3$  of the air mass after mixing? You may assume the conditions are such that no phase change occurs.
- (ii) In the jargon of Thermodynamics, is specific humidity an intensive or an extensive variable?

**Q5** (i) Show that in an isothermal atmosphere ( $T = T_o$ ) the pressure decays exponentially with height with a scale  $H_s = k_B T_o / mg$  (the scale height), in which  $g$  is the gravity of the planet and  $m$  is the mass of an atmospheric molecule. (ii) Estimate  $H_s$  in the lower atmosphere for each of the planet listed in Table 1.1.

**Q6** Show that the specific volume  $\alpha$  of a sample of air can be approximated as,

$$\alpha \approx \alpha_d(1 - q_t) \quad (1.21)$$

in which  $\alpha_d = R_d T / P_d$  is the specific volume of dry air ( $R_d$  being the gas constant for dry air,  $P_d$  the partial pressure of dry air and  $T$  temperature). You might want to start by writing that  $\alpha = (V + V_l + V_i) / (m_d + m_v + m_l + m_i)$  in which  $V$  is the volume of the sample occupied by the gas phase,  $V_l$  and  $V_i$  that of the liquid and ice phases, respectively.

**Q7** By inspection of a surface pressure map (for example from the on-line ERA40Atlas<sup>2</sup>), work out whether the Rocky mountains tend to increase or decrease atmospheric angular momentum.

**Q8** A simple view of the Tropics is that it is primarily independent of longitude, i.e., rings of air flow upward at the equator in the ascending branch

<sup>2</sup>See the web link on Blackboard.

of the Hadley cell, and flow poleward at upper levels, conserving their angular momentum. Estimate the implied zonal velocity  $u$  (relative to the solid body rotation of the Earth) at  $30^\circ$  of latitude. How does it compare with the observed velocity? Hint: you may assume that the relative velocity  $u$  of the ring is very small near the ground.

**Q9** Using the numbers in Fig. 1.9, discuss whether the atmosphere can be reasonably described as transparent to solar radiation.

# Chapter 2

## Radiative heating and cooling of the atmosphere

**Key concepts:** solid angle, irradiance, radiation balance, greenhouse effect, Beer's law, Schwarzschild's equation, infrared cooling to Space.

### 2.1 Concepts and definitions

#### 2.1.1 Intensity of radiation

The intensity of electromagnetic radiation at wavelength  $\lambda$  measures the energy crossing a unit area perpendicular to the direction of propagation per unit time, per unit wavelength interval, and per unit solid angle (Fig. 2.1). The “per unit area” and “per unit time” are familiar, but the “per unit wavelength interval” and “per unit solid angle” is less so. The “per unit wavelength interval”, or “per wavelength” for short, is needed to account for the spectrum of electromagnetic radiation, the total energy flux being computed as the integral over all wavelengths (i.e.,  $\int F_\lambda d\lambda$ ). In absence of scattering or absorption, the intensity of radiation, denoted by  $I_\lambda$ , is conserved (see the Appendix if you're interested to read more about this).

The “per unit solid angle” is included to represent the 3D nature of electromagnetic radiation. The radiation reaching P in Fig. 2.1 in a given direction is made of an infinitesimal cone of rays, or “radiation pencil”, filling a certain fraction of the sky. This fraction is measured by solid angle  $\Omega$ , exactly like an angle is a measure of length on a unit radius circle (Fig. 2.2). Solid angle is expressed in steradians ( $sr$ ) and the maximum solid angle attainable (the amount of space filled by the sky if we were floating in the air) is  $4\pi \approx 12.5sr$  (an hemisphere is  $2\pi$ ).

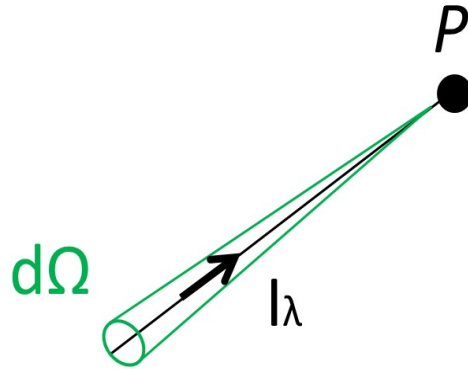


Figure 2.1: The intensity of radiation at wavelength  $\lambda$  is denoted by  $I_\lambda$  and measures the energy flow along the direction of propagation per unit area ( $dS$ ) and time ( $dt$ ), per unit wavelength ( $d\lambda$ ) and unit solid angle ( $d\Omega$ ).

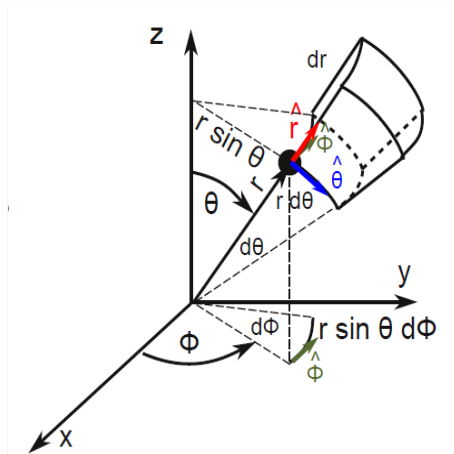


Figure 2.2: From vector Calculus (year 1), the area element on a sphere of unit radius  $r = 1$  is  $d\Omega = \sin\theta d\theta d\phi$ . This is the infinitesimal solid angle which we will use throughout in this chapter.

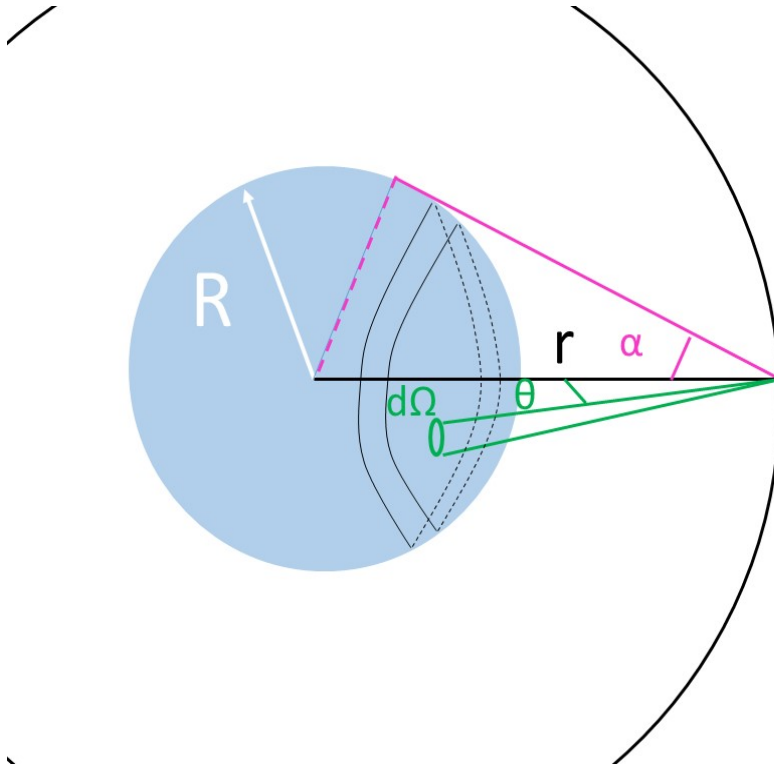


Figure 2.3: Example of calculation of solid angle. The total solid angle of the Sun at a distance  $r$  is the sum over the angle  $\theta$  (from 0 to  $\alpha$ ) of all the small solid angles  $2\pi \sin \theta d\theta$  indicated by the black shell.

*Example: Compute the solid angle of the Sun (radius  $R$ ), as seen from a distance  $r$  to its center (Fig. 2.3). The Sun is seen by an observer on the sphere of radius  $r$  with a solid angle  $\Omega(r) = \int_0^{2\pi} \int_0^\alpha \sin \theta d\theta d\phi = 2\pi(1 - \cos \alpha)$  where the angle  $\alpha$  satisfies  $\tan \alpha = R/r$  (note the right angle magenta triangle defining  $\alpha$  in Fig. 2.3). It covers a solid angle  $\Omega \approx 2\pi$  very close to the source ( $\alpha = \pi/2$ ) and  $\Omega \approx \pi(R/r)^2$  for  $r \gg R$  since  $1 - \cos \alpha \approx \alpha^2/2$  when  $\alpha$  is small.*

### 2.1.2 Blackbody radiation

As taught in Year 2 (Thermodynamics and Statistical Physics), blackbody radiation is the radiation emitted by a body in thermal equilibrium. It is isotropic and only depends on the temperature  $T$  characterizing the equilibrium, not on the nature of the material making the body. Its intensity, at a

given wavelength  $\lambda$  is given by the Planck function,

$$B_\lambda(T) = \frac{2hc^2\lambda^{-5}}{e^{hc/\lambda k_B T} - 1} \quad (2.1)$$

which has units of  $Wm^{-2}$  per wavelength per solid angle.

### 2.1.3 Shortwave and longwave radiation

We saw in section 1.4 that there is a small overlap of the Planck functions associated with terrestrial (infrared) and solar (visible) emissions (Fig. 1.6 –note the scaling of the Planck function by the solid angle of the Sun as seen from the Earth which is, from the calculation in section 2.1.1, equal to  $\pi(R/r)^2$ ). It is, as a result, common practice to separate “longwave” and “shortwave” radiations. Typically,  $4\mu m$  is used as the separation between the two. As we shall see the difference in wavelength will lead to important differences with respect to the role played by scattering and absorption/emission in the conservation of radiation intensity for longwave (scattering negligible, absorption/emission important) and shortwave radiation (scattering important, absorption important, emission negligible).

### 2.1.4 Irradiance

The energy of radiation passing through an horizontal plane, per unit area of that plane, per unit wavelength is called the monochromatic irradiance  $F_\lambda$ . It requires integrating  $I_\lambda$  over solid angle ( $2\pi$  at most for either upward or downward hemispheres) and taking into account the angle between the beam and the normal to the horizontal plane.

Consider for example the geometry in Fig. 2.4 and take the horizontal plane to be the  $x, y$  plane. The net downward radiation across the horizontal plane is made of several “radiation pencils”, each coming from different angles  $\theta$  with the  $z$  direction and the polar angle  $\phi$  in the horizontal plane. It is thus a matter of summing over all these pencils, each of infinitesimal solid angle  $d\Omega$ , and projecting onto the vertical  $I_\lambda \rightarrow I_\lambda \cos \theta$ . Thus,

$$F_\lambda = \int I_\lambda \cos \theta d\Omega \quad (2.2)$$

or using  $d\Omega = \sin \theta d\theta d\phi$ ,

$$F_\lambda = \int_{\phi=0}^{2\pi} \int_{\theta=0}^{\pi/2} I_\lambda \cos \theta \sin \theta d\theta d\phi \quad (2.3)$$

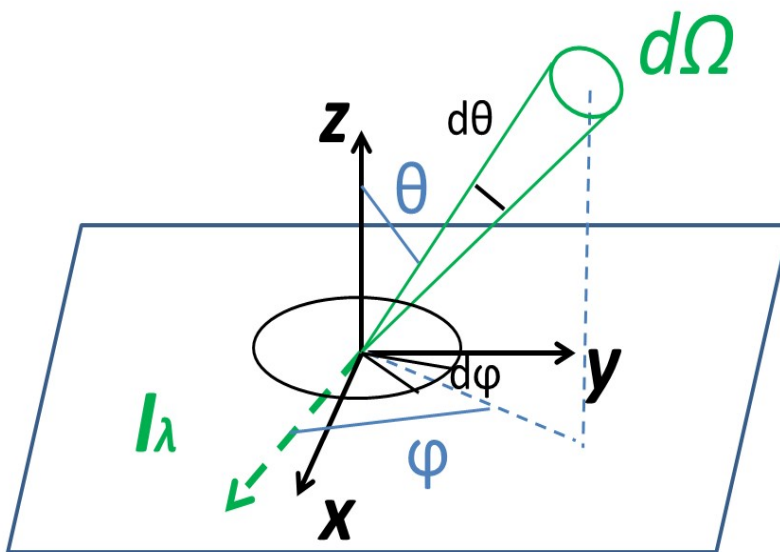


Figure 2.4: Geometry for the calculation of irradiance, given a pencil of monochromatic radiation (green cone) of intensity  $I_\lambda$  propagating downward (green dashed arrow) across the horizontal plane at an angle  $\theta$ .

If the radiation is isotropic (i.e., independent of  $\theta$  and  $\phi$ ), then the integral simplifies to

$$F_\lambda = 2\pi I_\lambda \int_{\theta=0}^{\pi/2} \cos\theta \sin\theta d\theta = \pi I_\lambda \quad (2.4)$$

This result is exact for Blackbody radiation, for which  $I_\lambda = B_\lambda$  in (2.1), and so  $F_\lambda = \pi B_\lambda$  (if one were to integrate the latter over all wavelengths, one would obtain  $\int \pi B_\lambda d\lambda = \sigma T^4$  in which  $\sigma$  is Stefan-Boltzmann's constant).

NB: The irradiance just defined is, strictly speaking, a downward irradiance (we counted solid angles from above). We'll denote it by  $F_\lambda^\downarrow$  in the following. We could also have computed the energy flux received from below, producing, for  $I_\lambda = B_\lambda$ , the same result:  $F_\lambda^\uparrow = \pi B_\lambda$  ("upward irradiance").

### 2.1.5 Kirchoff's law

In practice, most components of the climate system do not behave like black bodies, or only do so over a limited range of wavenumbers. For example the spectrum of most gases is made of sharp spectral lines, not a continuum; in addition, gases not only absorb radiation but also transmit it, unlike blackbodies. We'll see indeed in section 2.3 that the atmosphere is almost transparent to infrared radiation in the 10–12 $\mu m$ , the so-called "atmospheric window" region (this is the spectral region chosen to make infrared pictures of the Earth since in this region infrared radiation either originates from the Earth's surface or from cloud tops –see for example Fig. 1.5).

Surprisingly, even though the atmosphere does not emit according to  $B_\lambda(T)$ , one can relate atmospheric emission and absorption to  $B_\lambda(T)$  by using Kirchoff's law. To see this, define the emissivity of a particular body at temperature  $T$  (e.g., sample of air) according to,

$$\epsilon_\lambda \equiv I_\lambda(\textit{emitted})/B_\lambda(T) \quad (2.5)$$

and define its absorbtivity as,

$$\alpha_\lambda \equiv I_\lambda(\textit{absorbed})/I_\lambda(\textit{incident}) \quad (2.6)$$

Kirchoff's law states that, remarkably, irrespective of what the body is made, and irrespective of the nature of the radiation (isotropic or not),

$$\epsilon_\lambda = \alpha_\lambda \quad (\textit{Kirchoff's law}) \quad (2.7)$$

NB: For a blackbody,  $\epsilon_\lambda = \alpha_\lambda = 1$  for all wavelengths. Note also that Kirchoff's law only applies to systems in thermodynamic equilibrium with

their immediate surroundings (“local” thermodynamic equilibrium). This condition is satisfied in the troposphere and the stratosphere but less so above these regions.

### 2.1.6 The “solar constant”

We now apply the concept of radiation intensity and radiation pencils to estimate the amount of solar energy received per unit time by the Earth. This quantity is referred to as the solar constant  $S_o$  (in units of  $W$ ), although it fluctuates on many timescales (e.g., the decadal solar cycle)<sup>1</sup>

So we consider a point P on Earth at latitude  $\phi$  and longitude  $\gamma$  (Fig. 2.5) and first estimate the flux of energy received at that point. We will then sum over all points to obtain an expression for  $S_o$ . Because the Sun is so far away from the Earth, we are going to treat the solar radiation received at P, at a given wavelength  $\lambda$ , as made of only one pencil of radiation. Indeed, as the calculation in section 2.1.1 showed, the Sun covers a solid angle  $\delta\Omega \approx \pi(R_s/1AU)^2$  where  $R_s$  is the Sun’s radius and  $1AU$  (astronomical unit) is the mean Earth-Sun distance, that is a very small solid angle. This is just a mathematical way to say that the Sun covers only a small fraction of the sky. In addition, because the Sun is so far away from the Earth, we also approximate the angle made between this pencil and the local vertical as the latitude  $\phi$  in a plane of constant longitude (Fig. 2.5). This is just saying that we are treating the impinging solar radiation as a plane wave. Note that Fig. 2.5 only shows this projection in a plane of constant longitude. You would need to view the figure from the North pole to see the same effect in a plane of constant latitude, the result being that the angle between the pencil and the local vertical in that plane is approximately  $\pi/2 - \gamma$  if  $0 \leq \gamma \leq \pi$ .

With these approximations, the flux of energy per wavelength  $\Phi_\lambda$  received from the Sun at P is,

$$\Phi_\lambda \approx I_\lambda \cos \phi \sin \gamma \delta\Omega, \quad (2.8)$$

so that the power  $P_\lambda$  per unit wavelength integrated over the Earth is simply,

$$P_\lambda \approx \int \Phi_\lambda R^2 \cos \phi d\phi d\gamma \quad (2.9)$$

Note that in this expression the latitude  $\phi$  is integrated from South to North pole ( $-\pi/2$  and  $\pi/2$ , respectively) but the longitude is only integrated over

---

<sup>1</sup>Once you realise how amazingly active the Sun is this is not a surprise. Have a look at the fantastic movies NASA has made from the SDO mission (e.g., google “thermonuclear art SDO”).

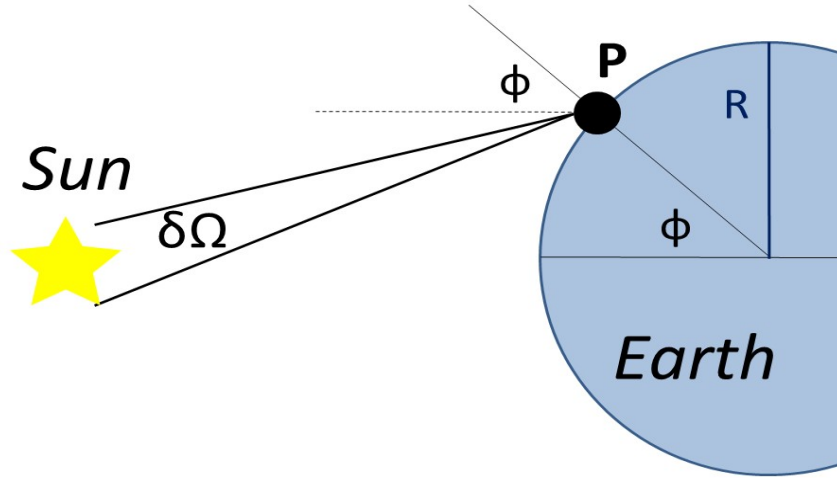


Figure 2.5: Schematic for the calculation of the Solar constant. Note that the diagram is (obviously!) not on the correct scale.

the day hemisphere, i.e. from 0 to  $\pi$ . Inserting (2.8), we obtain,

$$P_\lambda \approx I_\lambda \delta\Omega \int R^2 \cos^2 \phi \sin \gamma d\phi d\gamma = (I_\lambda \delta\Omega) \pi R^2 \quad (2.10)$$

The above relation shows that, under our approximation of parallel incoming solar radiation, it all looks as if the Earth was a disk of radius  $\pi R^2$ . Integrating over wavelength, we define the Solar constant as,

$$S_o \equiv \int I_\lambda \delta\Omega d\lambda \approx 1,361 W m^{-2} \quad (2.11)$$

so that the net power received by the Earth is  $S_o \pi R^2$ .

NB: This is a calculation valid for equinoctial conditions, or annual mean conditions, only. One would need to include the tilt of  $23.5^\circ$  of the ecliptic plane to estimate the total energy gained at the solstices.

### 2.1.7 Radiation balance and emission temperature

A simplified energy balance for the Earth is given in Fig. 2.6. A fraction  $\alpha_P$  (the planetary albedo) of the Solar radiation discussed in the previous subsection is reflected. At equilibrium, the same amount of power must be

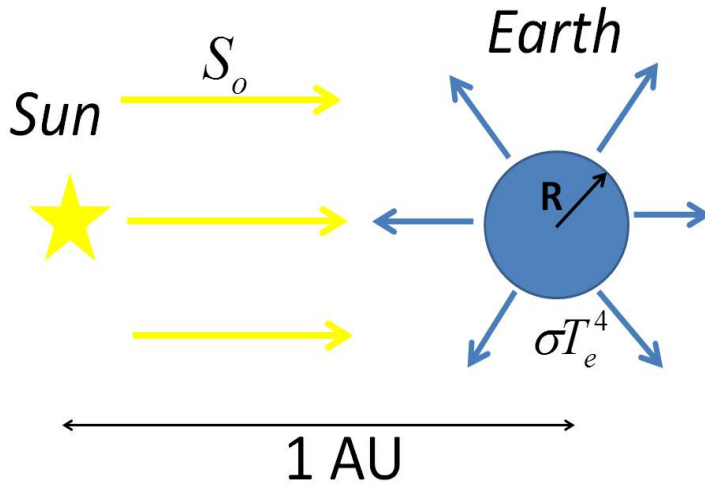


Figure 2.6: Radiation balance of the Earth. The incoming solar radiation is treated as a parallel beam impinging on a spherical Earth. The outgoing infrared radiation is isotropic.

lost by the Earth. The emission temperature is defined as the temperature required to achieve this, were the Earth a perfect blackbody in the infrared:

$$\pi R^2 S_o (1 - \alpha_P) = 4\pi R^2 \sigma T_e^4 \quad (2.12)$$

leading to

$$T_e \equiv \left( \frac{S_o (1 - \alpha_P)}{4\sigma} \right)^{1/4} \quad (2.13)$$

NB: note the factor of 4 coming from the geometry of the problem (plane radiation impinging a sphere as opposed to radial emission).

The idea of radiative balance at the TOA is an idealization. Global conservation of energy requires that any imbalance be reflected in a change in heat content. This, in practice, is dominated by oceanic heat storage (largest heat capacity in the climate system) which fluctuates on very long timescales (decades and longer) because of the slow ocean dynamics. Thus the TOA net radiative fluxes are not expected to vanish on timescales shorter than at least a few decades. We will come back to this in Chapter 5 when discussing anthropogenic climate change.

For Earth annual average,  $\alpha_P = 0.3$  so that  $T_e = 255K$  or  $-18^\circ C$  (very cold!). The Earth's surface temperature is about  $288K$ , or about  $+15^\circ C$ .

Thus, by contrast with the present model which omits entirely the atmosphere, we can say that the atmosphere is responsible for a  $\approx 288 - 255 = 33K$  increase in surface temperature. The way this works is disentangled in the simple model coming next. Before doing so, it is worth mentioning a couple of other interesting aspects of this model:

- it suggests that the bulk of the infrared radiation seen from Space originates from the atmosphere itself rather than from the surface because  $255K$  is found typically at an altitude of  $5km$  above the Earth's surface.
- the Planck function for a blackbody at  $255K$  is centered near  $15\mu m$  (Fig. 1.6). This happens to be a wavelength at which the  $CO_2$  molecule absorbs strongly radiation, hence the strong “leverage” of  $CO_2$  on climate.

## 2.2 A simple model of the greenhouse effect

We consider a 0D model of radiative balance (averaged over the whole Earth's surface area and expressed in  $Wm^{-2}$ ) and go a little beyond the previous section by explicitly introducing the surface temperature  $T_s$  (Fig. 2.7).

In the shortwave, the solar flux impinging at the TOA is still  $S_o(1 - \alpha_P)/4$  which we denote by  $F_o$ . We further assume that only a fraction  $T_{sw}$  of this radiation reaches the surface, to account for absorption by atmospheric molecules and aerosols. (we'll call  $T_{sw}$  the transmissivity of the atmosphere in the shortwave in the following). From Kirchoff's law, if some radiation is absorbed it must also be emitted. However, at terrestrial temperature the emission in the range of wavelengths where the bulk of solar radiation resides is negligible, and  $\epsilon_\lambda B_\lambda(T) \ll \alpha_\lambda I_{incoming}$ . As a result, even though  $\alpha_\lambda = \epsilon_\lambda$  for wavelengths  $\lambda$  in the shortwave part of the spectrum, we can safely neglect the emission of shortwave radiation by the atmosphere.

In the longwave, we take the atmosphere to be at constant temperature  $T_a$  and denote by  $F_a$  the longwave flux it emits upward and downward. The surface is treated as a blackbody, thus emitting  $F_s = \sigma T_s^4$  upward. A fraction  $T_{LW}$  of this radiation reaches the top-of-the-atmosphere (we'll call this fraction the transmissivity of the atmosphere in the longwave). Fig. 2.7 summarizes the energy flows.

We can predict what the surface temperature should be solely from energy conservation arguments. At equilibrium, the net flow of energy across any surface must be zero. Applying this at the Earth's surface yields (see Fig. 2.7):

$$F_o T_{sw} + F_a = F_s \quad (2.14)$$

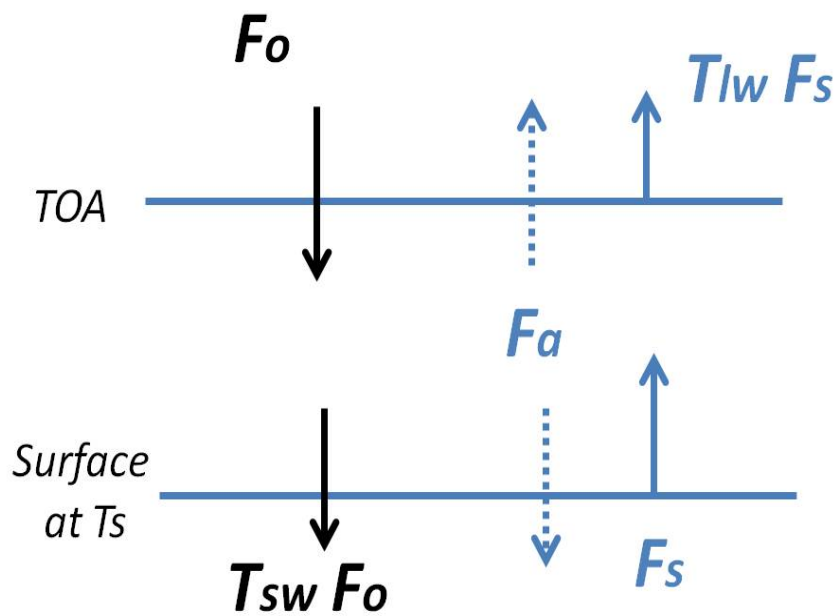


Figure 2.7: A simple model of the greenhouse effect. TOA denotes the “top-of-the-atmosphere” where pressure vanishes. The shortwave fluxes are indicated in black, the longwave ones in blue.

while, at the “top-of-the-atmosphere”, it produces:

$$F_o = F_a + F_s T_{lw} \quad (2.15)$$

By assumption  $F_s = \sigma T_s^4$  while, using (2.13),  $F_o = \sigma T_e^4$ . As a result, after elimination of  $F_a$  from the above two energy conservation equations, we obtain,

$$T_s = T_e \left( \frac{1 + T_{sw}}{1 + T_{lw}} \right)^{1/4} \quad (2.16)$$

This equation is remarkably simple and shows that the surface temperature and the emission temperature differ only by a factor proportional to the transmissivities in the shortwave and the infrared. If there were no atmosphere,  $T_{sw} = T_{lw} = 1$  and  $T_s = T_e = 255K$ . With an atmosphere, and if  $T_{sw} > T_{lw}$ , the surface temperature will then exceed  $T_e$ . In the Earth atmosphere,  $T_{lw} \approx 0.2$  while  $T_{sw} \approx 0.9$ , leading to  $T_s \approx 286K$ .

The agreement of this prediction with the observed  $T_s = 288K$  is fortuitous because of the extreme simplicity of the model (isothermal atmosphere, surface treated as a blackbody). The key point though is that because the atmosphere is more transparent to shortwave than it is to longwave ( $T_{sw} > T_{lw}$ ), there is a “recycling” of energy towards the surface:

$$F_o T_{sw} + F_a = F_o \frac{1 + T_{sw}}{1 + T_{lw}} > F_o \quad (\text{surface heating}) \quad (2.17)$$

The added heating leads to a larger surface temperature –this effect is called the greenhouse effect.

## 2.3 Beer’s law

*NB: The “atmospheric window”, absorption, emission and scattering of radiation by atmospheric molecules and aerosols is discussed in the ppt slide for this chapter.*

Consider a monochromatic beam of wavelength  $\lambda$  and of intensity  $I_\lambda$ . We want to derive the change in intensity ( $dI_\lambda$ ) of this beam along its direction of propagation (measured by the coordinate  $s$ ). This change is caused either because some air molecules scatter the radiation (net loss of radiation intensity along the path but no change in radiation intensity integrated over all directions), or absorb it (net loss of radiation intensity along the path but no change in radiation intensity in other directions). If we denote by  $q_a$  the mass of these molecules per unit mass of air,  $\rho q_a$  is the mass of these

molecules per unit volume and  $\rho q_a ds$  is the mass of those molecules per unit area perpendicular to the direction of propagation.

Beer's law states that,

$$dI_\lambda = -I_\lambda k_\lambda \rho q_a ds \quad (2.18)$$

in which  $k_\lambda$  (in  $m^2 kg^{-1}$ ), called the extinction coefficient, measures the intensity of absorption or scattering of radiation of wavelength  $\lambda$ ,

$$k_\lambda = \beta_\lambda(\text{absorption}) + \sigma_\lambda(\text{scattering}) \quad (2.19)$$

Equation (2.18) can be integrated along the path of the beam as,

$$I_\lambda(s) = I_\lambda(s_o) e^{-\int_{s_o}^s k_\lambda \rho(s') q_a(s') ds'} \quad (2.20)$$

In this expression  $s_o$  is a starting point where the radiation intensity is  $I_\lambda(s_o)$ . It is convenient to introduce the following quantities,

$$T_\lambda(s_o, s) = e^{-\int_{s_o}^s k_\lambda \rho(s') q_a(s') ds'} \quad (\text{transmittance}) \quad (2.21)$$

$$\tau_\lambda(s_o, s) = \int_{s_o}^s k_\lambda \rho(s') q_a(s') ds' \quad (\text{optical depth}) \quad (2.22)$$

Note that both  $\tau_\lambda > 0$  and  $0 \leq T_\lambda \leq 1$  are non dimensional functions (i.e., they are just numbers, without SI units). One measures the opacity of the atmospheric layer over a given path ( $\tau_\lambda$ , the larger the more opaque the layer; hardly any radiation escapes a layer with optical depth much greater than unity), while the other measures its transparency ( $T_\lambda$ , the closer to unity the more transparent the layer –see for example the discussion of the greenhouse effect earlier in this chapter).

With these notations, (2.20) can be rewritten more compactly as:

$$I_\lambda(s) = I_\lambda(s_o) T_\lambda(s_o, s) \quad (2.23)$$

expressing that if only extinction is considered, the intensity at  $s$  is that at  $s_o$  times the transmittance along the path  $(s_o, s)$ .

## 2.4 Schwarzschild's equation

### 2.4.1 Derivation

Beer's law only considers removal of radiation from a beam. Radiation can however also be added to the beam due to the emission from the layer or

to radiation incident from another direction being scattered into the beam. The additional elements also depend on the amount of radiatively active constituent  $\rho q_a ds$  so Beer's law can be modified to include them by introducing a source function  $J_\lambda$ ,

$$dI_\lambda = -k_\lambda \rho q_a ds I_\lambda(s) + k_\lambda \rho q_a ds J_\lambda(s) \quad (2.24)$$

This can be simplified by introducing again the optical depth –see eq. (2.22) in which  $s_o$  is simply taken as a reference location,

$$d\tau_\lambda = k_\lambda \rho q_a ds \quad (2.25)$$

Doing so allows a change of variables ( $s \rightarrow \tau_\lambda$ ) and (2.24) can be rewritten as,

$$d(I_\lambda e^{\tau_\lambda})/d\tau_\lambda = J_\lambda e^{\tau_\lambda} \quad (2.26)$$

Integrating from  $s_o$  to  $s$ , and noting that  $\tau_\lambda(s_o, s_o) = 0$ , we obtain,

$$I_\lambda(s) = I_\lambda(s_o) e^{-\tau} + \int_0^\tau J_\lambda(\tau') e^{-(\tau-\tau')} d\tau' \quad (2.27)$$

with  $\tau' = \tau_\lambda(s_o, s')$  and  $\tau = \tau_\lambda(s_o, s)$  (to simplify notations).

### 2.4.2 Physical interpretation

Let us step back a little from these calculations. The first term on the r.h.s. of the previous equation is readily interpreted as the radiation emitted at  $s_o$ , a fraction  $e^{-\tau}$  making to  $s$ , in agreement with Beer's law. The second term, the integral, reflects the contribution to the radiation at  $s$  emitted from all layers between  $s_o$  and  $s$ . To see this more clearly, consider the following. Measuring the location of any of these layers by  $s'$  with  $s_o \leq s' \leq s$ , we know from (2.24) that they emit an amount of radiation  $J_\lambda(s') k_\lambda \rho q_a ds = J_\lambda(s') d\tau'$ . From the definition of transmittance, only  $T_\lambda(s', s) J_\lambda(s') d\tau'$  reaches  $s$ . This is nothing else than  $J_\lambda(s') e^{-(\tau-\tau')} d\tau'$  since  $T_\lambda(s', s) = T_\lambda(s_o, s)/T_\lambda(s_o, s')$ . Thus we can as well rewrite (2.27) as,

$$I_\lambda(s) = I_\lambda(s_o) T_\lambda(s_o, s) + \int_0^{\tau_\lambda(s_o, s)} T_\lambda(s', s) J_\lambda(\tau') d\tau' \quad (2.28)$$

### 2.4.3 Final form

Eq. (2.28) has a clear physical interpretation but, for practical purposes, the initial form (2.27) can be put to better use. Start from:

$$dT_\lambda(s', s) = e^{-(\tau-\tau')} d\tau' \quad (2.29)$$

(NB: here  $s$  is constant and the derivative applies to the variable  $s'$ , or  $\tau'$ ). After division by  $ds'$ , this reads simply:

$$I_\lambda(s) = I_\lambda(s_o)T_\lambda(s_o, s) + \int_{s_o}^s J_\lambda(s') \left( \frac{dT_\lambda(s', s)}{ds'} \right) ds' \quad (2.30)$$

This is the most convenient form of Schwarzschild's equation to use because:

- (i) the contribution from atmospheric layers to the radiation intensity at  $s$  (the integral term) is expressed using the natural coordinate  $s'$  rather than the mathematical function  $\tau'$ .
- (ii) this form suggests that the contribution to intensity at  $s$  from the emission by a layer at  $s'$  (i.e.,  $J_\lambda(s')$ ) is weighted by the gradient of the transmissivity between  $s'$  and  $s$  (i.e.,  $dT_\lambda(s', s)/ds'$ ). As the section below shows, this turns out to be very useful to gain a bit more intuition about how radiative transfer works.

## 2.5 Some applications of Schwarzschild's equation

### 2.5.1 No scattering

So far the exact form of the source function  $J_\lambda$  has not been discussed. When scattering is important as a source of radiation along a particular line-of-sight (or "pencil of radiation"), the problem is mathematically difficult as one must integrate over all solid angles a probability function that photons have been scattered into that line-of-sight. So it would be useful to know when we can neglect this complexity.

In the infrared part of the spectrum, scattered radiation can typically be neglected compared to the radiation emitted directly in a given line of sight so the approximation is usually adequate. In the shortwave part of the spectrum, *except for a line-of-sight directed at the Sun*, all pencils of radiation are made of scattered radiation, and so the complexity has to be met fully.

If scattering can be neglected, i.e.,  $\sigma_\lambda = 0$  in (2.19) (so typically for the infrared radiation, based on the previous discussion), the Schwarzschild's equation takes a particularly simple form. Indeed, in that case, the absorptivity of the layer of thickness  $ds$  is,

$$\alpha_\lambda = I_\lambda \beta_\lambda \rho q_a ds / I_\lambda = I_\lambda k_\lambda \rho q_a ds / I_\lambda = k_\lambda \rho q_a ds \quad (2.31)$$

while its emissivity is,

$$\epsilon_\lambda = J_\lambda k_\lambda \rho q_a ds / B_\lambda \quad (2.32)$$

Using Kirchoff's law (2.7),  $\epsilon_\lambda = \alpha_\lambda$  which leads to  $1 = J_\lambda/B_\lambda$  and so Schwarzschild's equation can be simply rewritten as,

$$I_\lambda(s) = I_\lambda(s_o)T_\lambda(s_o, s) + \int_{s_o}^s B_\lambda(s') \left( \frac{dT_\lambda(s', s)}{ds'} \right) ds' \quad (2.33)$$

### 2.5.2 Infrared radiation by an isothermal atmosphere

Consider the case of an isothermal atmosphere and neglect scattering. The downward infrared radiation measured at a distance  $s$  from the top-of-the-atmosphere ( $s = s_o$ ) can be computed from (2.33) as follows.

First, acknowledge that for downward infrared radiation,  $I_\lambda(s_o) = 0$ , so that the first term on the r.h.s of (2.33) vanishes. For the integral term, one can take  $J_\lambda = B_\lambda$  outside it since the atmosphere is isothermal (say  $B_\lambda = B_o$ ). We thus have,

$$I_\lambda(s) = B_o[T_\lambda(s, s) - T_\lambda(s_o, s)] = B_o[1 - T_\lambda(s_o, s)] \quad (2.34)$$

since the transmissivity between  $s$  and  $s$  is unity.

Apply this result to absorption/emission by water vapour for example. We can very reasonably neglect the amount of water vapour above the tropopause, so the transmittance, measured from  $s_o$  (the top-of-the-atmosphere) to  $s$  will look like schematized in Fig. 2.8 (red curve): unity until the tropopause is reached and then decaying towards the surface. Conversely, the radiation intensity is initially zero until the tropopause is reached, and then increases towards the Earth's surface. Note that the intensity at the Earth's surface approaches  $B_o$  as the transmittance of the atmosphere decreases ( $T_\lambda \rightarrow 0$ ). This is expected since in this limit the troposphere behaves like a Blackbody. The spectral line (or wavelength  $\lambda$ ) is then said to be "saturated".

### 2.5.3 Remote sensing of temperature

A useful application of Schwarzschild equation is the measurement of atmospheric temperature from satellites. For a passive instrument, we would consider the upward radiation of longwave radiation emitted by the atmosphere and the surface. We thus consider the full expression (2.33), with  $s_o$  being at the Earth's surface and  $I_\lambda(s_o) = B_\lambda(SST)$  (assuming we are over the oceans, which are excellent blackbodies in the longwave –SST is the sea surface temperature). The path variable  $s$  thus increases upwards and the transmittance  $T_\lambda(s_o, s)$  is measured from the sea to any point in the atmosphere above. We are interested in the radiation received by a satellite, i.e., at very large  $s$ .

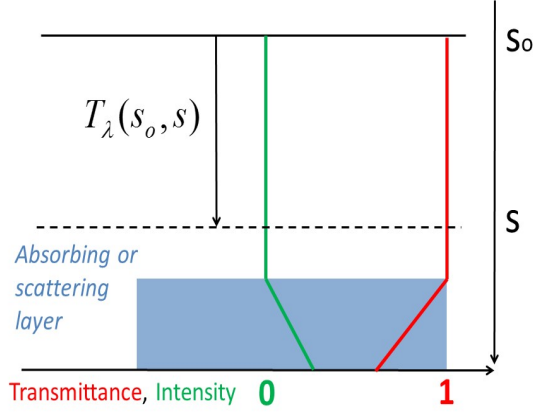


Figure 2.8: Simple application of Schwarzschild's equation to downward long-wave radiation. The lower atmosphere (blue region) is assumed to be radiatively active at this wavelength but not the layer above it. In the latter  $I_\lambda = 0$  and  $T_\lambda(s_o, s) = 1$ .

Imagine that there is a strong absorption of infrared radiation at wavelength  $\lambda$  at a distance  $s_a$  from the sea, and very little absorption elsewhere (Fig. 2.9). The transmittance  $T_\lambda(s', s)$  would then be nearly zero for  $s' \leq s_a$  (the  $(s', s)$  layer would then include the absorbing layer), while it would be close to unity for  $s' \geq s_a$  (the  $(s', s)$  layer would then be above the absorbing layer). As a result, the derivative  $dT_\lambda(s', s)/ds'$  would have a “narrow bell” shape centred at  $s' = s_a$  (Fig. 2.9). The intensity measured at  $s$  (say aboard a satellite) would then be

$$I_\lambda(s) = \int_{s_o}^s J_\lambda(s') \left( \frac{dT_\lambda(s', s)}{ds'} \right) ds' \approx J_\lambda(s_a) \quad (2.35)$$

where I have used the fact that  $T_\lambda(s_o, s) = 0$  in eq. (2.33) in this example, and I have approximated the narrow bell shaped derivative as a Dirac function. The source function  $J_\lambda(s_a)$  is a strong function of temperature and so, after calibration, the previous equation provides an estimate of temperature of the atmosphere at  $s = s_a$ .

In practice, rather than measuring temperature at a precise location, the measurement provides temperature over a weighted layer (i.e., the bell shaped derivative is not exactly a Dirac function. In addition one could more realistically consider absorbers with a uniform mixing ratio and use the different strength of absorption lines –see some examples in the slides for

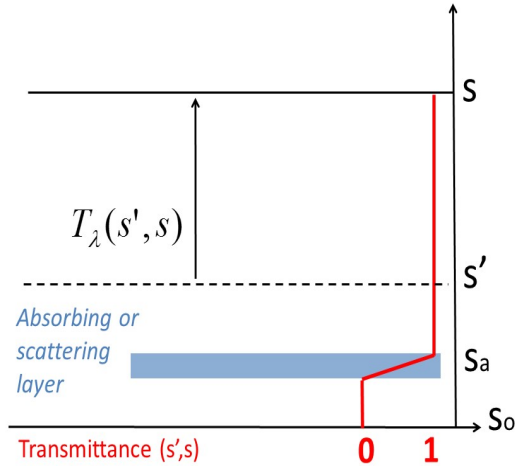


Figure 2.9: Same as Fig. 2.8 but for upward longwave radiation in the presence of a localized absorbing layer.

this chapter). Typical wavelengths used are the  $15\mu m$  and  $4.3\mu m$  bands of  $CO_2$  and the microwave ( $5mm$ ) band of  $O_2$ .

## 2.6 Radiative heating and cooling rates

The difference between the radiation incoming and outgoing from the sides of a given volume of air is, by conservation of energy, a heating rate. Although conceptually simple, the calculation of this heating rate is made difficult in practice because of the need to integrate the radiation coming/outgoing from all sides of the sample. In the case of the global atmosphere, the sides in question are spheres of constant radius, or, in the Cartesian geometry adopted here for simplicity, planes of constant height. We will thus concentrate in this section on the heating of a layer sandwiched between height  $z$  and  $z + dz$ .

From section 2.1.4, the total flux of radiation across an horizontal plane due to a beam of intensity  $I_\lambda$  was defined as the irradiance  $F_\lambda$ . To distinguish between radiation coming from above and below, we will separately consider  $F_\lambda^\uparrow$  and  $F_\lambda^\downarrow$ . The heating rate  $Q_\lambda$  of an infinitesimal layer of air sandwiched between height  $z$  and  $z + dz$  is thus (Fig. 2.10),

$$Q_\lambda = \frac{d}{dz}(F_\lambda^\downarrow - F_\lambda^\uparrow) \quad (2.36)$$

Because  $F_\lambda$  is in units of  $Wm^{-2}$  per wavelength,  $Q_\lambda$  is in units of  $Wm^{-3}$  per

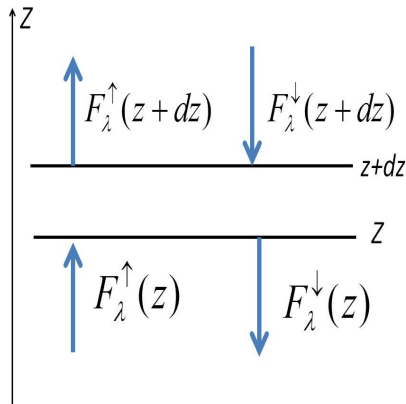


Figure 2.10: Schematic of the various terms in the heat budget of an infinitesimal layer sandwiched between  $z$  and  $z + dz$ . The heat gained per unit time, area and wavelength is  $F_{\lambda}^{\uparrow}(z) + F_{\lambda}^{\downarrow}(z + dz)$ . Likewise, the heat lost per unit time, area and wavelength is:  $F_{\lambda}^{\uparrow}(z + dz) + F_{\lambda}^{\downarrow}(z)$ . Thus the net heat gained per unit area, time and wavelength is  $F_{\lambda}^{\uparrow}(z) - F_{\lambda}^{\uparrow}(z + dz) + F_{\lambda}^{\downarrow}(z + dz) - F_{\lambda}^{\downarrow}(z) = (dF_{\lambda}^{\downarrow}/dz - dF_{\lambda}^{\uparrow}/dz)dz$ . Dividing this expression by  $dz$  gives the heating per unit volume, wavelength and unit time.

wavelength. The total heating rate due to radiation is thus  $Q_{rad}$ ,

$$Q_{rad} \equiv \int_0^{+\infty} Q_{\lambda} d\lambda \quad (2.37)$$

which has units of  $Wm^{-3}$ . As we shall see, and consistent with the numbers in Fig. 1.9, the heating due to shortwave absorption is more than offset by radiative cooling due to longwave emission so that in the net,  $Q_{rad} < 0$  (cooling).

### 2.6.1 Shortwave heating

Let's take advantage of the hard work in section 2.1.6, where we showed by surface integration on a sphere that the solar energy received by the Earth was, at a given wavelength  $\lambda$ , equal to,

$$P_{\lambda} = (I_{\lambda} \delta\Omega) \pi R^2 \quad (2.38)$$

In this expression, both the  $I_{\lambda}$  and  $R$  are strictly speaking referring to quantities at the top-of-the-atmosphere since we did not account for atmospheric absorption and scattering and we were, in this section, only interested in the

energy available as a whole by the Earth. But we can re-interpret this result as saying that, per unit horizontal area at a height  $z$ , the irradiance is,

$$F_{\lambda}^{\downarrow}(z) = I_{\lambda}(z)\delta\Omega\pi R^2/4\pi R^2 = I_{\lambda}(z)\delta\Omega/4 \quad (2.39)$$

Using Beer's law, we have  $I_{\lambda}(z) = I_{\lambda,TOA}e^{-\tau_{\lambda}(z)}$  where  $\tau_{\lambda}(z)$  is the optical thickness of the atmosphere from the top-of-the-atmosphere to a height  $z$ . Hence we write,

$$F_{\lambda}^{\downarrow}(z) = F_{\lambda,TOA}^{\downarrow}e^{-\tau_{\lambda}(z)} \quad (2.40)$$

where  $F_{\lambda,TOA}^{\downarrow} = I_{\lambda,TOA}\delta\Omega/4$ .

The contribution to  $Q_{\lambda}$  coming from  $F_{\lambda}^{\downarrow}$  is then,

$$Q_{\lambda} = \frac{d}{dz}[F_{\lambda,TOA}^{\downarrow}e^{-\tau_{\lambda}(z)}] \quad (2.41)$$

$$= (-F_{\lambda,TOA}^{\downarrow}e^{-\tau_{\lambda}(z)})(-\rho q_a k_{\lambda}) \quad (2.42)$$

$$= F_{\lambda}^{\downarrow}\rho q_a k_{\lambda} \quad (2.43)$$

in which we have used (2.22). Fig. 2.11 gives a schematic of the vertical variations of  $F_{\lambda}^{\downarrow}$  and  $\rho q_a = \rho_a$ , as well as a scale for the optical depth. The downward radiation decreases monotonically as we go downward, as expected, and the density of absorber is assumed to be exponential-like. As can be seen,  $Q_{\lambda}$ , the product of these two<sup>2</sup>, peaks at a height where the optical depth is close to unity. Physically, well above the level of unit optical depth, the incoming beam is virtually undepleted, but the density is so low that there are too few molecules to produce significant absorption and heating. Likewise, well below the level of unit optical depth, there are a lot of molecules to produce absorption and heating, but there is not much left to absorb as the beam has been mostly depleted. You are invited to prove this result mathematically in Q5 below.

Detailed calculations, using a ‘‘line-by-line radiation code’’ and including the contribution to  $Q_{\lambda}$  from  $F_{\lambda}^{\uparrow}$ , are shown in Fig. 2.12 (focus here on the right hand side, i.e., shortwave heating rates). The heating rates are given in units of  $K/day$ , i.e.,  $Q_{\lambda}/(\rho c_p)$  is plotted rather than  $Q_{\lambda}$ . Absorption by ozone in the stratosphere dominates the heating rate, on the order of  $5 - 10K/day$ . After this and  $O_2$  at high altitude (above the mesopause), the next most important absorber of solar radiation is water vapour, which contributes to a relatively uniform heating of the troposphere on the order of  $0.5K/day$ .

<sup>2</sup>We are neglecting here the temperature and pressure dependence of  $k_{\lambda}$ .

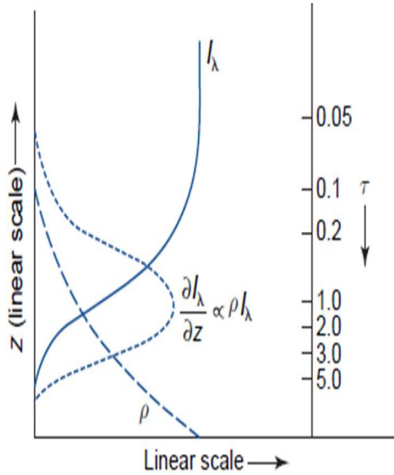


Figure 2.11: Schematic of heating rate due to solar absorption of radiation of intensity  $I_\lambda$ . See text for explanations. Figure from the Wallace and Hobbs' textbook.

*NB: Why divide by  $c_p$  and not  $c_v$  to express heating rates in K/day? This is an interesting question. In the 1st law of Thermodynamics,  $dU = \delta Q + \delta W = \delta Q - PdV$ , the heating  $\delta Q$  is not a state function, i.e., it depends on the path considered. Radiative cooling/heating does not involve adding/subtracting mass, and mass is constant within a given pressure layer under the hydrostatic approximation. Thus, we can consider that an infinitesimal layer of air (thickness  $dz$ ) of fixed mass has a constant pressure (the pressure variations within the layer are of order  $dP \ll P$  so the pressure of the layer is constant at  $\approx P$ ). This suggests to use instead  $dU = \delta Q - d(PV) + VdP$  which, after using  $PV = Nk_B T$  leads to  $(C_V + Nk_B)dT \equiv C_p dT = \delta Q + VdP$ . At constant pressure, a given amount of heat will lead to a temperature change after division by  $C_p$ . At constant volume, the same amount of heat would lead to a larger temperature change since  $C_V < C_p$ .*

## 2.6.2 Longwave cooling

It is impossible to neglect the upward irradiance of longwave radiation (this is the physical mechanism allowing the Earth to cool to Space, see Chapter 1).

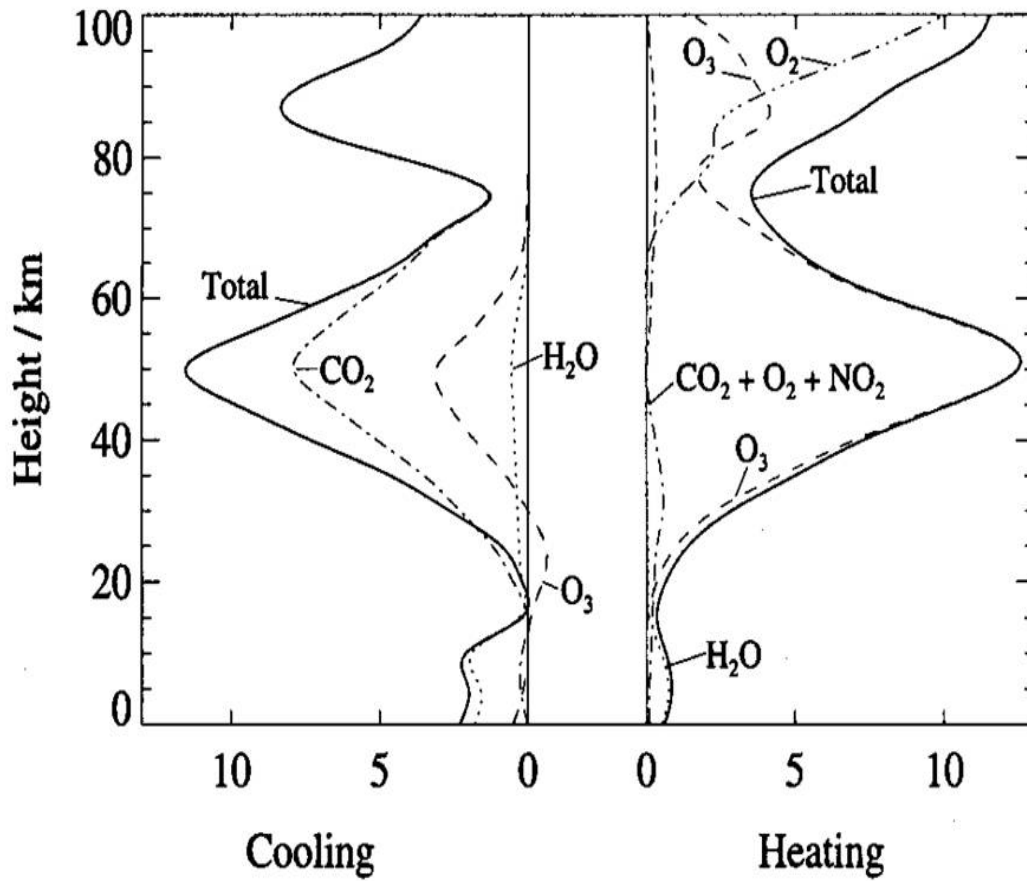


Figure 2.12: Global mean longwave (left panel) and shortwave (right panel) heating rates in  $K/day$  as a function of altitude showing contributions of the major gases. After D. Andrews' textbook.

Nor is it possible to neglect the downward infrared irradiance responsible for the greenhouse effect. We'll thus compute both terms in this section. Besides this, the other important difference between the calculation here and that in the previous section regards the transformation from  $I_\lambda$  to  $F_\lambda$ . As illustrated in fig. 2.13 this simply reflects the well defined source of shortwave radiation (the Sun) as opposed to the more diffuse sources of longwave radiation (Earth's surface, atmospheric molecules, clouds, etc). Note that the different pencils in Fig. 2.13 have also different path lengths. To treat this effect explicitly without enhancing the complexity too much we'll use the "parallel plane approximation", which treats the atmosphere as homogeneous in the horizontal direction: one can then use for all pencils the optical thickness measured along the direction  $z$ , after taking into account the increase in path length by the factor  $1/\cos\theta$  (see Fig. 2.13).

In the calculations below we'll neglect scattering of longwave radiation and will accordingly use  $J_\lambda = B_\lambda$  (section 2.4.2) in Schwarzschild equation, i.e.,

$$I_\lambda(s) = I_\lambda(s_o)e^{-\tau} + \int_0^\tau B_\lambda(\tau')e^{-(\tau-\tau')}d\tau' \quad (2.44)$$

with  $\tau = \tau_\lambda(s_o, s)$  and  $\tau' = \tau_\lambda(s_o, s')$ .

### Upward irradiance

Let's first consider the contribution to  $F_\lambda^\uparrow$  arising from emission by the Earth's surface, i.e., the term corresponding to  $I_\lambda^\uparrow(s_o) = B_\lambda(T_s)$  where  $T_s$  is the Earth's surface temperature. Taking into account the  $1/\cos\theta$  term, the contribution  $F_{\lambda,surf}^\uparrow$  to the upward irradiance from the Earth's surface is,

$$F_{\lambda,surf}^\uparrow(z) = \int_0^{2\pi} B_\lambda(T_s)e^{-\tau(z)/\cos\theta} \cos\theta d\Omega \quad (2.45)$$

in which  $\tau(z) = \tau_\lambda(0, z)$  now measures the optical depth of the air column from the surface to height  $z$ , and  $\theta$  is the angle made by each pencil of radiation with the vertical. Consistent with the parallel plane approximation, we assume that  $T_s$  does not vary too much, which allows us to take the  $B_\lambda(T_s)$  term outside the integral. After doing this, and introducing  $\mu = \cos\theta$ , we have,

$$F_{\lambda,surf}^\uparrow(z) = 2\pi B_\lambda(T_s) \int_0^1 e^{-\tau(z)/\mu} \mu d\mu \quad (2.46)$$

A useful approximation is that  $2 \int_0^1 e^{-\tau/\mu} \mu d\mu \approx e^{-\tau/\cos(53^\circ)} = e^{-1.66\tau}$  ("diffuse approximation"). As a result,

$$F_{\lambda,surf}^\uparrow(z) \approx \pi B_\lambda(T_s) e^{-1.66\tau(z)} \quad (2.47)$$

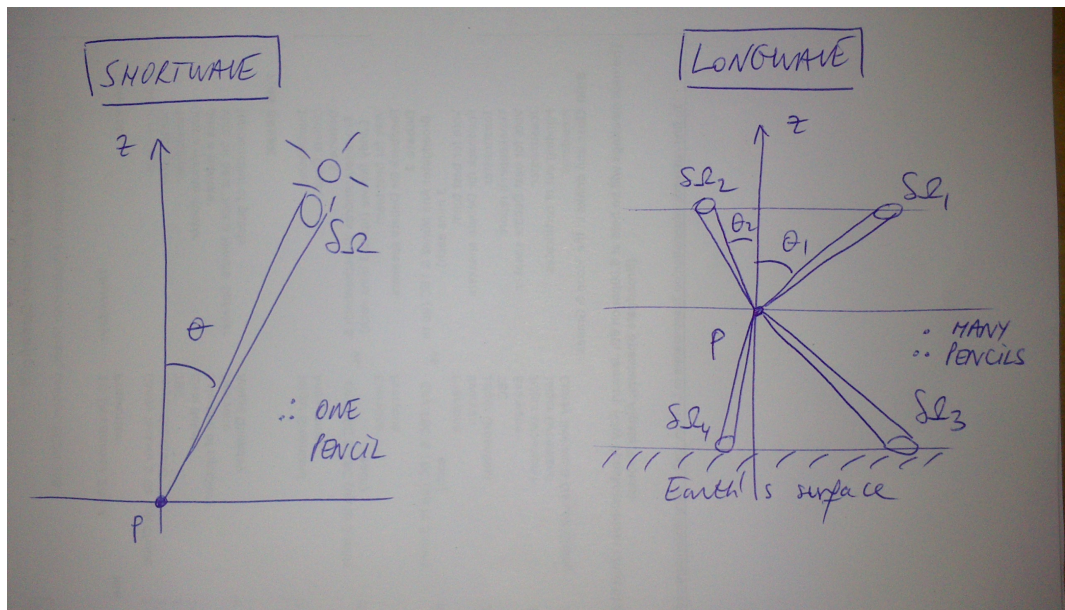


Figure 2.13: Schematic of the “radiation pencils” to be considered when computing irradiances at point  $P$  for the shortwave (left) and longwave (right) part of the spectrum. In absence of scattering, only one radiation pencil (the one covering the small solid angle  $\delta\Omega$  subtended by the Sun) would need to be considered for the shortwave part of the spectrum –but many need to be taken into account for infrared radiation. The distance  $ds$  along a path making an angle  $\theta$  with the vertical is related to  $dz$  by  $ds = dz / \cos\theta$ , hence the factor  $1 / \cos\theta$  in the calculations in this section.

The total upward irradiance at  $z$  is then,

$$F_{\lambda}^{\uparrow}(z) \approx \pi B_{\lambda}(T_s) e^{-1.66\tau(z)} + F_{\lambda,lay}^{\uparrow}(z) \quad (2.48)$$

where the second term on the r.h.s is the contribution of the atmospheric lower hemisphere (or layer), to the irradiance. Let's see how we would estimate it if we were climate modellers, equipped with a (fast) computer. For a given direction, i.e. a given slanted path, we would calculate the integral term on the r.h.s of (2.44). Because of the plane parallel approximation, the result will not depend on the azimuthal direction, but only on  $z$  and  $\theta$ . Writing it as  $\Phi^{\uparrow}(z, \theta)$ ,

$$\Phi^{\uparrow}(z, \theta) \equiv \int_0^{\tau(z)/\cos\theta} B(\tau') e^{\tau'} d\tau' \quad (2.49)$$

where  $\tau'$  measures the optical depth along the slanted path, the contribution of the atmospheric layer to the total irradiance would then be,

$$F_{\lambda,lay}^{\uparrow}(z) = 2\pi \int_0^1 \Phi^{\uparrow}(z, \mu) e^{-\tau(z)/\mu} \mu d\mu. \quad (2.50)$$

### Downward irradiance

Because of the negligible amount of photons emitted by the Sun at wavelength  $\geq 4\mu m$ , the “surface term” for downward infrared radiation can be set to zero. Hence the downward irradiance at a height  $z$  only reflects the emission from the atmospheric column sandwiched between the “top-of-the-atmosphere” and  $z$ . The result would thus simply be the analog of (2.50) for downward rather than upward integration. We can simply use the previous result and write,

$$F_{\lambda}^{\downarrow}(z) = F_{\lambda,lay}^{\downarrow}(z) = 2\pi \int_0^1 \Phi^{\downarrow}(z, \mu) e^{-\tau(z)/\mu} \mu d\mu. \quad (2.51)$$

in which  $\tau(z) = \tau_{\lambda}(TOA, z)$  is now the optical depth measured downward from the “top-of-the-atmosphere”.

An illustration of the calculation is provided using the result in section 2.5.2 for an isothermal atmosphere at  $T = T_o$ . Based on this the result, the downward irradiance is,

$$F_{\lambda}^{\downarrow}(z) = 2\pi \int_0^1 B_{\lambda}(T_o) (1 - e^{-\tau_{\lambda}(z)/\mu}) \mu d\mu \approx \pi B_{\lambda}(T_o) (1 - e^{-1.66\tau_{\lambda}(z)}). \quad (2.52)$$

The contribution of this irradiance to the heating rate can then be estimated from (2.36) and an illustration is provided in Fig. 2.14 for an idealised water

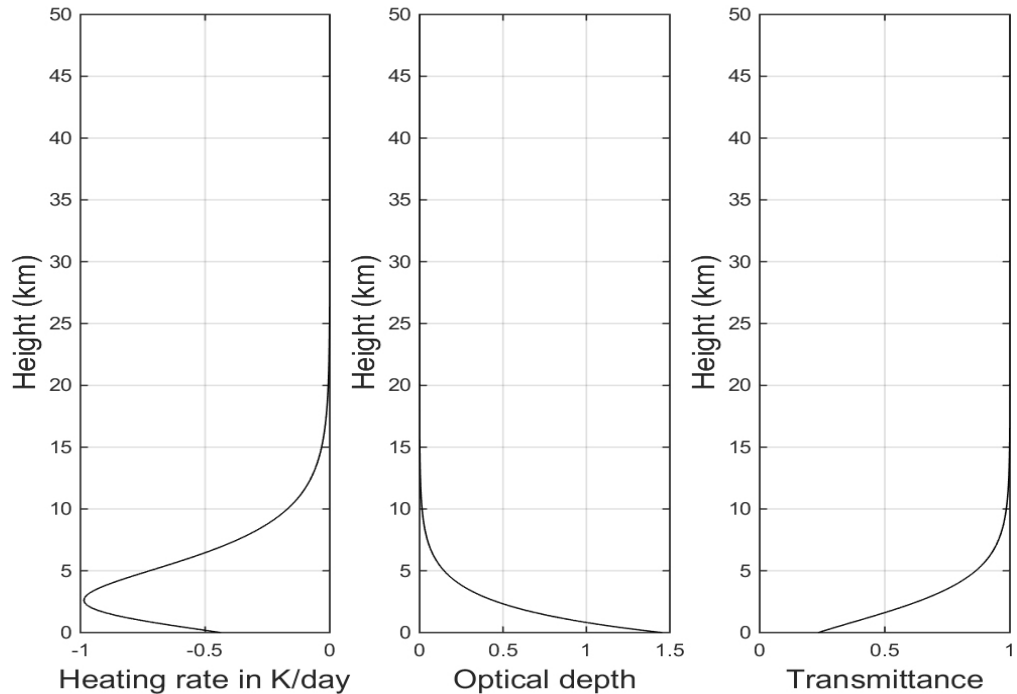


Figure 2.14: A simple calculation of radiative cooling due to water vapour for an isothermal atmosphere at  $T = T_o = 255K$ . The specific humidity is taken as  $q_a = 0.005e^{-z/3km}$  and the background density is taken as  $\rho = 1.2e^{-z/8km}$ . An extinction coefficient  $k_\lambda = 0.03m^2/kg$  was used over the  $5\mu m \leq \lambda \leq 50\mu m$ . The heating rate (integrated over  $\lambda$ , in  $K/day$ ) is displayed as a function of height, as are the optical depth and associated transmissivity. The Matlab code is available on Blackboard.

vapour profile (i.e., the calculation assumes an exponential  $q_a$  and a broad range of wavenumbers –see caption). A mid-tropospheric peak in cooling is predicted, with a magnitude on the order of  $1K/day$ . The formula can also be applied for a “ $CO_2$  case” by making the mixing ratio  $q_a$  uniform as a function of height, by narrowing the range of wavenumbers and increasing the opacity in that range. As seen in Fig. 2.15, the peak of cooling now moves upward, with very little cooling below  $5km$  (this is because the irradiance is “saturated” at these levels and so does not vary with height).

Realistic numerical calculations of upward (red), downward (blue) and the net (upward-downward, green) are shown in Fig. 2.16. These were carried out for typical summertime conditions over the Northern Hemisphere (only three infrared absorbers were included, water vapour, carbon dioxide and

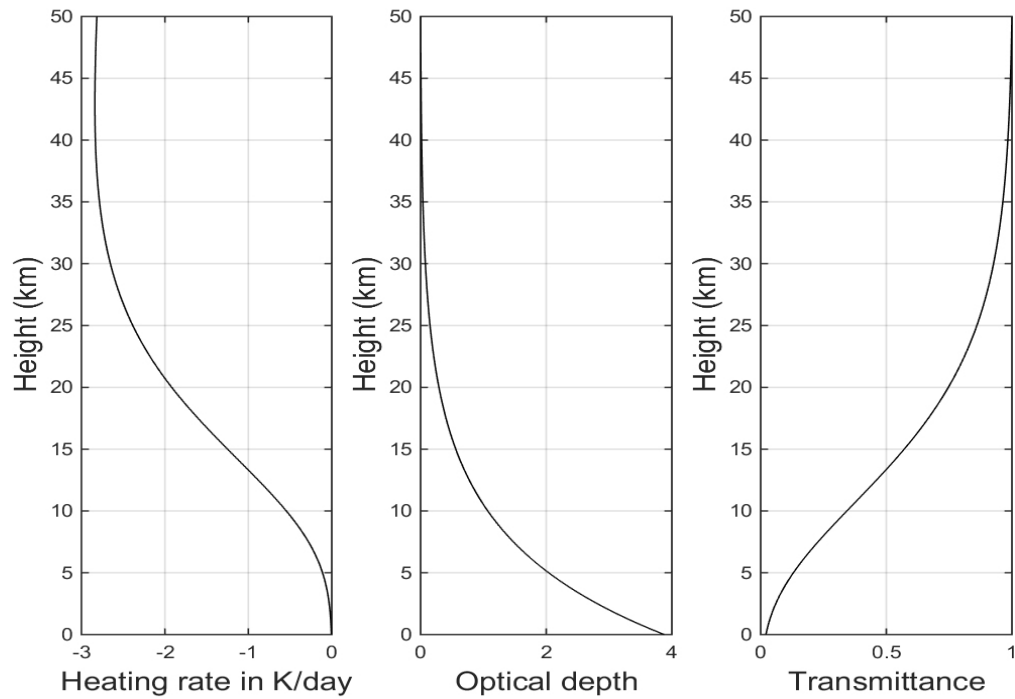


Figure 2.15: Same as Fig. 2.14 but for an idealised  $CO_2$  case. The mixing ratio is now taken as  $q_a = 400ppm$  and an extinction coefficient  $k_\lambda = 1m^2/kg$  was used over the  $12.5\mu m \leq \lambda \leq 17.5\mu m$ . The heating rate (integrated over  $\lambda$ , in  $K/day$ ) is displayed as a function of height, as are the optical depth and associated transmissivity. The Matlab code is available on Blackboard.

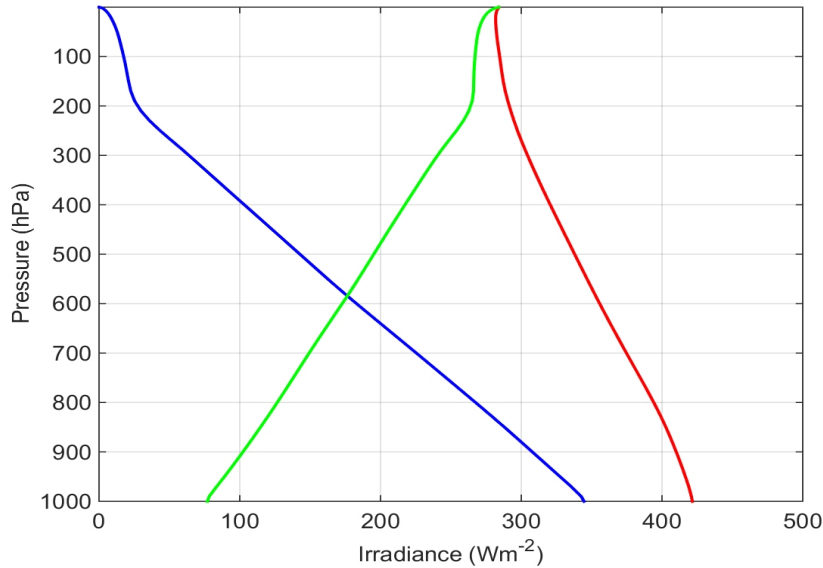


Figure 2.16: Calculations of upward (red), downward (blue) and net (green) irradiances for summertime conditions in the Northern Hemisphere. Courtesy of Wenyi Zhong and Jo Haigh from the SPAT group. The data and the Matlab code used to generate the plot are available on Blackboard.

ozone). Note that the irradiances are integrated over all wavelengths and are displayed as a function of pressure. The general shape is that of decreasing intensity as one goes up in the atmosphere for the upward irradiance: the upward infrared radiation is absorbed in the atmosphere and is re-emitted less strongly at upper (lower temperature, lower number density) than at low levels (high temperature, high number density). Conversely, the general shape for the downward irradiance is that of increase as one goes to lower levels: downward infrared is more effectively emitted at low levels where the temperature and the number density are higher.

### Heating rate

The net heating rates will reflect the competition between heating due to absorption of the radiation emitted by other atmospheric layers and the ground, and the cooling due to the emission of longwave radiation. Detailed calculations of the resulting heating rates, integrated over wavelengths, are shown in Fig. 2.12 (left panel). The first thing to note is that, except for  $O_3$  near  $25\text{km}$ , longwave heating rates are negative, on the order of several  $K/day$ . Infrared radiation thus cools the atmosphere globally, which opposes the heating due

to absorption of shortwave radiation (previous subsection). Inspection of Fig. 2.16 suggests that the cooling reflects the fact that downward irradiance (blue curve) diverges more (i.e., cools atmospheric layers) than upward irradiance (red curve) converges (i.e., heats atmospheric layers).

The primary reason why net cooling is found in the infrared is that the radiation that a given atmospheric layer exchanges with the ground and other layers tend to cancel out, but there is no cancellation when it comes to exchange of radiation with Space. Restating the arguments first put forward in Chapter 1 (Fig. 1.7), a given atmospheric layer emits upwards and downwards towards layers above and below, but it also receives radiation from them. Likewise, it emits towards the Earth's surface but also receives upwards radiation from the Earth's surface. Each of these exchanges approximately cancel out. In addition, the atmospheric layer in question also emits infrared radiation to Space but it does not receive such radiation in return. Hence a net cooling is expected, the so-called "cooling to Space" approximation (clearly visible in Fig.2.16 as the increase of the green curve towards lower pressure). As Fig. 2.12 shows, this is mostly due to water vapour in the troposphere, and carbon dioxide in the stratosphere and the mesosphere.

### 2.6.3 Net radiative heating rates

The compensation between infrared cooling and shortwave heating is imperfect in the troposphere, where a net cooling of about  $1K/day$  is suggested in Fig. 2.12. This is expected since the troposphere receives energy from the oceans and the land (heat and moisture exchange). Likewise in the mesosphere (height above  $\approx 50km$  in Fig. 2.12) a net radiative heating is suggested (this is opposed by molecular diffusion of heat upward at these levels—the density of air is so small there that molecular diffusion becomes a major player in the heat budget). In the stratosphere however the compensation between infrared cooling and shortwave heating is good: the stratosphere is close to a radiative equilibrium.

One way to visualize this competition is proposed in Fig. 2.17. In the right panel is shown the downward net shortwave flux: largest at the TOA and decreasing slightly towards the Earth's surface as a result of absorption by atmospheric gases, aerosols and clouds. On the left panel is shown the net longwave flux, which is upward at all levels: at the TOA it must be nearly equal in length to the solar flux since the Earth is approximately in radiative balance. At the surface its length must be less than the downward solar flux since the Earth's surface itself is in equilibrium and cools by surface evaporation and heat transfer, in addition to emitting infrared radiation. At a given level, the air cools through radiative exchanges in the infrared (the

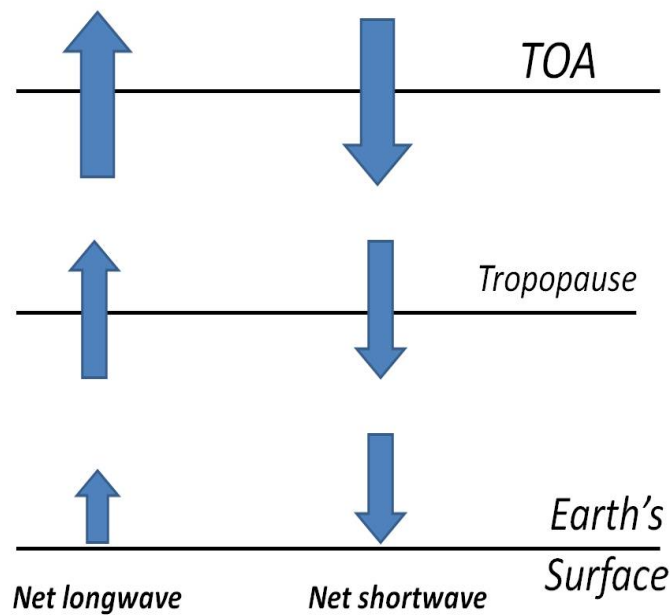


Figure 2.17: Schematic of the compensation between longwave cooling and shortwave heating. The arrows represent the net fluxes, i.e., the sum of upward and downward radiative fluxes in each frequency band. The fluxes are shown at the top-of-the-atmosphere (TOA), the tropopause and the Earth's surface. For the magnitude of arrows shown, the portion of air above the tropopause is in radiative equilibrium while the troposphere cools in the net. This is a good approximation for the troposphere-stratosphere system. See text for explanations.

upward arrows diverge in the direction of propagation) and heats up through radiative exchanges in the shortwave (the downward arrows converge in the direction of propagation).

## 2.7 Problems

**Q1** Calculate the ratio of the solar radiation incident on northward and southward facing slopes (i.e., the latter faces the Sun in the Northern Hemisphere), each angled  $\alpha = 20^\circ$  to the horizontal, if the solar zenith angle  $\theta_S$  (the angle between the vertical and the line of sight to the Sun) is: (i)  $30^\circ$  (ii)  $60^\circ$ . See Fig. 2.18 for a schematic.

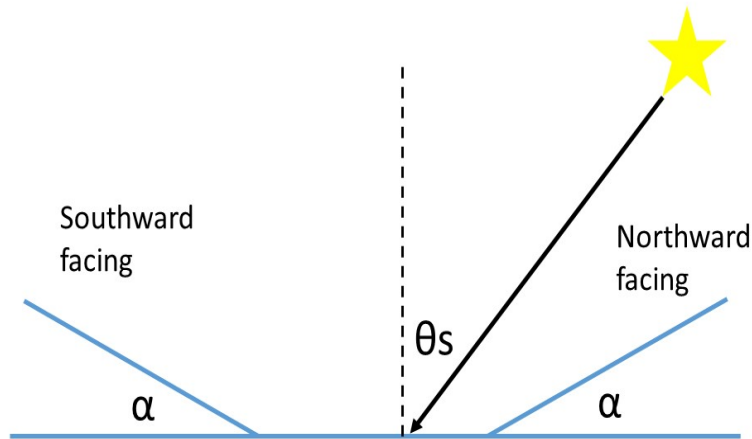


Figure 2.18: Geometry for Q1.

**Q2** Calculate the intensity  $I$  of solar radiation at the top-of-the-atmosphere (TOA), given the irradiance  $F = 1361 \text{ W m}^{-2}$  at zero zenith angle. The radius of the Sun is  $R_s = 7 \times 10^8 \text{ m}$  while the Earth-Sun distance is  $d = 1.5 \times 10^{11} \text{ m}$ .

**Q3** Consider monochromatic radiation passing through a gas with absorption coefficient  $\beta_\lambda = 0.01 \text{ m}^2 \text{ kg}^{-1}$ . (i) What fraction of the beam is absorbed in passing through a layer containing  $1 \text{ kg m}^{-2}$  of the gas? (ii) What mass per unit area would the gas layer have to have in order to absorb half the incident radiation?

**Q4** Suppose the gas in the previous question is present with uniform mass mixing ratio  $q = 10^{-3}$  in an atmosphere in hydrostatic equilibrium. Take surface pressure to be  $P_s = 1000 \text{ hPa}$ . (i) Show that the optical depth measured from the top of the atmosphere is linearly proportional to pressure. What is the constant of proportionality? (ii) Estimate the pressure of the level that is one optical depth from the top of the atmosphere.

**Q5** Show that, for a beam of monochromatic solar radiation  $F_\lambda$  incident

vertically on an atmosphere in which the mixing ratio of the radiatively active gas is independent of height and the density decreases exponentially with height, the heating rate per unit volume is greatest at unit optical depth.

**Q6** Show that, for the situation in the previous question, the heating rate per unit mass is greatest near the top of the atmosphere.

**Q7** Now consider infrared radiation traveling upwards (optical depth measured from Earth's surface) in an atmosphere where the total optical depth at the wavelength of the radiation considered is  $\tau_\infty = 5$ . (i) What fraction of the monochromatic intensity emitted by the ground is absorbed in passing through the layer of atmosphere extending from optical depth 0.2 to 4.0? (ii) What fraction of the intensity emitted to space is emitted by the layer between 0.2 and 4.0 optical depth? You may assume the atmosphere to be isothermal for this part, and at the same temperature as the Earth's surface.

**Q8** Past exam question (2005, No 3).

- (i) Derive an expression for the emission (or effective) temperature of the Earth as a function of solar constant and albedo.
- (ii) Estimate numerically the sensitivity of the effective temperature to fluctuations in albedo. (Solar constant  $S_o = 1370 \text{ W m}^{-2}$ , planetary albedo  $\alpha_P = 0.3$  and Stefan-Boltzmann constant  $\sigma = 5.67 \times 10^{-8} \text{ W m}^{-2} \text{ K}^{-4}$ ).
- (iii) Over the last 10 years the global mean temperature has risen by about  $0.2^\circ \text{C}$ . If clouds have an albedo of 0.8 and the surface has an albedo of 0.1, what change in the cloud percentage cover could account for this temperature rise? State any assumption you make.
- (iv) If the transmissivity of clouds increased by 10 % but the cloud cover stayed the same what would the new equilibrium temperature be?
- (v) Why is the observed surface temperature larger than the effective temperature?
- (vi) In which direction must the observed net radiation at the surface be and why?

**Q9** Figure 2.19 shows an estimate of the flux of solar radiation impinging on the Earth (the solar constant  $S_o$ ). Show that it is in good agreement with a pen and paper prediction assuming only knowledge of the radius of the Sun

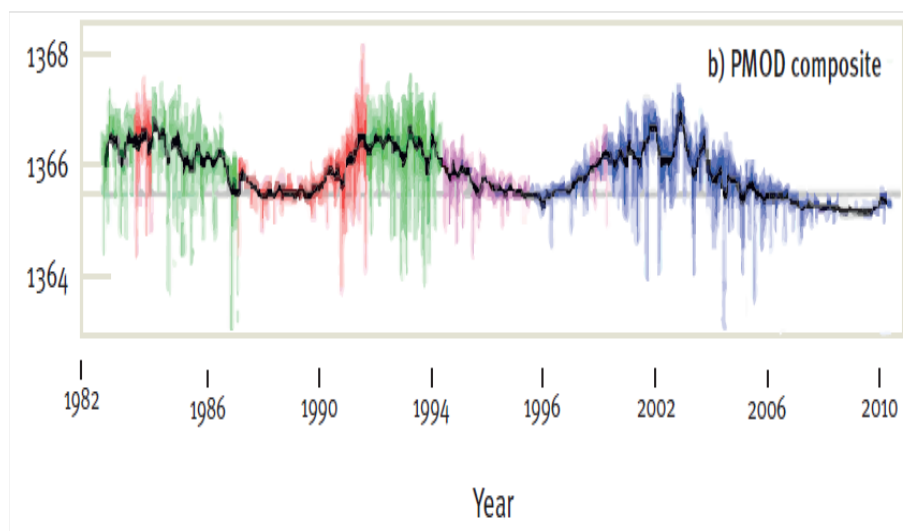


Figure 2.19: Composite measurement of the Solar “constant”  $S_o$  from Space through time (in  $Wm^{-2}$ ). From Joanna Haigh’s briefing paper published by the Grantham Institute for Climate Change at Imperial College in 2011.

$r_{sun} = 6.96 \times 10^8 m$ , the Sun’s emission temperature  $T_{sun} = 5780K$ , and the mean Earth-Sun distance  $d = 1AU = 1.5 \times 10^{11}m$ .

**Q10** A sunphotometer is an instrument designed to measure the optical thickness of the atmosphere due to scattering and absorption of solar radiation by air molecules and aerosols. At the ground, two measurements of the incident solar radiation at a wavelength  $\lambda = 1\mu m$ , denoted by  $I_\lambda$ , are made. These are made at two different solar zenith angles  $\theta_1 = 20^\circ$  and  $\theta_2 = 40^\circ$ .

- (i) Show that the ratio  $r_\lambda = (I_\lambda)_1 / (I_\lambda)_2$  of the two intensities satisfy,

$$\ln r_\lambda = \tau_\lambda (\sec \theta_2 - \sec \theta_1) \quad (2.53)$$

in which  $\tau_\lambda = \int_0^{+\infty} k_\lambda \rho q_a dz$  is the “column” optical depth.

- (ii) The ratio of the two intensity measurements is  $r_\lambda = 1.12$ . Compute the column’s optical depth using the data above, stating any assumptions made.



# Chapter 3

## Radiative-convective equilibrium

**Key concepts:** radiative equilibrium, fluid parcel, environment, buoyancy, Brunt-Vaisala frequency, radiative-convective equilibrium.

The preceding chapters showed that the atmosphere cools through (net) radiative processes (Chapter 2) and is heated from below through surface evaporation and sensible heat fluxes (Chapter 1). This situation destabilizes the atmosphere because, *at same pressure* warm air is lighter than cold air, and thus rises, while cold air sinks. The effect is to generate a convective cell which restores the equilibrium by carrying heat upward. In this chapter we study simple models of this interaction between radiation (destabilizing) and convection (stabilizing).

### 3.1 Radiative equilibrium

Mathematically, the state of radiative equilibrium is such that the net radiative heating (i.e., the sum of shortwave and longwave parts) is zero at all heights. Using the result from Chapter 2, this reads,

$$Q_{rad} = \int_0^{+\infty} Q_{\lambda} d\lambda = \frac{d}{dz} \int_0^{+\infty} (F_{\lambda}^{\downarrow} - F_{\lambda}^{\uparrow}) d\lambda = 0 \quad (\text{for all } z) \quad (3.1)$$

Since the longwave emission depends on temperature, there must be a particular choice of this variable allowing (3.1) to be satisfied. It is referred to as the “radiative equilibrium” temperature.

Figure 3.1 (left panel) provides an example of a radiative equilibrium temperature calculation. The input for such calculation is the distribution

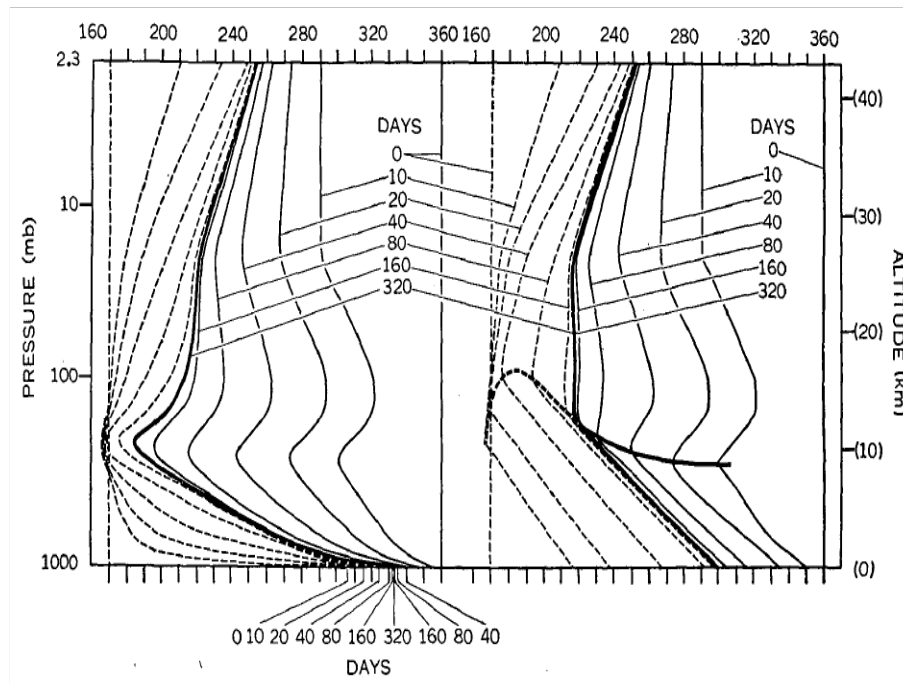


Figure 3.1: Approach to radiative (left) and radiative-convective (right) equilibrium in a time dependent calculation (Manabe and Strickler, 1964). Each curve represents temperature ( $x$ -axis) vs pressure ( $y$ -axis). Dashed curves refer to a cold start while continuous lines refer to a warm start. The thick lines indicate the equilibrium temperature profile in each case. In the right panel, they also locate the region of minimum temperature, the model's "tropopause".

of radiatively active constituents as a function of height, and the incident solar radiation at the TOA. (note that in this example, clouds were omitted and water vapour as well as ozone and carbon dioxide distributions were specified). When starting for example from a cold isothermal state at  $T = 160K$  (dashed lines), one observes a systematic warming at all levels as time increases, reaching a steady state after about 300 days (thick continuous curve). This warming is pronounced near the surface and at upper levels. Note that the same equilibrium is reached if one starts from a warm state  $T = 360K$  (continuous lines).

What happens in these experiments is that the shortwave part of the heating rate is essentially fixed (it does not depend on temperature). The longwave cooling, however strongly depends on temperature through Schwarzschild's equation (Chapter 2). In the cold start for example, a given layer of air does not emit enough longwave radiation to offset the shortwave heat gain and,

as a result, it warms. By warming up, it emits more in the infrared (the blackbody radiation term in Schwarzschild's equation) and so the net warming decreases. When the equilibrium temperature is reached, the layer cools as much by infrared than it gains heat from shortwave absorption. No further temperature change can arise.

An interesting feature of Fig. 3.1 is that it displays the time evolution of the temperature profile. Whether starting from a cold or a warm state, it takes several months to reach the final equilibrium temperature profile. This suggests that atmospheric motions such as weather disturbances, convective cloud systems, and others, can be considered as adiabatic since their timescale is much shorter than a few months.

## 3.2 Convection

If we were to perturb slightly the radiative temperature equilibrium, say by allowing a small upward velocity at low level, and wait long enough, would the same temperature profile be found? In other words, is the radiative temperature equilibrium stable to “dynamical” as opposed to thermal changes?

Unfortunately, the answer is a clear no, and this is the main reason why weather and climate predictions are difficult to make! The radiative temperature profile is not stable to displacements of the layers: convective motion will develop and change the final temperature. We first study the basics of this instability and return to the problem of the radiative temperature equilibrium later in the chapter.

### 3.2.1 The “parcel’s equation”

The key concept to understand convection is that of buoyancy whom you might remember from Archimede’s principle. In Atmospheric sciences this concept is tied to that of an air parcel, a small enough sample of air that it describes locally what happens in the atmosphere, but made of a large enough number of molecules that we can apply thermodynamics to it.

Consider such parcel initially at a reference height  $z_o$  in the atmosphere. We ignore horizontal variations. From Newton’s second law, the motion of the parcel obeys,

$$\frac{dw_p}{dt} = \sum_i F_i \quad (3.2)$$

where  $F_i$  refers to any force per unit mass acting on the parcel of upward velocity  $w_p$ . The forces in question here are simple gravity and the pressure

gradient force,

$$\frac{dw_p}{dt} = -g - \alpha_p \frac{dP}{dz} \quad (3.3)$$

in which  $\alpha_p$  is the volume per unit mass (or specific volume) of the parcel and  $P$  is the pressure. We wish to establish whether, once displaced initially, the parcel will come back to  $z_o$  (stable case) or move away from it (unstable case).

We will carry out a thorough investigation of all the forces acting on a parcel of air in chapter 4 (including Coriolis and centrifugal forces, as well as transport of momentum by the flow). As it turns out, the approximation (3.3) will be shown to be accurate.

The key concept to answer this question is that of the “environment”, i.e., the atmosphere before we displaced the parcel. In the question at hand (stability of the radiative equilibrium state), the environment is simply a state of rest (no motion) with the temperature equal to the radiative equilibrium temperature. The environment (subscript  $e$ ) thus satisfies,

$$0 = -g - \alpha_e \frac{dP_e}{dz} \quad (3.4)$$

Note that this equilibrium is the “hydrostatic balance” (1.8) introduced in Chapter 1.

To make further predictions regarding the parcel’s fate, we will make two assumptions:

- (i) the pressure field is not modified by the parcel’s motion, so the  $P$  in (3.3) and in (3.4) are equal
- (ii) the parcel does not acquire any heat as it moves (consistent with the short timescale of this process compared to radiative processes, see Fig. 3.1) and the ascent does not involve irreversibilities such as mixing with surrounding air, friction, etc. As a result the entropy of the parcel is conserved during the ascent (second law of Thermodynamics).

As a result of (i), we can rewrite (3.3) as,

$$\frac{dw_p}{dt} = g \frac{(\alpha_p - \alpha_e)}{\alpha_e} \quad (3.5)$$

This equation shows that if the specific volume of the parcel is greater than that of the environment, the parcel will exhibit upward acceleration ( $dw_p/dt > 0$ ). Likewise, if the parcel has a smaller specific volume than the

environment, it will be accelerated downwards. The r.h.s in (3.5) is called the buoyancy force  $B$ ,

$$B = g \frac{(\alpha_p - \alpha_e)}{\alpha_e} \quad (3.6)$$

### 3.2.2 Potential temperature

Up to now the derivation has been fairly general. We restrict from now on the discussion to the case of dry air so that the pressure  $P = P_d$  and the equation of state for the parcel is simply the ideal gas law  $P_d \alpha_d = R_d T$  (see Chapter 1). This allows to rewrite (3.5) as<sup>1</sup>,

$$\frac{dw_P}{dt} = -g \frac{(T_e - T_p)}{T_e} \quad (3.7)$$

The goal of this subsection is to introduce a quantity called “potential temperature”, which is going to allow us to solve (3.7) by using the second assumption above (isentropic ascent).

Potential temperature is simply meteorologist’s jargon for entropy. The concept is best illustrated with the following calculation. Consider an air parcel at upper levels where its temperature is  $T$  and its pressure is  $P$ . Suppose we bring this parcel adiabatically to the surface where the pressure is  $P_{ref} = 1000hPa$ . What would be its new temperature? We’ll call the latter potential temperature, with the variable  $\theta$ , to express that it is the temperature an air parcel at  $T, P$  would have if it were brought adiabatically to the surface.

To find a formula for  $\theta$ , use that in an adiabatic process, entropy is conserved. For dry air, this reads,

$$c_{p,d} dT/T - R_d dP/P = 0 \quad (3.8)$$

since the specific entropy of dry air is  $s_d = c_{p,d} \ln T - R_d \ln P$  (in this expression  $c_{p,d}$  is the specific heat capacity at constant pressure). This can be integrated from  $P$  to  $P_{ref}$  and  $T$  to  $\theta$ ,

$$\int_{\theta}^T dT/T = \frac{R_d}{c_{p,d}} \int_{P_{ref}}^P dP/P, \quad (3.9)$$

---

<sup>1</sup>In doing so one must neglect the difference between the pressure of the parcel ( $P_p$ ) and that ( $P_e$ ) of the environment: otherwise the ratio of specific volumes  $\alpha_p/\alpha_e$  would include a term  $P_p/P_e$ . It can be shown that this is valid as long as the velocity of the parcel is less than the speed of sound, which is valid for the atmospheric applications considered here (i.e.,  $P_p \approx P_e$  for the motions considered in this course).

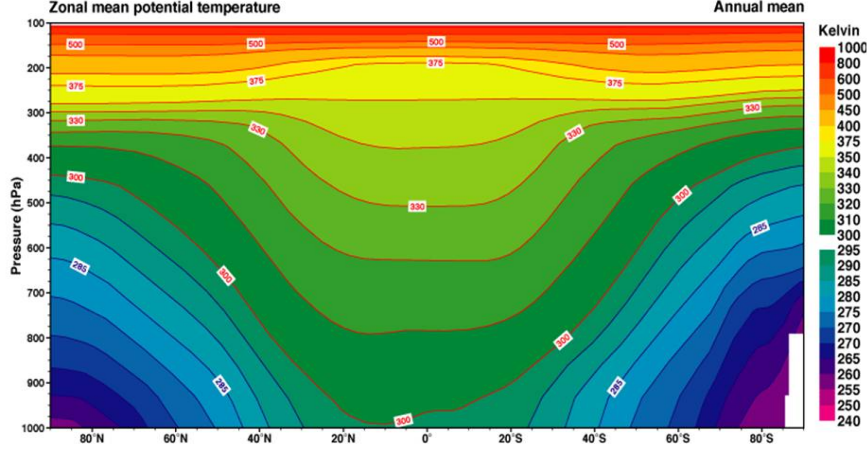


Figure 3.2: Annual and zonal mean distribution of potential temperature  $\theta$  as a function of latitude and pressure. Figure obtained from the on-line ERA40 Atlas.

leading to

$$\theta = T \left( \frac{P}{P_{ref}} \right)^{-R_d/c_{p,d}} \quad (\text{potential temperature}) \quad (3.10)$$

For a parcel initially near the tropopause with  $P = 250hPa, T = 210K$ , we find  $\theta = 312K!!$  So although it is true that the in-situ temperature high up above our head is colder, bringing these parcels to us would raise their temperature tremendously because of the work of compression they would experience during the adiabatic descent.

Figure 3.2 illustrates the zonal mean (i.e., averaging along a latitude circle) and time mean distribution of  $\theta$ . Stratospheric air is seen as the region of the atmosphere where  $\theta$  is very high ( $\theta \approx 500K$ ), that is very buoyant. The downward doming of  $\theta$  surfaces near low latitudes reflect, at a given pressure level, the higher temperature in these regions compared to higher latitudes.

### 3.2.3 Stability of temperature profiles to vertical displacements of air parcels

Replacing  $T$  in (3.7) by  $\theta$  (note that the pressure terms cancel), we obtain,

$$\frac{dw_P}{dt} = -g \frac{(\theta_e - \theta_p)}{\theta_e} \quad (3.11)$$

At first sight, not much is gained. Upon reflection though we see that we have replaced  $T$ , a non conserved variable during the ascent, by  $\theta$  which is conserved (you can easily check that  $ds = 0$  implies  $d\theta = 0$ ). In particular, if we start the parcel at  $z_o$  with the same temperature as the environment,  $\theta_p(z_o) = \theta_e(z_o)$  while at  $z$ ,  $\theta_e(z) = \theta_e(z_o) + d\theta_e/dz(z - z_o)$ . This shows that, since the parcel conserves its entropy during the ascent, i.e.,  $\theta_p(z) = \theta_p(z_o)$ ,

$$\frac{d^2(z_p - z_o)}{dt^2} + \frac{g}{\theta_e} \frac{d\theta_e}{dz}(z_p - z_o) = 0 \quad (3.12)$$

in which we have used  $w_p = dz_p/dt$ ,  $z_p$  being the height of the parcel.

This equation shows that the fate of the parcel is governed by the sign of the quantity  $N^2$ , defined as,

$$N^2 \equiv \frac{g}{\theta_e} \frac{d\theta_e}{dz} \quad (\text{the Brunt-Vaisala frequency}) \quad (3.13)$$

When  $N^2 > 0$ , (3.12) is an harmonic oscillator with angular frequency  $N$ : the parcel undergoes stable oscillations around  $z = z_o$ . When  $N^2 < 0$ , the parcel displacement is unstable: if initially displaced upwards, it will keep going upwards, being constantly accelerated upwards by the buoyancy force (and likewise if initially displaced downwards, the parcel will keep accelerating downwards). The Brunt-Vaisala frequency is clearly a very important variable describing the atmosphere (see section 3.5).

A couple of important comments:

- (i) From Fig. 3.2 we see that the atmosphere has, in the mean,  $N^2 > 0$ . So it is stable to vertical displacements of air parcels.
- (ii) From the plot, one can estimate roughly that  $N = [(9.81/315) \times (330 - 300)/5km]^{1/2} \simeq 10^{-2} s^{-1}$ . This corresponds to a period of oscillation of about 10 minutes.
- (iii) The fact that the time mean and zonal mean picture has  $N^2 > 0$  does not mean that the atmosphere is always everywhere, and at all times, stable. Indeed the deep anvil clouds that one sometimes experiences on a summer day (Fig. 3.3) are the manifestation of a region of  $N^2 < 0$ . This arose because parcels at low levels increased their entropy tremendously through heating with the hot Earth's surface while, aloft, they cooled through infrared radiation. This state of affair generates high  $\theta_p$  at low levels and low  $\theta_e$  at upper level and thus a positive buoyancy for air parcels from (3.11). NB: clearly moisture effects must be invoked to discuss this aspect fully, and this is postponed to section 3.4.



Figure 3.3: An intense “anvil cloud”. Surface heating throughout the day increased the entropy of air parcels at low levels while infrared radiative cooling decreased that of air parcels at upper levels (this latter effect is admittedly weaker than the heating due to heat exchange with the Earth’s surface). Note that air parcels seem “stuck” at the top and spread laterally. This reflects that even though they acquire large buoyancy through surface heating, this buoyancy was still less than that of the environmental air at upper levels (the tropopause here). Thus in this example the spreading allows you to “see” the tropopause!

### 3.3 Radiative-convective equilibrium

#### 3.3.1 Stability of the radiative equilibrium temperature profile

We now return to Fig. 3.1 (left column) and the stability of the radiative temperature equilibrium. At the surface, the temperature is  $T \approx 330K$  with a pressure  $P = 1000hPa$ . Higher up, there is a minimum temperature of about  $180K$ , reached at a pressure  $\approx 300hPa$ . Application of (3.10) with  $P_{ref} = 1000hPa$  shows that the surface potential temperature is  $330K$  while at  $300hPa$  it is  $\approx 254K$ . Hence  $\theta$  decreases with height ( $N^2 < 0$ ) and the radiative equilibrium temperature profile is unstable!

What this says is that radiative processes destabilize the atmosphere and that consideration of radiation only cannot provide a realistic prediction for the temperature structure of the atmosphere. The right panel in Fig. 3.1 is an attempt to represent the effect of convection, by bringing artificially the atmosphere into a state with  $N^2 = 0$  (i.e., neutral to vertical displacements of air parcels –see section 3.4.2 below). Independently of the type of convective parameterization used, we will refer to this state as one of radiative-convective equilibrium.

The radiative - convective equilibrium state has a weaker change of temperature with height, i.e., a weaker “lapse-rate”  $\Gamma$  in the right compared to the left panel,

$$\Gamma \equiv -\frac{dT}{dz} \quad (\text{definition of lapse-rate}) \quad (3.14)$$

It also has colder surface temperature (about  $290K$ ), and higher temperature aloft. This reflects that by carrying high  $\theta$  parcels upwards and replacing them by cold  $\theta$  parcels going downward, convection carries heat upward. Denoting the associated heating rate per unit volume as  $Q_{conv}$ , we extend the mathematical definition of radiative equilibrium definition in eq. (3.1) to that of radiative-convective equilibrium:

$$Q_{rad} + Q_{conv} = 0 \quad (\text{“Radiative-convective” equilibrium}) \quad (3.15)$$

#### 3.3.2 The Tropopause

An interesting feature in Fig. 3.1 is the presence of a clear discontinuity in the lapse-rate (from being positive to negative) around  $300hPa$ . This discontinuity is very pronounced in the radiative equilibrium (left panel), with a sharp transition between the lower ( $\Gamma > 0$ ) and upper atmosphere ( $\Gamma < 0$ ). In the radiative - convective equilibrium state, the discontinuity

is still seen, but is less pronounced, the layer between 10 and 25km being nearly isothermal ( $\Gamma \approx 0$ ).

Returning to Chapter 1 (Fig. 1.4), we identify this discontinuity in lapse rate as the tropopause. The previous paragraph makes it clear that it arises primarily as a result of radiative constraints: the absence of significant absorption of solar radiation below about 10km leads, in pure radiative equilibrium, to a region of positive lapse-rate (see the simple calculations in Q4 below). Conversely, in a region where there is absorption of solar radiation, pure radiative equilibrium leads to negative lapse-rate (so that this region can cool by emitting more infrared radiation at its top than at its bottom). The “dynamics” (convective adjustment here) merely modulates the exact value of the height at which this transition happens.

Returning to Fig. 3.1, the fact that the two temperature profiles (left and right panels) differ below the tropopause is expected from the fact that the radiative calculation has  $N^2 < 0$  there. Above the tropopause, the radiative equilibrium temperature is very stable (a region of  $\Gamma < 0$  has a very large  $N^2$ ), so no instability is expected and the difference between the two temperature profiles is more surprising. What we are seeing in action here is the interaction of convection with radiation: changing the tropospheric temperature through convection affects the upward infrared radiation reaching the stratosphere, and thus perturbs radiative heating rates in this region. The calculation shows that above  $\approx 25km$  this effect becomes negligible and the radiative and radiative-convective equilibrium temperature profiles are the same.

## 3.4 Dynamical effects of moisture<sup>\*</sup>

### 3.4.1 Dry and moist adiabatic lapse-rates

We have managed to get a long way by simply considering the buoyancy of dry air. However, as a buoyant air parcel rises, its internal energy (temperature) decreases because of the work of expansion done by the parcel on the surrounding air. As a result, phase change can occur. As we shall see, the latent heat released at this stage increases significantly the buoyancy of the parcel. Thus, in addition to important radiative effects, moisture also plays a key role in the dynamics.

To isolate clearly this role we are going to consider the case of cloudy, as opposed to pure dry, air. We will restrict ourselves to a mixture of dry air, water vapour and liquid water, the two latter phases being in thermodynamic equilibrium. This means that the vapour pressure  $e$  is solely a function of

temperature, given by the Clausius-Clapeyron equation (Thermodynamics, year 2):

$$e = e_{eq}(T) \quad \text{with} \quad \left( \frac{de_{eq}}{dT} \right)_{p.b} = \frac{\Delta s}{\Delta \alpha} \quad (3.16)$$

Note that in this equation,  $\Delta$  refers to a change across the phase boundary (subscript *p.b*), i.e.,  $\Delta s = s_v - s_l = l_v/T$  ( $l_v$  being the latent heat of vaporization introduced in Chapter 1) and  $\Delta \alpha = \alpha_v - \alpha_l \approx \alpha_v$  (a given mass of water vapour occupies a much larger volume than the same mass of liquid water). So we can approximate it as,

$$\left( \frac{de_{eq}}{dT} \right)_{p.b} \approx \frac{l_v}{\alpha_v T} \quad (3.17)$$

Before proceeding, a few comments need to be made:

- The assumption that gas and liquid phases are in equilibrium is very important. This can occur at the core of a cloud but, in general, we must acknowledge that the two phases do not coexist in a state of equilibrium (net evaporation or net condensation occurs). So we are considering the effect of moisture in a very idealised case (cloudy air).
- The phase change occurring as a parcel ascends is adiabatic. What is said here is that latent heating is internal to the parcel. It is not heat taken from the environment, as occurs for example when a cold continental air mass flows over a warm ocean. So we can still assume that the parcel conserves its entropy during ascent.

The calculation below addresses the question: what is the lapse rate when the environment is neutral to vertical displacement of air parcels? That is, what is  $\Gamma$  when  $N^2 = 0$ . In such cases, the buoyancy experienced by the parcel is zero throughout its displacement –see (3.12)– so that  $\alpha_p = \alpha_e$ . Since the environment satisfies the hydrostatic balance itself  $\alpha_p \partial P / \partial z = -g$ , and since the pressure of parcels and environment are the same by assumption, this means that the parcel also satisfies the hydrostatic balance,

$$\alpha \frac{dP}{dz} = -g \quad (3.18)$$

(in this equation, and from now on, the subscript *p* has been dropped). To see how we can use this to predict the lapse-rate, let's first start with the dry case. For an adiabatic displacement,  $ds = 0$  leads to

$$c_{p,d} dT/T - R_d dP/P = 0 \quad (3.19)$$

After dividing by  $dz$  and using the ideal gas law and the hydrostatic balance, we obtain,

$$\Gamma_d = \frac{g}{c_{p,d}} \quad (\text{“dry adiabatic lapse - rate”}) \quad (3.20)$$

In the case of moist air, we accept the result that the entropy of cloudy air is approximately given by,

$$s = s_{ref} + c_{p,d} \ln(T/T_{ref}) - R_d \ln(P_d/P_{ref}) + \frac{l_v q_v}{T} \quad (3.21)$$

in which  $q_v$  (specific humidity) was introduced in chapter 1 (the appendix provides a derivation of this expression for  $s$  if you’re interested). Using again the hydrostatic equilibrium (being careful that now the  $P$  in the hydrostatic balance refers to the total pressure  $P = P_d + e$ ), applying  $ds = 0$  to this equation leads to<sup>2</sup>,

$$\left(1 + \frac{\alpha_d}{\alpha_v} \frac{l_v}{c_{p,d} T}\right) \frac{dT}{dz} = - \left(\frac{\alpha_d}{\alpha}\right) \frac{g}{c_{p,d}} - \frac{T}{c_{p,d}} \frac{d}{dz} (l_v q_v / T) \quad (3.22)$$

The first term on the r.h.s is similar to the case of dry air, the factor in parenthesis being close to unity. The second term on the r.h.s is new and clearly reflects the effect of phase change. In a realistic range of temperature, this term can be approximated as,

$$- \frac{T}{c_{p,d}} \frac{d}{dz} (l_v q_v / T) \approx - \frac{l_v}{c_{p,d}} \frac{dq_v}{dz} \quad (3.23)$$

Likewise, the second term in parenthesis on the l.h.s is small compared to unity so that,

$$\Gamma_m \approx \frac{g}{c_{p,d}} + \frac{l_v}{c_{p,d}} \frac{dq_v}{dz} \quad (\text{“moist adiabatic lapse - rate”}) \quad (3.24)$$

Because specific humidity decreases with height (water vapour condensing to liquid water in ascending air, liquid water evaporating in descending air), the second term on the r.h.s is negative so that the moist adiabatic lapse rate is weaker (typically  $6.5K/km$ ) than the dry adiabatic one. Physically, as a parcel rises and performs work against the environment, its temperature decreases. In the cloudy air case, the decrease is however not as pronounced as in the dry air case because of the release of latent heat during condensation.

---

<sup>2</sup>the Appendix provides a general derivation of  $N^2$  which shows that, even for cloudy air,  $N^2 = 0$  implies  $ds = 0$ .

### 3.4.2 Application of “dry and moist adiabats thinking”

#### Parameterisation of convective instability

In either the dry or moist case, the state of neutrality to vertical displacement of air parcels is one in which no energy can be extracted from the “environment”, i.e., air parcels cannot gain kinetic energy through the work of buoyancy forces (identically zero). This is what motivates the parameterisation of convection in Fig. 3.1 (right panel): radiation generates an unstable temperature profile but convection uses rapidly the energy stored in that profile to generate motions so that there is never any “left over” energy available. Setting  $\Gamma$  to be equal to  $\Gamma_m$  in the calculation in Fig. 3.1 (right panel), and thus imposing  $N^2 = 0$  throughout the calculation, is a very powerful and simple way to represent this state of affair.

#### Conditional instability

The calculations above for a dry and a cloudy parcel are exact when the environment is neutral ( $N^2 = 0$ ). When  $N^2 \neq 0$ , they would have to be modified by replacing  $g$  by  $g\alpha_p/\alpha_e$ , since the parcel is now experiencing a buoyancy force<sup>3</sup>. This correction is small. For example, for dry air,  $\alpha_p/\alpha_e = \theta_p/\theta_e$  is at most  $300 \pm 10K/300K$ , i.e., a 3% error. Thus in practice, we can consider that the temperature lapse rate of a dry parcel during its adiabatic displacement follows approximately  $\Gamma_d$ . Likewise for a moist parcel and  $\Gamma_m$ . This is very useful, as the exemple below shows.

Consider the temperature profile in Fig. 3.4 (black), whose lapse rate  $\Gamma$  is somewhere in between dry and moist adiabats (i.e.,  $\Gamma_m \leq \Gamma \leq \Gamma_d$ ). If we were to lift an air parcel from the surface upward (for example as a result of a large scale convergence of air near the surface), would it continue to go up? Here we take into account moisture and do not assume that the parcel is already in equilibrium of phases (i.e., the relative humidity is less than unity at the surface).

Starting at the surface at A, we displace the parcel upward following a dry adiabat since no liquid water is yet present<sup>4</sup>. For the case shown, this displacement is stable since the temperature decreases faster with height along a dry adiabat (blue) than it does for the environment (black). Nevertheless,

<sup>3</sup>This is because we can only use  $\alpha_p \partial P / \partial z = -g$  when  $\alpha_p = \alpha_e$  since it is only the environment which is in hydrostatic balance when  $N^2 \neq 0$ .

<sup>4</sup>Some of you might rightly question the use of a dry adiabat for the isentropic ascent of a mixture of dry air and water vapour considered here. Doing the calculation properly would only change the lapse rate slightly but would require using an exotic quantity called “virtual potential temperature”. For simplicity I decided not to do this.

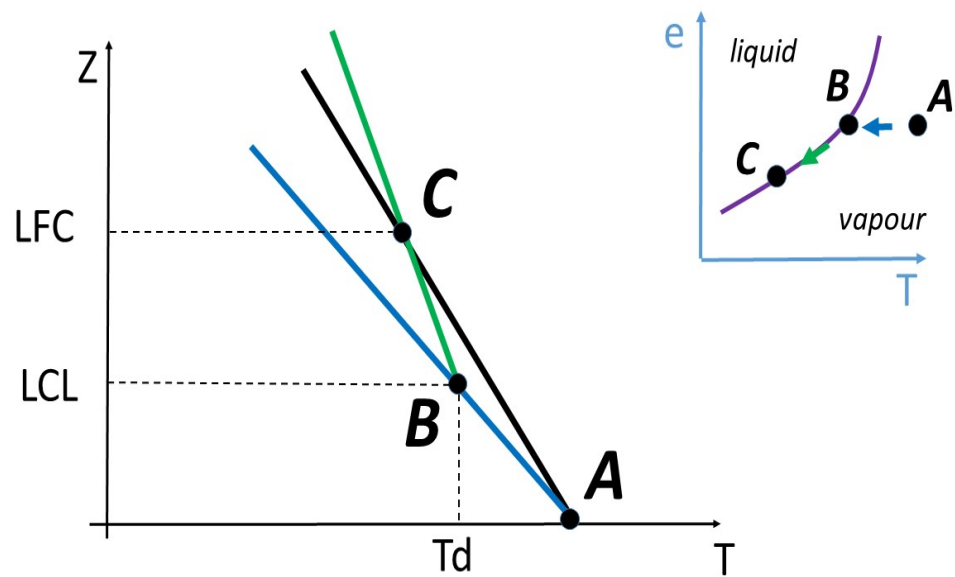


Figure 3.4: An idealized temperature profile (black) with dry (blue) and moist (green) adiabats superimposed. The LCL is the “lifting condensation level” where the temperature equals the dewpoint temperature (i.e., where the first drop of liquid water is produced by condensation). The LFC is the “level of free convection”, beyond which the parcel’s displacement would become unstable. In the lower panel, the trajectory of the sample is shown in the temperature ( $T$ ) - vapour partial pressure ( $e$ ) space. The displacement from  $A$  to  $B$  is on the vapour side of the phase diagram, and follows approximately a line of constant  $e$ . From then on, the displacement is along the phase boundary (purple curve).

at some point the temperature of the parcel has dropped enough that condensation occurs. This happens at a temperature  $T_d$  (dewpoint temperature) such that:

$$e_{eq}(T_d) = e \quad (3.25)$$

in which  $e_{eq}$  is the equilibrium vapor pressure (a function of temperature only, given by integration of the Clausius-Clapeyron equation –see eq. (3.16) in section 3.4.1) and  $e$  the vapor pressure in the sample. The level at which this occurs is called the “lifting condensation level” (point B in the figure). From this point onward our sample is in thermodynamic equilibrium of phases (i.e., the relative humidity is unity) so further adiabatic lifting will proceed along the moist adiabat (green curve). For the case shown, the parcel is still less buoyant than the surrounding from B to C, the latter being the point where the parcel’s temperature equals that of the environment. Thus the displacement is overall stable from A to C. Beyond C however, the displacement is unstable, since the parcel’s temperature exceeds that of the environment (and its pressure equals that of the environment).

In summary, if the parcel has enough kinetic energy when it starts at the surface, it could reach C at which point buoyancy forces will accelerate it further upward. This type of instability is called “conditional instability”. This situation occurs frequently in the atmosphere, and the LCL is readily identified as the cloud base. Deep convective clouds are those where enough energy was available at low levels to reach the LFC. We’ll return to these ideas in the lecture on clouds (powerpoint file on Blackboard).

### 3.5 Radiative-convective equilibrium and the real world

The main message from all the above is that there is a competition between radiative processes, which tend to destabilize the atmosphere, and dynamical processes, which tend to stabilize the atmosphere. The 1D case illustrated in Fig. 3.1 showed that radiation acts relatively slowly (it took several months to achieve radiative equilibrium on the left panel). Convection is expected to be much faster (a moderate updraft of  $10\text{cm/s}$  would reach the tropopause in typically  $10\text{km}/10\text{cms}^{-1} \approx 1\text{day}$ ). As a result, the prediction is that convection should dominate and we do not expect to observe unstable temperature profiles.

Figure 3.5 displays the observed ratio  $(\Gamma_m - \Gamma)/\Gamma_m$ . It is clearly seen that in the Tropics (equatorward of  $30^\circ$  of latitude), and above the near surface layer ( $P \leq 900\text{hPa}$ ), observed lapse rates are within 10 % of the moist adi-

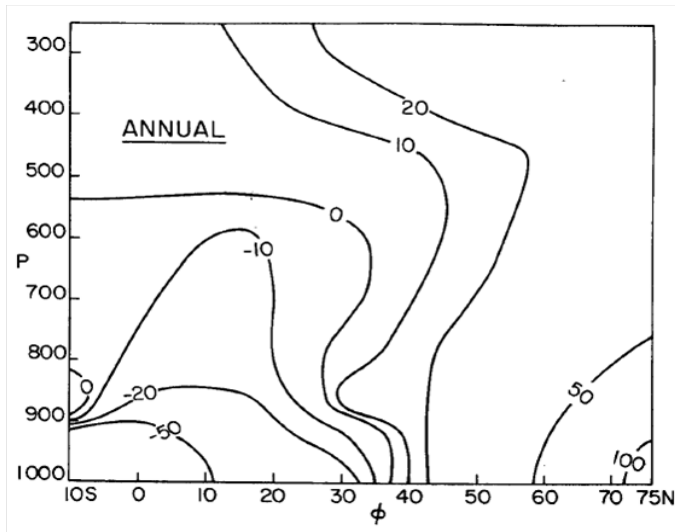


Figure 3.5: Observed tropospheric lapse rate, expressed as percentage of the moist adiabatic value (i.e.,  $(\Gamma_m - \Gamma)/\Gamma_m$ ). From Stone and Carlson (1979).

adiabatic value. (They are slightly greater than  $\Gamma_m$  below  $500hPa$  and slightly smaller above this level which reflects the curvature of the moist adiabats and the more linear temperature variations –see the ppt slide discussed in the lecture for this section). This is suggestive of a strong role of convective processes at low latitudes and has deep implications for a variety of problems. For example, it suggests that any change in surface temperature will be quickly felt throughout the atmosphere through adjustment to a new (warmer) moist adiabatic profile. This is indeed one of the prediction of the Intergovernmental Panel on Climate Change (IPCC) to which we will come back later in the course. Another interesting idea is that since observations suggest  $\Gamma \simeq \Gamma_m$  in the Tropics, this could be used to parameterize convection in climate models (these do not resolve individual clouds, and not even their aggregation into clusters), like was done in Fig. 3.1. This is what all climate models do...but you'll be surprised (interested?) to know that there is to present day no theory which explains why it should be so.

In mid and high latitudes, observed lapse rates are weaker than moist adiabatic values ( $\Gamma \leq \Gamma_m$ ), i.e., atmospheric motions stabilize radiative effects beyond what is expected from a consideration of their tropical counterparts. Thus in addition to the vertical convection discussed above, something else must be stabilizing the atmosphere. We all know this something else: the weather systems we experience daily at the latitude of England. We show next that these motions can also be thought of as resulting from a convective

instability, but with 3D motion of air parcels rather than 1D (purely vertical) being involved. We'll go deeper in their dynamics in Chapter 4.

## 3.6 Sloping convection

To explain why the observed lapse rates are significantly smaller than moist adiabatic in mid and high latitudes compared to low latitudes (Fig. 3.5), we start by looking at the distribution of potential temperature  $\theta$  (Fig. 3.2). The latter shows a striking distinction between the Tropics and higher latitudes. To within a few tens of degree of latitude off the equator,  $\theta$ -surfaces are nearly flat while they slope upward in the extra-tropics. This distribution reflects the presence of marked horizontal temperature gradients away from the equator (we will see in Chapter 4 that this difference in slopes of  $\theta$ -surfaces between low and high latitudes arises because of the effect of rotation on motions). By consideration of the energetics associated with parcels' displacements in the latitude-height plane, rather than purely in the vertical, we can get a sense as to why storms help to create larger values of  $N^2$  in midlatitudes. As it turns out the basic physics is well captured by ignoring the effect of moisture on buoyancy, so we will use the framework in section 3.2.2.

Starting from the "parcel's equation" (3.5) in the form,

$$\frac{dw_p}{dt} = g \frac{(\theta_p - \theta_e)}{\theta_e} \quad (3.26)$$

we can say something about displacements of air parcel's in the latitude-height plane (Fig. 3.6). For example, imagine swapping point  $A$  with either point  $B$ ,  $C$  or  $D$ . We note that:

- $A \leftrightarrow B$ : this is the situation discussed in section 3.2 when the Brunt-Vaisala frequency is positive ( $\theta$  increases upward,  $\theta(A) < \theta(B)$ ). Thus work would have to be done against the buoyancy force to achieve this displacement. This is a stable situation.
- $A \leftrightarrow C$ : this displacement is along a  $\theta$  surface so the parcels experience no buoyancy force ( $\theta_e = \theta_p$ ).
- $A \leftrightarrow D$ : this time  $\theta(A) > \theta(D)$  so the displacement would be unstable, i.e., the buoyancy force would do work on the parcels.
- $A \leftrightarrow E$ : again  $\theta(A) > \theta(E)$  but no work by the buoyancy force can be generated since the displacement is horizontal (i.e., at right angle to the force). This situation will thus not occur spontaneously.

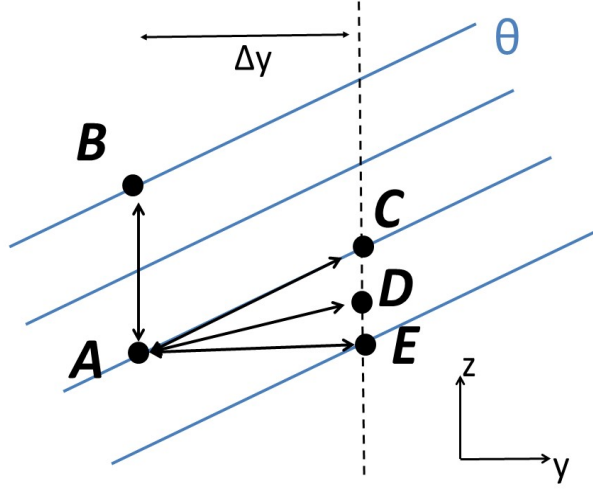


Figure 3.6: Sloping convection in the latitude ( $y$ ) - height ( $z$ ) plane. Kinetic energy can be gained in certain swapping of parcels while they conserve their potential temperature  $\theta$ .

This suggests that if the displacement of fluid parcels follows a sloping path shallower than the isentropic slope, kinetic energy can be gained in the process: an instability occurs.

*NB: the paths shown in Fig. 3.6 are imposed, and all we do is compute the work done by buoyancy forces for a given path. You can easily convince yourself that the work done must be path dependent (e.g., it is zero along A-C but  $> 0$  along A-E-C with same start and end points).*

The gain in kinetic energy after a time  $t$  has elapsed since the swap can be estimated from the parcel's equation, having in mind  $\theta_p = \theta(A)$ ,

$$\Delta \frac{1}{2} (w_p^2) = \int_0^t w_p \frac{dw_p}{dt} dt = \int_0^t g \frac{(\theta_p - \theta_e)}{\theta_e} w_p dt = \int_{z_A}^{z_D} g \frac{(\theta_p - \theta_e)}{\theta_e} dz \quad (3.27)$$

where the integral is along the slanted path  $A \leftrightarrow D$ . Define  $\Delta z = z_D - z_A$  and rewrite the integral as,

$$\Delta \frac{1}{2} (w_p^2) = g \Delta z \left\langle \frac{(\theta_p - \theta_e)}{\theta_e} \right\rangle \quad (3.28)$$

where the bracket  $\langle \rangle$  denotes an average along the path. Approximate the latter using a Taylor expansion, as,

$$\left\langle \frac{(\theta_p - \theta_e)}{\theta_e} \right\rangle \approx -\frac{1}{2} \left( \frac{\partial \theta}{\partial z} \Delta z + \frac{\partial \theta}{\partial y} \Delta y \right) / \theta_e \quad (3.29)$$

in which  $\Delta y = y(D) - y(A) > 0$  is the gain in latitude of the parcel and we have introduced the vertical ( $\partial\theta/\partial z > 0$ ) and meridional ( $\partial\theta/\partial y < 0$ ) temperature gradients. Note that the implicit assumption used here is that the parcel conserves its  $\theta$  from  $A$  to  $D$  ( $\theta_p - \theta_e = 0$  at  $A$  while  $\theta_e - \theta_p = \Delta z \partial\theta/\partial z + \Delta y \partial\theta/\partial y$  at  $D$ , hence the factor  $1/2$  and the negative sign). Inserting this result, and after introducing the slope of the displacement  $\mu = \Delta z/\Delta y$  and the isentropic slope  $\mu_\theta = -(\partial\theta/\partial y)/(\partial\theta/\partial z) > 0$ , we have,

$$\Delta \frac{1}{2} (w_p^2) \approx \frac{N^2(\Delta y)^2}{2} \mu(\mu_\theta - \mu) \quad (3.30)$$

For a fixed displacement  $\Delta y$ , we recover the discussion at the beginning of this section:

- $A \leftrightarrow B$ :  $\mu > \mu_\theta$  and the kinetic energy gained is negative!
- $A \leftrightarrow C$ :  $\mu = \mu_\theta$  and the kinetic energy gained is zero.
- $A \leftrightarrow E$ :  $\mu = 0$  and the kinetic energy gained is zero.
- $A \leftrightarrow D$ :  $0 < \mu < \mu_\theta$  and the kinetic energy gained is positive. The maximum possible kinetic energy gained is when  $\mu = \mu_\theta/2$ ,

$$KE_{max} = \frac{N^2(\Delta y)^2}{8} \mu_\theta^2 = \frac{g(\Delta y)^2}{8\theta_e} \left( \frac{\partial\theta}{\partial y} \right)^2 / \left( \frac{\partial\theta}{\partial z} \right) \quad (3.31)$$

Not all air parcels can go on average upward and poleward –otherwise mass would be continuously lost at low latitudes and low levels. So we should think of a swap: parcel  $A$  replacing parcel  $D$  and parcel  $D$  replacing parcel  $A$ . What would be the kinetic energy gained in the displacement  $D \rightarrow A$ ? This can be computed from the previous result by simply making the substitution  $\Delta y \rightarrow -\Delta y$  and  $\Delta z \rightarrow -\Delta z$ . As you can check, it yields the exact same result. This is really what happens in midlatitude weather systems, a swap of low  $\theta$ , low level, low latitude air with high  $\theta$ , high latitude, high level air. This takes the form of a wave, as schematized in Fig. 3.7. Interestingly, eq. (3.31) indicates that the larger the meridional scale of the swap ( $\Delta y$ ), the larger the kinetic energy released. So it is not a surprise that midlatitude storms are so big and span such a large range of latitudes (typically  $20^\circ - 60^\circ$ ).

The bottom line is that we can understand the extra-tropical storms in Fig. 1.5 (the “wavy bits”) in the same way as we understand their tropical counterparts (the “spotty bits”). They result from a convective instability, “sloped”, as opposed to vertical. The distortion of  $\theta$  surfaces brought about

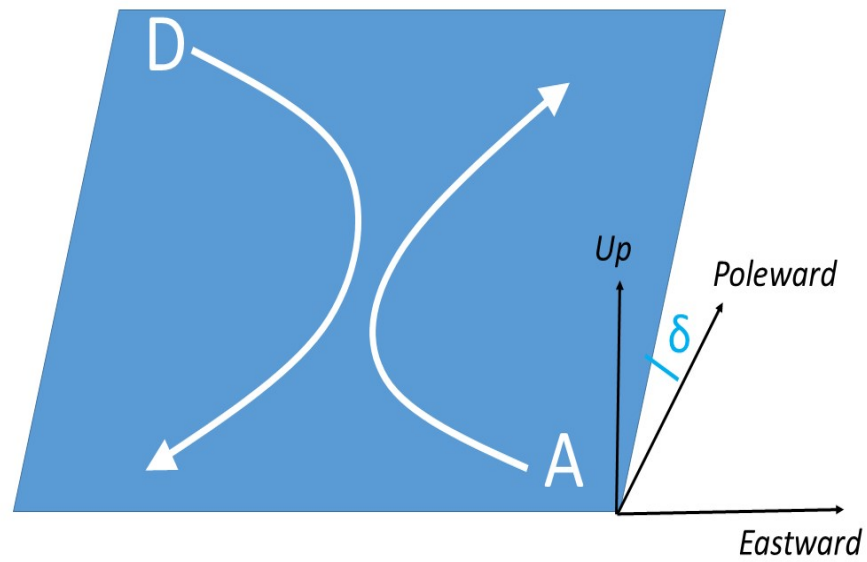


Figure 3.7: Schematic of an Eady wave, after the Imperial College physicist Eric Eady who came up with the simplest theory for weather systems in the 1950s. The swap of two air parcels in a plane making an angle  $\delta$  with the horizontal is shown. Eady reasoned that the wave could grow if  $\delta \approx \mu_\theta/2$ .

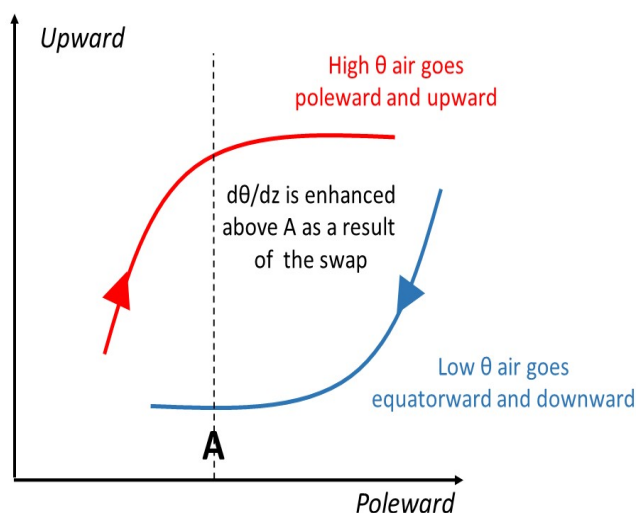


Figure 3.8: Schematic of how the swap of air parcels in sloping convection leads to an increase in the Brunt-Vaisala frequency  $N$  in eq. (3.13) in mid-latitudes (column of air above A).

by the swapping of air parcels at a shallow angle ( $\mu \leq \mu_\theta$ ) lead to an enhancement of the local Brunt-Vaisala frequency in the extra-tropics, as seen in Fig. 3.5. This effect is illustrated in Fig. 3.8.

### 3.7 Summary

Figure 3.9 offers a graphical summary of the various ideas discussed in this chapter:

- Above the tropopause, the atmosphere can be thought to be in radiative equilibrium: the sum of shortwave and longwave irradiances (grey and black arrows, respectively), does not converge or diverge in the vertical. Radiative heating in the shortwave balances exactly radiative cooling in the longwave:  $Q_{rad,SW} + Q_{rad,LW} = 0$ .
- Below the tropopause, radiative effects alone lead to a strong lapse-rate. Displacements of air parcels either purely upward (section 3.2) or in a slanted way (section 3.6) are unstable and convective motions develop. The troposphere as a whole (Tropics, midlatitudes and high-latitudes) can be thought of being in a state of convection.

- Convection carries heat upwards (blue arrows, converging upward at a rate  $Q_{conv}$  from the surface to the tropopause). This transfer cools the surface and heats the upper levels, leading to a weaker (but still positive) lapse-rate.
- Convective heating is opposed by a net radiative cooling, seen in the vertical divergence of the net longwave irradiances (black arrows):  $Q_{rad,SW} + Q_{rad,LW} + Q_{conv} = 0$ .

### 3.8 Problems

**Q1.** In this question we treat the Earth's atmosphere as dry and in hydrostatic equilibrium.

- Show that the adiabatic lapse rate is simply  $\Gamma = \Gamma_d = g/c_{p,d}$  where  $c_{p,d} = 1005 \text{ J kg}^{-1} \text{ K}^{-1}$  is the specific heat capacity of dry air at constant pressure and  $g = 9.81 \text{ m s}^{-2}$  is gravity. Compute its numerical value in  $\text{K/km}$ .
- Show that the actual lapse rate is  $\Gamma = \Gamma_d - \frac{T}{\theta} \frac{\partial \theta}{\partial z}$ .
- In light of the result in (ii) discuss whether a dry atmosphere can have a lapse rate greater (or lower) than  $\Gamma_d$ .

**Q2.** Air flows over the ocean (so it is well-supplied with moisture), across the coast, over a mountain which is 4 km high and down to a plateau on the far side at 1 km above sea level. Estimate the difference in temperature between sea level on the windward side and at the surface of the plateau. [Take  $\Gamma_d = 10 \text{ K/km}$  and  $\Gamma_m = 6.5 \text{ K/km}$ ].

**Q3.** Relative humidity ( $RH$ ) is defined as the ratio of the vapour pressure found in a sample of air at temperature  $T$  to that found when vapour and liquid water are in thermodynamic equilibrium at the same temperature:  $RH = e/e_{eq}(T)$ . Discuss whether the situations below correspond to a state of thermodynamic equilibrium: (i) Room temperature,  $RH = 0.7$  (ii) precipitation falling into a dry air mass,  $RH = 0.5$  (as can happen on the edge of a cloud).

**Q4.** We study a simple model of radiative equilibrium (Fig. 3.10) by treating the atmosphere as a two-layer system. Each of these layers is assumed to

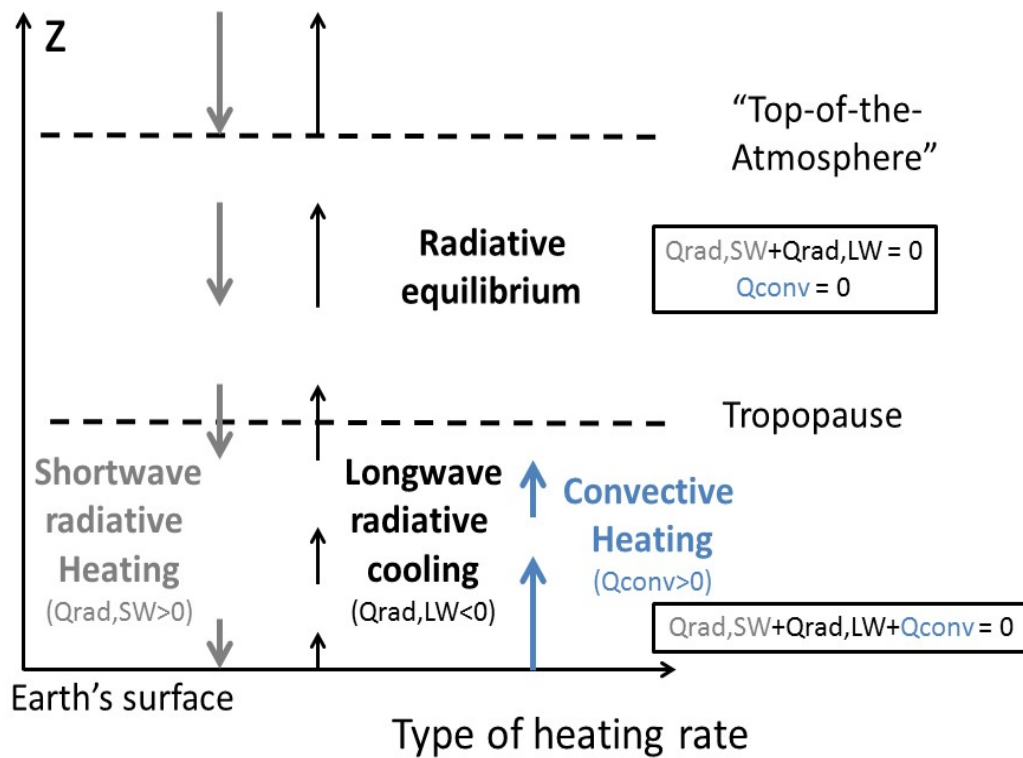


Figure 3.9: A summary schematic of the radiative - convective equilibrium view of the atmosphere. Black upwards arrows denote net (i.e., upward minus downward) longwave irradiances while grey downward arrows denote net (downward minus upward) shortwave irradiances (see Chapter 2). Blue upwards arrows indicate the vertical heat flux driven by convective motions.

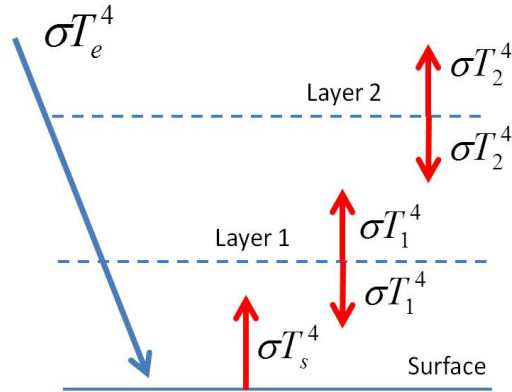


Figure 3.10: Simple radiative equilibrium model. The surface receives solar radiation ( $\sigma T_e^4 \equiv S_o(1 - \alpha_P)/4$ ) and emits infrared radiation upward. The atmosphere consists of two layers of longwave emissivity unity and shortwave absorptivity zero.

radiate like a blackbody in the infrared. The Earth's surface is also treated like a blackbody. The atmosphere is assumed to be completely transparent to solar radiation, so that at each level, the solar flux is  $S_o(1 - \alpha_P)/4$ . Compute the radiative equilibrium temperatures  $T_s$  (surface),  $T_1$  (lower atmosphere) and  $T_2$  (upper atmosphere).

**Q5.** The temperature profile predicted in the previous question is not stable to vertical displacements of air parcels. The latter lead to convective motions and a new temperature distribution close to an adiabat. To represent this simply, we fix the temperature difference  $\Delta T = T_1 - T_2 = T_s - T_1$  in the previous model, and also acknowledge the presence of additional heating terms: a surface heat exchange  $F_s$  and a convective heat flux  $F_c$  (Fig. 3.11).

- (i) Taking the two atmospheric layers to be at a pressure of  $700hPa$  and  $400hPa$  respectively, and using your answers in Q3, check that indeed the radiative equilibrium temperature profile is unstable. You may take the surface pressure to be  $1000hPa$ .
- (ii) Before doing any calculation, do you expect the surface temperature to decrease or increase when the fluxes  $F_s$  and  $F_c$  are included in the model?

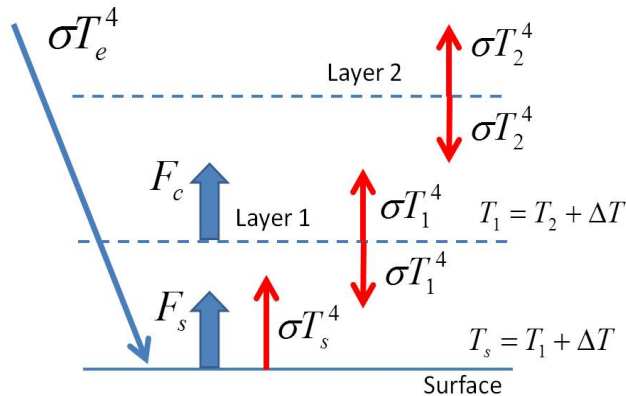


Figure 3.11: Addition of convective fluxes,  $F_s$  and  $F_c$  to the simple radiative equilibrium model.

- (iii) Solve for the temperature  $T_s$ ,  $T_1$  and  $T_2$  as a function of  $T_e$  and  $\Delta T$ .
- (iv) Solve for the convective flux  $F_c$  and the surface heat exchange  $F_s$ . Express your answer as a function of  $T_e$  and the non dimensional parameter  $x = \Delta T/T_e$ .
- (v) Find a plausible value for  $x$  and discuss the range of values of this parameter for which the model makes sense. Also check that for this range of values the model agrees with your answer in (ii).

**Q6.** Using Figs. 1.5 and 3.2, estimate the kinetic energy gain in sloping convection –eq. (3.31). How does this compare with your guess for the kinetic energy in storms?

**Q7.** A parcel of air has the same potential temperature than the environment at  $t = 0$  and  $z = 0$ , and an upward velocity  $w_o = 10\text{cm/s}$ . Find its height after 1mn if (i)  $N^2 = 10^{-4}\text{s}^{-2}$  (ii)  $N^2 = -10^{-4}\text{s}^{-2}$ . (iii)  $N^2 = 0$ . Neglect the effects of moisture on the motion.

**Q8.** The temperature structure in Fig. 1.3 in the mesosphere is very strange. In the Summer Hemisphere, the mesopause has  $T \leq -100^\circ\text{C}$  while it is about  $70^\circ\text{C}$  warmer in the Winter Hemisphere!

- (i) Estimate the mesospheric lapse rate (i.e., from stratopause to mesopause) in the summer and winter hemispheres
- (ii) Sketch how  $\theta(z)$  looks like in the summer and winter hemispheres
- (iii) Show that the profiles you have plotted in (ii) are consistent with the Brewer-Dobson circulation sketched in the ppt slides for Chapter 1.

# Chapter 4

## Atmospheric motions

**Key concepts:** Eulerian and Lagrangian descriptions of motions, material derivative, Coriolis force, Rossby number, geostrophic balance, “thermal wind”, rotational and divergent flows, vorticity, Rossby waves.

The vertical instability associated with  $N^2 < 0$  in Chapter 3 is at the heart of convective cells and cloud clusters with horizontal scales ranging from a few  $km$  up to  $100km$ . Updrafts and downdrafts in such systems are however not the sole motions driven by radiative processes. Indeed, the net radiative loss at high latitudes and the net radiative heat gain at the equator set up a whole range of motions. On scales of  $\approx 1000km$ , we find the traveling weather systems familiar at our latitudes, and their embedded cold and warm fronts ( $\approx 100km$ ). On even larger scale ( $10,000km$ ) we find planetary cells organized in east - west (Walker cell) and north-south (Hadley cell) directions –see Fig. 4.1 for a summary. In this chapter we study these motions from first principles (Newton’s second law in a rotating frame of reference). As we shall see, the Earth’s rotation has a profound impact on the dynamics, giving a (counter-intuitive) rigid or solid - like behavior to atmospheric motions on large scales.

### 4.1 Equations of motions

These are simply the three components of the “momentum” equation (Newton’s second law). Compared to the classical mechanics you have dealt with so far, the difficulties and novelty lie in:

- (i) the “fluid nature” of the motion, air parcels transporting their own momentum (material derivative)

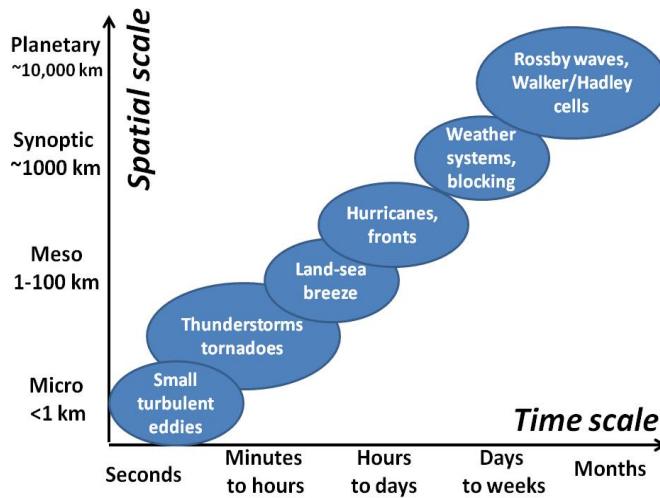


Figure 4.1: Space and time scales of atmospheric motions.

- (ii) the Earth rotation, which introduces new forces as seen by an observer at a fixed location on the planet. The effects of rotation on motions are huge as is most spectacularly illustrated with the “Taylor columns” (see Youtube video and the paper by Taylor (1923) on Blackboard).
- (iii) the sphericity of the Earth, which introduces mathematical complexity and a “channel-like” geometry to the study of atmospheric motions.

### 4.1.1 Forces acting on a parcel of air

Per unit mass, these are simply: the acceleration due to gravity (kept to a constant  $g = 9.81ms^{-2}$  for practical purposes, owing to the thinness of the atmosphere compared to the Earth’s radius), the pressure gradient force we’ve seen in Chapter 3 (but now in 3D), and frictional (or viscous) forces,

$$\mathbf{a} = \mathbf{g} - \alpha \nabla P + \mathbf{F}_{fric} \quad (4.1)$$

Note that in this equation  $\mathbf{a}$  is the acceleration vector in an inertial frame (say from an observer looking at the Earth from deep space), and  $\alpha$  is the volume per unit mass used extensively in Chapter 3.

### 4.1.2 Material derivative

Imagine a parcel of air undergoing an adiabatic ascent. Following the parcel, there is no change in its entropy. At a fixed location, however, an observer

might see a change in entropy since the parcel might originate from a warmer region than that in which the observer is sitting. To make it clear that the change “following the parcel” is a special case of derivative, we will write it as  $D/Dt$ . In the previous example, we would thus write,

$$\frac{Ds}{Dt} = 0 \quad (4.2)$$

Mathematically, the change following the parcel (also called “Lagrangian derivative”) includes the parcel’s displacement. If we write that entropy is a function of space and time, i.e.,  $s = s(x(t), y(t), z(t), t)$ , a small change in entropy  $\delta s$  in a small time interval  $\delta t$  is, after Taylor expansion,

$$\delta s = \left(\frac{\partial s}{\partial t}\right) \delta t + \left(\frac{\partial s}{\partial x}\right) \delta x + \left(\frac{\partial s}{\partial y}\right) \delta y + \left(\frac{\partial s}{\partial z}\right) \delta z \quad (4.3)$$

Dividing by  $\delta t$  and taking the limit, we thus identify  $D/Dt$  as,

$$\frac{Ds}{Dt} \equiv \lim_{\delta t \rightarrow 0} \frac{\delta s}{\delta t} = \frac{\partial s}{\partial t} + u \frac{\partial s}{\partial x} + v \frac{\partial s}{\partial y} + w \frac{\partial s}{\partial z} \quad (4.4)$$

Note that we have used the fact that the velocity components satisfy  $u = \lim_{\delta t \rightarrow 0} \delta x / \delta t$ ,  $v = \lim_{\delta t \rightarrow 0} \delta y / \delta t$  and  $w = \lim_{\delta t \rightarrow 0} \delta z / \delta t$ .

The local change with time can then be mathematically identified with,

$$\frac{\partial s}{\partial t} = \frac{Ds}{Dt} - \mathbf{u} \cdot \nabla s \quad (4.5)$$

in which we have introduced the velocity vector  $\mathbf{u} = (u, v, w)$ . This equation states that the local change in entropy results from the change following the parcel minus that due to advection. The view encapsulated in (4.5) is referred to as “Eulerian” (fixed location), as opposed to the “Lagrangian” (following a parcel) view in (4.2).

We used entropy in the previous example, but the concept applies to any variable, and even vector (applying the material derivative to each of its component). For example, for the velocity vector,

$$\mathbf{u} = \frac{D\mathbf{r}}{Dt} \quad (4.6)$$

(You can readily check that this expression provides the identity  $u = u \partial x / \partial x = u$ , etc... since the coordinates  $x, y, z, t$  are independent).

Applying the notation to Newton’s second law, we obtain:

$$\mathbf{a} = \mathbf{g} - \alpha \nabla P + \mathbf{F}_{fric} = \frac{D\mathbf{u}}{Dt} = \lim_{\delta t \rightarrow 0} \frac{\delta \mathbf{u}}{\delta t} \quad (4.7)$$

This is the Navier-Stokes equation for fluid flow in an inertial frame of reference. What is meant here is that the momentum of a fluid parcel changes along its trajectory due to the gain / loss associated with gravitational, frictional and pressure forces. Note that the  $D\mathbf{u}/Dt$  is a vector with components  $(Du/Dt, Dv/Dt, Dw/Dt)$ . Each of those are non linear expressions, for example, for the third component of momentum,

$$\frac{Dw}{Dt} = \frac{\partial w}{\partial t} + u \frac{\partial w}{\partial x} + v \frac{\partial w}{\partial y} + w \frac{\partial w}{\partial z} \quad (4.8)$$

showing that the upward motion carries its own upward momentum and that the latter is also carried by the horizontal flow.

### 4.1.3 Rotating frame of reference

The choice of the Earth as a frame of reference is natural. However, this is not an inertial frame because it is accelerating (rotating) with respect to a coordinate system fixed in space. Newton's law can be applied in the non-inertial frame if the acceleration of the coordinates is taken into account, introducing "apparent forces" in the equation of motion.

To introduce those, we need to relate the change of momentum of a parcel in the inertial frame<sup>1</sup>, denoted by  $(D\mathbf{u}_I/Dt)_I$  to that measured in the rotating frame of the Earth, denoted by  $(D\mathbf{u}_R/Dt)_R$ . In this notation,  $\mathbf{u}_I$  and  $\mathbf{u}_R$  refer to the velocity of a parcel in the inertial and rotating frames, respectively, while  $(D./Dt)_I$  and  $(D./Dt)_R$  denote the change following a parcel in the inertial and reference frames, respectively. Two important points need to be emphasized:

- we are talking about the same parcel of air here and we just describe differently its momentum "history" (see Fig. 4.2) by measuring changes as  $(D\mathbf{u}_I/Dt)_I$  or  $(D\mathbf{u}_R/Dt)_R$ .
- such change in momentum history only arises because momentum is a vector. In other words, in general

$$\left(\frac{D\mathbf{A}}{Dt}\right)_I \neq \left(\frac{D\mathbf{A}}{Dt}\right)_R \quad (4.9)$$

---

<sup>1</sup>We will consider that a coordinate system with the Earth's centre as its origin (orbiting around the Sun) provides such inertial frame. This is the idea introduced in Year 1 (Classical mechanics) that a free falling object under the action of gravity behaves approximately like an inertial frame.

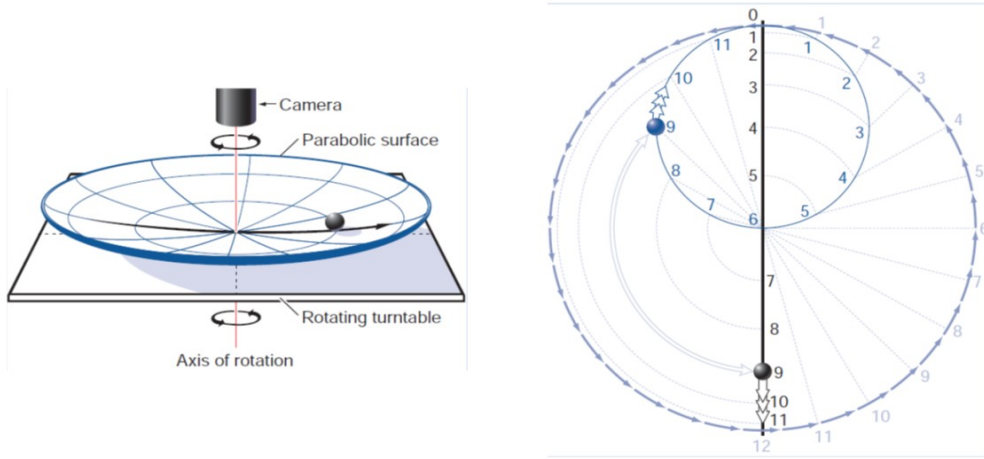


Figure 4.2: A simple apparatus (left) to illustrate how the trajectory of an object appears different in an inertial and a rotating frame of reference. In the inertial frame, a small ball thrown at point  $O$  on a parabolic dish moves forward and backward (black trajectory on the right). Viewed in the rotating frame of the dish, it describes a circle (blue trajectory). Friction has been ignored. Picture taken from Wallace and Hobbs' textbook.

for any vector  $\mathbf{A}$  (simply think about a constant vector in a rotating frame: it will have a zero value of  $D/Dt$  in the rotating frame, but a non zero value in the inertial frame), but

$$\left(\frac{DB}{Dt}\right)_I = \left(\frac{DB}{Dt}\right)_R \quad (4.10)$$

is always true for any scalar  $B$  since we follow the same parcel (think about measuring temperature of the parcel in Fig. 4.2: it does not matter whether we describe its trajectory as a circle or a straight line, it is still the same temperature we measure since it is the same parcel).

We accept the result (proven in the Appendix) that, for any vector  $\mathbf{A}$ , we have:

$$\left(\frac{D\mathbf{A}}{Dt}\right)_I = \left(\frac{D\mathbf{A}}{Dt}\right)_R + \boldsymbol{\Omega} \times \mathbf{A} \quad (4.11)$$

in which  $\boldsymbol{\Omega}$  is the Earth's rotation vector. Applying (4.11) to the vector position  $\mathbf{A} = \mathbf{r}$  (measured from the centre of the Earth), one recovers the

Galilean transformation of velocities between reference frames,

$$\mathbf{u}_I = \mathbf{u}_R + \boldsymbol{\Omega} \times \mathbf{r} \quad (4.12)$$

Applying it to  $\mathbf{A} = \mathbf{u}_I$  provides,

$$\left( \frac{D\mathbf{u}_I}{Dt} \right)_I = \left( \frac{D\mathbf{u}_I}{Dt} \right)_R + \boldsymbol{\Omega} \times \mathbf{u}_I \quad (4.13)$$

which, after using (4.12), reads,

$$\left( \frac{D\mathbf{u}_I}{Dt} \right)_I = \left( \frac{D\mathbf{u}_R}{Dt} \right)_R + 2\boldsymbol{\Omega} \times \mathbf{u}_R + \boldsymbol{\Omega} \times (\boldsymbol{\Omega} \times \mathbf{r}) \quad (4.14)$$

(to obtain this result we acknowledge that  $(D\boldsymbol{\Omega}/Dt)_R$  represents the change in the vector  $\boldsymbol{\Omega}$  at the location of the parcel, as seen in the rotating frame. At any given point along the trajectory,  $\boldsymbol{\Omega}$  is always the same since it is not affected by the rotation effect encapsulated in (4.11). Thus  $(D\boldsymbol{\Omega}/Dt)_R = \mathbf{0}$ .)

Rearranging, and using (4.7), we finally obtain,

$$\left( \frac{D\mathbf{u}_R}{Dt} \right)_R = \mathbf{g} - \alpha \nabla P + \mathbf{F}_{fric} - 2\boldsymbol{\Omega} \times \mathbf{u}_R - \boldsymbol{\Omega} \times (\boldsymbol{\Omega} \times \mathbf{r}) \quad (4.15)$$

#### 4.1.4 Coriolis and centrifugal forces

Comparing (4.15) with (4.7), one sees two new forces on the r.h.s, namely the Coriolis and centrifugal forces. The latter only depends on the position of the parcel (like a conservative force), and in effect acts to reduce gravity,

$$\mathbf{g}' \equiv \mathbf{g} - \boldsymbol{\Omega} \times (\boldsymbol{\Omega} \times \mathbf{r}) \quad (4.16)$$

After noticing that  $-\boldsymbol{\Omega} \times (\boldsymbol{\Omega} \times \mathbf{r}) = \Omega^2 \mathbf{r}_H = \nabla(\Omega^2 r_H^2/2)$  where  $\mathbf{r}_H$  is the component of  $\mathbf{r}$  perpendicular to  $\boldsymbol{\Omega}$ , it is sometimes convenient to introduce a slightly modified gravitational potential  $\Phi$  such that,

$$\mathbf{g}' = -\nabla(\Phi_{gravi} - \Omega^2 r_H^2/2) \equiv -\nabla\Phi \quad (4.17)$$

We will in the following approximate surfaces of constant (net) gravitational potential  $\Phi$  as spheres, with the net gravity given by  $\mathbf{g}'$ .

The Coriolis force  $(-2\boldsymbol{\Omega} \times \mathbf{u}_R)$  is required to explain why an object moving in a straight line in an inertial frame appears to have a curved path in a rotating frame. (As will be apparent throughout this chapter, there is more to it than this.) For now, let's just analyze its effect on the momentum equation (4.15). Adopting the coordinate system in Fig. 4.3 (see also the

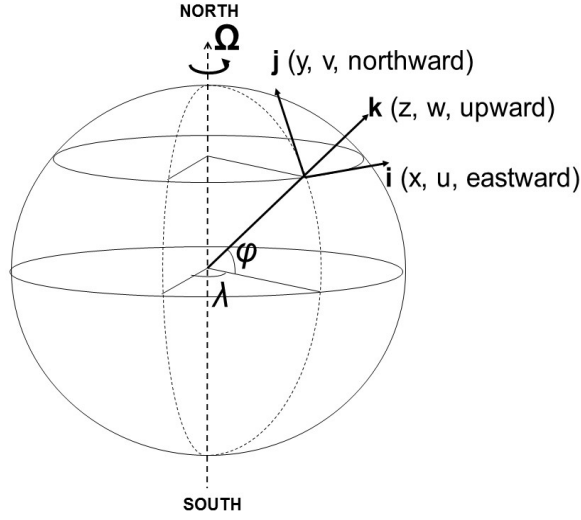


Figure 4.3: Local coordinate system  $(x, y, z)$ . Longitude is denoted by  $\lambda$ , latitude by  $\phi$ .

sidenote below),  $\mathbf{u}_R = (u, v, w)$  and  $\boldsymbol{\Omega} = \Omega(0, \cos \phi, \sin \phi)$  in which  $\phi$  is latitude and the three axes are  $\mathbf{i}$  (West to East),  $\mathbf{j}$  (South to North) and  $\mathbf{k}$  (anti-parallel with  $\mathbf{g}'$ ). Thus the Coriolis force will have the components,

$$-2\boldsymbol{\Omega} \times \mathbf{u}_R = -2\Omega[(w \cos \phi - v \sin \phi)\mathbf{i} + u \sin \phi \mathbf{j} - u \cos \phi \mathbf{k}] \quad (4.18)$$

Thus a parcel of air with a purely eastward velocity ( $u > 0, v = w = 0$ ) will be accelerated southward in the Northern hemisphere ( $-u \sin \phi < 0$ ) and northward in the Southern Hemisphere. The general rule is accelerated to the right of the motion in the Northern Hemisphere, and to the left in the Southern Hemisphere. You will also notice an upward acceleration, but this is pretty small in comparison to gravity. We will proceed to a more systematic analysis of the magnitude of each term in (4.15) in section 4.2.

*Technical sidenote: local coordinate system.* The  $(x, y, z)$  coordinate system in Fig. 4.3 is local and cartesian. As such, it has some advantages compared to that of spherical geometry. Specifically,

$$\mathbf{u}_R = u\mathbf{i} + v\mathbf{j} + w\mathbf{k} \quad (4.19)$$

with  $u = r \cos \phi \frac{D\lambda}{Dt}$ ,  $v = r \frac{D\phi}{Dt}$ ,  $w = \frac{Dr}{Dt}$ . Here  $r = R + z$  in which  $R$  is the (mean) Earth's radius, and since  $z \ll R$  for practical purposes, one can further simplify and use,

$$u \approx R \cos \phi \frac{D\lambda}{Dt}, v \approx R \frac{D\phi}{Dt}, w = \frac{Dz}{Dt} \quad (4.20)$$

This system of coordinate however has the complication that the  $\mathbf{i}, \mathbf{j}, \mathbf{k}$  vectors vary with location, and as a result,  $(D\mathbf{u}_R/Dt)_R \neq \mathbf{i}(Du/Dt)_R + \mathbf{j}(Dv/Dt)_R + \mathbf{k}(Dw/Dt)_R$ . Rather,

$$\left(\frac{D\mathbf{u}_R}{Dt}\right)_R = \mathbf{i}\left(\frac{Du}{Dt}\right)_R + \mathbf{j}\left(\frac{Dv}{Dt}\right)_R + \mathbf{k}\left(\frac{Dw}{Dt}\right)_R + u\left(\frac{D\mathbf{i}}{Dt}\right)_R + v\left(\frac{D\mathbf{j}}{Dt}\right)_R + w\left(\frac{D\mathbf{k}}{Dt}\right)_R \quad (4.21)$$

We will accept the result that,

$$\left(\frac{D\mathbf{i}}{Dt}\right)_R = \frac{u \tan \phi}{R} \mathbf{j} - \frac{u}{R} \mathbf{k} \quad (4.22)$$

$$\left(\frac{D\mathbf{j}}{Dt}\right)_R = -\frac{u \tan \phi}{R} \mathbf{i} - \frac{v}{R} \mathbf{k} \quad (4.23)$$

$$\left(\frac{D\mathbf{k}}{Dt}\right)_R = \frac{u}{R} \mathbf{i} + \frac{v}{R} \mathbf{j} \quad (4.24)$$

As a result,

$$\left(\frac{D\mathbf{u}_R}{Dt}\right)_R = \left[\left(\frac{Du}{Dt}\right)_R - \frac{uv \tan \phi}{R} + \frac{uw}{R}\right] \mathbf{i} + \left[\left(\frac{Dv}{Dt}\right)_R + \frac{u^2 \tan \phi}{R} + \frac{vw}{R}\right] \mathbf{j} + \left[\left(\frac{Dw}{Dt}\right)_R - \frac{u^2 + v^2}{R}\right] \mathbf{k} \quad (4.25)$$

As can be easily checked the extra-terms purely reflect the spherical geometry of the Earth and disappear in the limit  $R \rightarrow \infty$ .

### 4.1.5 Mass conservation

Ignoring the loss of mass when it rains, and its gain when evaporation occurs above the Earth's surface, the conservation of mass can be written as

$$\frac{\partial \rho}{\partial t} + \nabla \cdot (\rho \mathbf{u}_R) = 0 \quad (4.26)$$

in which  $\rho = 1/\alpha$  is the density of an air parcel. This equation is sometimes called the "continuity equation".

One interesting feature of this equation is that it is invariant to a change of reference frame. Indeed, mass conservation in the inertial frame would read exactly the same with  $\mathbf{u}_R$  being replaced by  $\mathbf{u}_I$  (you can check this by yourself readily after noticing that solid body rotation is a non divergent motion). This is very unlike momentum conservation which, as we have just seen, requires a different formulation in the inertial and rotating frames. This is our first hint that momentum might not be the best variable to consider in rotating fluids. As we shall see later in this chapter, the *curl* of the velocity field is much better suited (and its conservation equation is also invariant under change of reference frame).

## 4.2 Scale analysis of the equation of motions

The momentum equation (4.15) is quite complicated and we would not go very far if we were not able to simplify it further. To do so we are going to use a technique similar to dimensional analysis in which we are going to put orders of magnitude on each terms in (4.15). We will ignore the effects of friction and focus here on scales of motions typical of those seen on weather charts, i.e. the sloping convection motions discussed at the end of Chapter 3:

Lengthscale (horizontal)  $L \simeq 10^6 m$  (a thousand kilometers)

Lengthscale (vertical)  $H \simeq 10^4 m$  (thickness of the troposphere)

Velocity ( $u, v$ )  $U \simeq 10 m s^{-1}$

Velocity ( $w$ )  $W \simeq 10^{-2} m s^{-1}$

Time ( $t$ )  $T = L/U \simeq 10^5 s$  (about one day)

Horizontal Pressure gradient  $\nabla_L P \simeq 10 hPa / 1000 km = 10^{-3} Pa m^{-1}$

Remember also that  $R = 6371 km$  and  $2\Omega = 4\pi / 1 day \approx 2 \times 10^{-4} s^{-1}$ .

NB: The scales for  $L, H, U, T$  and  $\nabla_L P$  are relatively intuitive (say from your own estimate of windspeed looking at cloud displacement and a casual inspection of weather charts). It is more difficult to estimate from observations what the scale for the vertical velocity  $W$  should be. One way to proceed is to use the continuity equation (4.26) and require that the horizontal and vertical derivatives contribute as much to the total divergence. You can easily check that this leads to  $W = HU/L \approx 0.1 m s^{-1}$ . This estimate is an order of magnitude larger than the one used above. The reason is that, we shall soon see, weather systems are in geostrophic balance with very little vertical motion (nearly non divergent motions).

### 4.2.1 Vertical momentum equation

The vertical component of (4.15) is, using (4.25),

$$\left( \frac{Dw}{Dt} \right)_R = \frac{u^2 + v^2}{R} + 2\Omega u \cos \phi - \alpha \frac{\partial P}{\partial z} - g \quad (4.27)$$

in which we have dropped  $g'$  for  $g$  and have ignored the friction force. The first two terms on the r.h.s scale respectively as,  $U^2/R$  and  $2\Omega U \cos \phi$ . Their strength relative to the acceleration of gravity are  $U^2/gR \simeq 10^{-6}$  and  $2\Omega U \cos \phi/g \approx 2 \times 10^{-4} \cos \phi$ , respectively. The l.h.s has several components

since,

$$\left(\frac{Dw}{Dt}\right)_R = \frac{\partial w}{\partial t} + u\frac{\partial w}{\partial x} + v\frac{\partial w}{\partial y} + w\frac{\partial w}{\partial z} \quad (4.28)$$

The first three have the same scale (since we have chosen  $T = L/U$ ), namely  $W/T$ , while the last term scales as  $W^2/H$ . The ratio of these to gravity is thus  $W/gT \approx 10^{-8}$  and  $W^2/gH = 10^{-9}$ , respectively. Note that because of the values listed above,  $U/L \approx 10W/H$  so from now on we will simply scale all  $D/Dt$  terms by simply dividing by  $T$  (i.e.,  $(Dw/Dt)_R \approx W/T$ ).

The bottom line is that all the terms considered are negligible compared to the acceleration of gravity and so, to a very good approximation, we can safely use,

$$0 \approx -\alpha\frac{\partial P}{\partial z} - g \quad (4.29)$$

This is the ‘‘hydrostatic equation’’ introduced earlier in Chapter 3, expressing a near cancellation between the acceleration due to gravity and that due to the vertical pressure gradient force.

To some extent the above scaling is misleading. It makes sense that gravity opposes the vertical pressure gradient, but the motions we are considering consist of pressure fluctuations superimposed on this state of pure hydrostatic equilibrium. (In other words, the pressure fluctuations used above, i.e.,  $10hPa$  has nothing to do with the much larger pressure changes between surface and tropopause which is  $\approx 750hPa$ ). What we should really check is whether this perturbed state satisfies the hydrostatic approximation. To do this, write

$$\alpha = \bar{\alpha} + \alpha' \quad \text{and} \quad P = \bar{P} + P' \quad (4.30)$$

where the bar denotes the background state in hydrostatic balance and the prime the fluctuations associated with weather systems. One can readily obtain that,

$$\alpha\frac{\partial P}{\partial z} + g \approx \bar{\alpha}\frac{\partial P'}{\partial z} - g\frac{\alpha'}{\bar{\alpha}} \quad (4.31)$$

Putting orders of magnitude on each term, we find,

$$\bar{\alpha}\frac{\partial P'}{\partial z} \simeq (1kgm^{-3})\frac{10hPa}{10km} = 10^{-1}ms^{-2} \quad (4.32)$$

and

$$-g\frac{\alpha'}{\bar{\alpha}} \approx -g\frac{\theta'}{\bar{\theta}} \simeq 9.81\frac{3}{300} = 10^{-1}ms^{-2} \quad (4.33)$$

These terms are still much larger than all the others in (4.27) and so the hydrostatic approximation also applies to dynamic, as opposed to purely

static situations,

$$0 \approx \bar{\alpha} \frac{\partial P'}{\partial z} - g \frac{\alpha'}{\bar{\alpha}} \quad (4.34)$$

Most climate models use this approximation. (Among other things it allows a change of vertical coordinate  $z \rightarrow P$  which simplifies considerably the model numerics).

*NB\**: You might rightly notice that the momentum balance (4.34) is different than the one used in Chapter 3 for sloping convection. What was missing there is the fact that the parcels ascending and descending are embedded in a wave, with associated pressure variations. Their vertical gradients are the primary mechanism opposing the buoyancy force, not vertical acceleration of the parcels. Returning to Fig. 3.7, as parcel A goes up, it gains kinetic energy through the work of buoyancy force (and as we know from section 3.6 this is maximized if it moves at an angle equal to half the slope of the  $\theta$  surfaces). From eq. (4.34), we now know that it loses kinetic energy because of adverse vertical pressure gradients. The latter act as a brake on the wave whose energy source is the work computed in section (3.6).

### 4.2.2 Horizontal momentum equation

The two components of the horizontal momentum equations take the form,

$$\left( \frac{Du}{Dt} \right)_R = -\frac{uw}{R} + \frac{uv \tan \phi}{R} + 2\Omega v \sin \phi - 2\Omega w \cos \phi - \alpha \frac{\partial P}{\partial x} \quad (4.35)$$

$$\left( \frac{Dv}{Dt} \right)_R = -\frac{vw}{R} - \frac{u^2 \tan \phi}{R} - 2\Omega u \sin \phi - \alpha \frac{\partial P}{\partial y} \quad (4.36)$$

Scaling these terms, we obtain (from left to right):  $U/T \approx 10^{-4}$ ,  $UW/R \approx 10^{-8}$ ,  $U^2/R \approx 10^{-5}$ ,  $\Omega U \sin \phi \approx 10^{-3} \sin \phi$ ,  $\Omega W \cos \phi \approx 10^{-6} \cos \phi$  and  $\alpha \nabla_L P \approx 10^{-3}$  (using the surface value for  $\alpha \approx 1 \text{ m}^3/\text{kg}$ ) for the zonal momentum equation. Likewise, for the meridional momentum equation:  $U/T \approx 10^{-4}$ ,  $UW/R \approx 10^{-8}$ ,  $U^2/R \approx 10^{-5}$ ,  $\Omega U \sin \phi \approx 10^{-3} \sin \phi$ , and  $\alpha \nabla_L P \approx 10^{-3}$ .

Looking at these numbers it becomes clear that, as long as we are not too close to the equator where  $\sin \phi = 0$ , the approximate form of the horizontal momentum equation is,

$$0 \simeq +2\Omega v \sin \phi - \alpha \frac{\partial P}{\partial x} \quad (4.37)$$

$$0 \simeq -2\Omega u \sin \phi - \alpha \frac{\partial P}{\partial y} \quad (4.38)$$

This approximation is called the geostrophic approximation, expressing a near cancellation between the acceleration due to the horizontal pressure gradient and Coriolis forces. One way to “visualize” this balance is that air parcels tend to flow along lines of constant pressure (anticlockwise around a low pressure system in the extra-tropics in the Northern Hemisphere).

After these two terms the next larger one is  $(Du/Dt)_R$  for the zonal momentum equation and  $(Dv/Dt)_R$  for the meridional momentum equation. Both terms scale as  $U/T = U^2/L$ . How small is this term compared to the Coriolis force is measured by a non dimensional number called the Rossby number ( $R_o$ ),

$$R_o \equiv \frac{U}{2\Omega L} \quad (4.39)$$

In other words, the smaller the Rossby number, the closer we are to geostrophic balance. For the scales considered at the beginning of section 4.2,  $R_o \approx 0.1$ .

NB: Not all atmospheric motions have small Rossby numbers. For example, hurricanes have typical windspeed  $U = 30ms^{-1}$  and horizontal lengthscale  $L = 100km$ , yielding  $R_o \approx 30/(2 \cdot 10^{-4} \times 10^5) = 1.5$ . Thus the geostrophic approximation is not valid for hurricanes and advection of momentum by the horizontal flow plays a key role in their dynamics.

### 4.2.3 The thermal wind relation

The smallness of the Rossby number is the main reason why the Earth rotation has so much influence on weather systems and many other motions. We have everything at hand to see straight away one of the powerful constraints resulting from  $R_o \ll 1$ , namely a constraint on how motions vary with height.

All we need are the approximate momentum equations (4.29), (4.37) and (4.38). Take the vertical derivative of (4.37), yielding,

$$f \frac{\partial v}{\partial z} \approx \frac{\partial}{\partial z} \left[ \alpha \frac{\partial P}{\partial x} \right] \quad (4.40)$$

in which we have introduced the Coriolis parameter,

$$f \equiv 2\Omega \sin \phi \quad (4.41)$$

Using (4.29), this can be rewritten as,

$$f \frac{\partial v}{\partial z} \approx \frac{\partial \alpha}{\partial z} \frac{\partial P}{\partial x} - \frac{\partial \alpha}{\partial x} \frac{\partial P}{\partial z} \quad (4.42)$$

Likewise,

$$f \frac{\partial u}{\partial z} \approx -\frac{\partial \alpha}{\partial z} \frac{\partial P}{\partial y} + \frac{\partial \alpha}{\partial y} \frac{\partial P}{\partial z} \quad (4.43)$$

or, in vector form,

$$f \frac{\partial \mathbf{V}}{\partial z} \approx (\nabla \alpha \times \nabla P)_H \quad (4.44)$$

in which  $\mathbf{V} = u\mathbf{i} + v\mathbf{j}$  is the horizontal velocity vector and the subscript  $H$  indicates we only consider the horizontal component.

The terms on the r.h.s of (4.44) vanish if  $\alpha = \alpha(P)$ . That is, in such condition, the horizontal velocity field cannot vary with height! –see the note below on “Taylor columns”. More realistically, in the atmosphere  $\alpha = \alpha(T, P)$  and the terms on the r.h.s do not vanish. Rather they set a constraint on how much the horizontal wind can vary with height.

A geometrical derivation brings more insight into these relations. Using the triple product rule for mixed derivative and the hydrostatic approximation, one has,

$$\alpha \left( \frac{\partial P}{\partial x} \right)_z = -\alpha \left( \frac{\partial z}{\partial x} \right)_P \left( \frac{\partial P}{\partial z} \right)_x = g \left( \frac{\partial z}{\partial x} \right)_P \quad (4.45)$$

which relates the pressure gradient to the slope of a pressure surface. As a result, the difference in meridional wind ( $v$ ) between two heights ( $z_1 > z_2$ ) is, using the geostrophic balance,

$$v_2 - v_1 = \frac{g}{f} \left( \frac{\partial z}{\partial x} \right)_{P_2} - \frac{g}{f} \left( \frac{\partial z}{\partial x} \right)_{P_1} \quad (4.46)$$

Likewise, for the zonal wind,

$$u_2 - u_1 = \frac{g}{f} \left( \frac{\partial z}{\partial y} \right)_{P_1} - \frac{g}{f} \left( \frac{\partial z}{\partial y} \right)_{P_2} \quad (4.47)$$

These relations show that variations with height of the geostrophic wind reflect horizontal gradients in the thickness between two pressure surfaces (Fig. 4.4). The thickness is itself directly related to temperature since the hydrostatic equation can be rewritten, using the ideal gas law (and neglecting moisture), as,

$$\frac{\partial \ln P}{\partial z} = -\frac{g}{R_d T} \quad (4.48)$$

This indeed shows that for two given pressure surfaces ( $P_1, P_2$ ), the thickness between them ( $= z_1 - z_2$ ) increases with the temperature of the layer of air sandwiched between these two surfaces,

$$z_1 - z_2 = \int_{z_2}^{z_1} dz = \int_{P_1}^{P_2} \frac{R_d T}{g} d \ln P \quad (4.49)$$

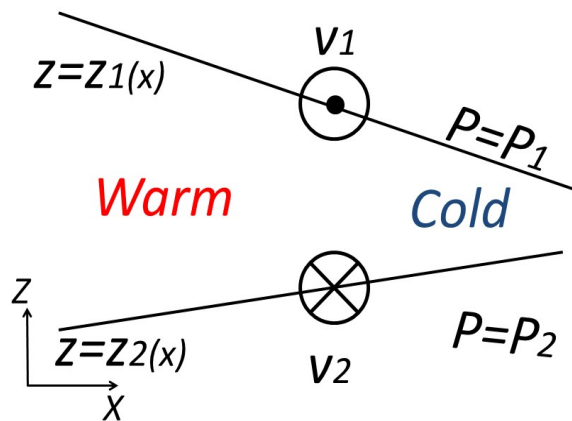


Figure 4.4: The variations of the geostrophic wind with height reflect horizontal temperature variations: in the Northern Hemisphere (shown in picture), winds increasing with height have cold air to their left (if  $x$  is interpreted as the east - west distance, the figure indicates southward wind  $v_1 < 0$  at upper level and northward wind  $v_2 > 0$  at low level). The distance between two pressure surfaces (the thickness) increases with temperature. In this diagram two pressure surfaces ( $P = P_1$  and  $P = P_2$ ) are shown in black, being at a height  $z = z_1(x)$  and  $z = z_2(x)$ , respectively.

This is why the wind variations in (4.46)-(4.47) are called the “thermal wind” relations.

A vivid illustration of the thermal wind relation is also found in Fig. 1.3 in Chapter 1. If we look for example at the winter hemisphere at  $30^\circ$ , one observes that the contours of velocity close on themselves at a height of about  $10\text{km}$  (i.e., there is a wind maximum here, the Jet Stream). Thus below the maximum the wind increases with height but above the maximum they decrease with height. The thermal wind relation shows that this must be associated with a reversal of the equator-to-pole temperature gradient. Indeed the Tropics are warmer than the Poles below  $10\text{km}$  but are colder (!) above this level in the lower stratosphere.

*NB\*: The thermal wind relation offers insight into the “Taylor’s column” effect discussed at the beginning of this chapter. In a fluid of constant density, it predicts  $\partial u/\partial z = \partial v/\partial z = 0$ . So the horizontal motion has to be independent of height and we cannot expect the motion above the obstacle to be solely limited to its vicinity. It happens that for small Rossby number and constant density, one can also predict  $\partial w/\partial z = 0$  which implies that there can be no motion above the obstacle at all (this would require having  $w$  non zero just above the obstacle but zero away from it).*

## 4.3 The vorticity view

### 4.3.1 The geostrophic flow, vorticity and divergence

The approximations derived in section 4.2 are very useful and allow to understand the basic structure of atmospheric motions. However, you might have noticed that they do not include time derivatives. In other words, they are just diagnostic relationships. Were you to forecast the weather based on them, you would go nowhere!

The breakthrough to achieve this task came in the 1950s when it was realized that the geostrophic flow is rotational: it goes around pressure centers (cyclones or anticyclones) but does not cross much the pressure lines. And so it became clear that what needs to be forecast is not momentum but vorticity  $\zeta$ , the rotational (or curl) of the velocity field,

$$\zeta \equiv \nabla \times \mathbf{u}_R \quad (4.50)$$

To see the importance of vorticity, simply consider its vertical component

( $\zeta$ ) in the local coordinate system,

$$\zeta \equiv \boldsymbol{\zeta} \cdot \mathbf{k} = \frac{\partial v}{\partial x} - \frac{\partial u}{\partial y} \quad (4.51)$$

On the scales considered in section 4.2, one can, for practical purposes further simplify the geostrophic balance as,

$$v \approx \frac{\alpha_o}{f_o} \frac{\partial P}{\partial x}, \quad \text{and} \quad u \approx -\frac{\alpha_o}{f_o} \frac{\partial P}{\partial y} \quad (4.52)$$

in which  $\alpha_o$  and  $f_o$  are typical values of the specific volume and the Coriolis parameter over the region of interest. From this,

$$\zeta \approx \frac{\alpha_o}{f_o} \left( \frac{\partial^2 P}{\partial x^2} + \frac{\partial^2 P}{\partial y^2} \right) \quad (4.53)$$

while, the horizontal divergence of the (relative) flow  $\delta$  is,

$$\delta \equiv \frac{\partial u}{\partial x} + \frac{\partial v}{\partial y} \approx 0 \quad (4.54)$$

Thus indeed, the geostrophic flow is close to being purely rotational, i.e., containing vorticity but no divergence. For such flows a streamfunction  $\psi$  can be introduced from the definition,

$$u \equiv -\frac{\partial \psi}{\partial y} \quad \text{and} \quad v = \frac{\partial \psi}{\partial x} \quad (4.55)$$

Comparison of (4.52) with (4.55) shows that  $\psi \approx \alpha_o P / f_o$ : the horizontal flow follows approximately lines of constant pressure.

The concept of vorticity comes from Fluid Mechanics and is thus much more general than the special case of geostrophic flows. The video shown in the lecture illustrates its presence or absence in simple flows (e.g., solid body rotation, source/sink flows in a kitchen sink –link provided on Blackboard).

*Technical note: An important result is that a flow in solid body rotation has a vorticity equal to twice the rate of rotation. A simple derivation can be obtained as follows. Consider a tank of water rotating around a vertical axis at a rate  $\Omega$ . One can compute the vorticity of any fluid parcel embedded in this flow by considering an anti-clockwise closed contour made of two lines  $r = r_1$  and  $r = r_2$  (with  $r_1 = r_2 + \delta r$ , i.e., we are considering a very small contour) joined by two radial lines making a small angle  $\delta\theta$ . From Stokes' theorem,  $\oint \mathbf{u} \cdot d\mathbf{l} = \iint (\nabla \times \mathbf{u}) \cdot d\mathbf{S} = \iint \zeta dS$ , which in polar cylindrical geometry, reads  $u_1 r_1 \delta\theta - u_2 r_2 \delta\theta = \zeta \delta r \delta\theta (r_1 + r_2) / 2$ . In solid body rotation  $u_1 = \Omega r_1$  and  $u_2 = \Omega r_2$ , hence,  $\Omega (r_1^2 - r_2^2) \delta\theta = \zeta \delta r \delta\theta (r_1 + r_2) / 2$ . Since  $r_1^2 - r_2^2 = (r_1 - r_2)(r_2 + r_1)$ , one obtains  $\zeta = 2\Omega$ .*

### 4.3.2 Predicting the vorticity of the flow: the vorticity equation

We are going to restrict ourselves to horizontal flows on the sphere, i.e., flows which have exactly zero vertical motion ( $w = 0$ ). In so doing we are admittedly taking an extreme limit (for example all types of motions discussed in Chapter 3 are excluded from this category), but it helps to see more clearly how vorticity can be predicted. As it happens, horizontal motions of planetary scales dominate the variability of atmospheric flows on timescales greater than a week or so, so this is not an academic problem but rather, one of great importance for seasonal and climate prediction (see section 4.3.3).

We thus consider the motion of an “air shell” sandwiched between the Earth and a concentric outer shell, and let us denote the (constant) distance between the two spheres, i.e., the height of the air column, by  $d$  (Fig. 4.5). We are going to follow in a Lagrangian sense an initial volume of air and we will neglect any effect of compressibility. Thus we take  $\alpha = cst = \alpha_o$ . As a result, the volume of this air sample remains constant. Since  $d$  is also constant, this implies that the surface area  $S$  of the sample is constant during its motion (it can deform and change shape but its total area has to remain the same). Focusing on flow of sufficiently large scale and small velocity amplitude, the Rossby number is very small. The thermal wind relation thus applies and without temperature variations ( $\alpha = cst$ ) this implies that the horizontal velocity vector is constant with height. We can thus think of the flow as simply representing the horizontal motion of a rigid column of fluid ( $w = 0$  by construction since the flow is bounded by two spherical shells—Fig. 4.5).

Let’s describe what happens to our column from the point of view of an observer in an inertial frame (say viewed from Space). Its velocity is,

$$\mathbf{u}_I = \mathbf{u}_R + \Omega \times \mathbf{r} \quad (4.56)$$

We are going to use the result, known as Kelvin’s identity (proven in Appendix), that if we follow a circuit made of fluid elements (hereafter called a “material contour”), i.e., any closed circuit within the column, we have,

$$\left( \frac{D}{Dt} \oint \mathbf{u}_I \cdot d\mathbf{s} \right)_I \equiv \oint \left( \frac{D\mathbf{u}_I}{Dt} \right)_I \cdot d\mathbf{s}, \quad (4.57)$$

in which  $d\mathbf{s}$  denotes an infinitesimal segment of the circuit. Using the equation of motion in an inertial frame (4.7), this can be rewritten as,

$$\left( \frac{D}{Dt} \oint \mathbf{u}_I \cdot d\mathbf{s} \right)_I = \oint (-\mathbf{g} - \alpha \nabla P + \mathbf{F}_{fric}) \cdot d\mathbf{s}, \quad (4.58)$$

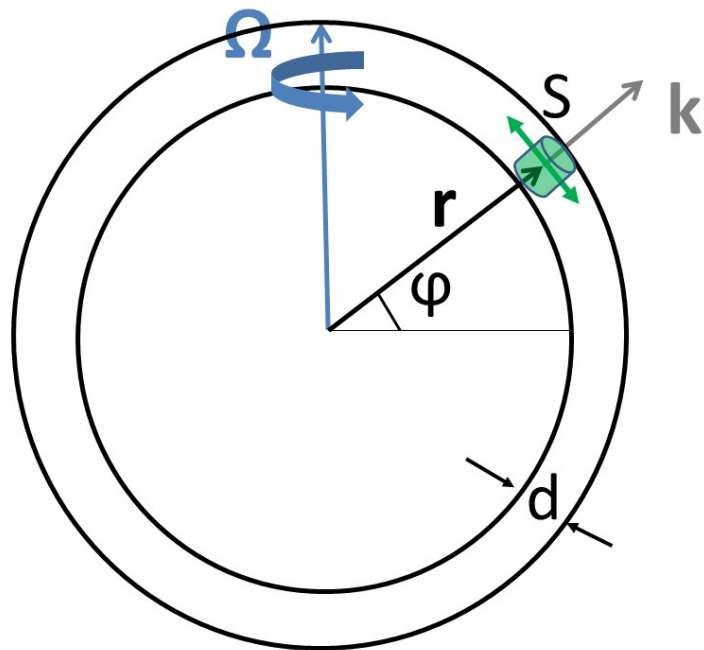


Figure 4.5: Horizontal motion of a column of fluid (green shading, height  $d$ , horizontal surface area  $S$ ) sandwiched between the Earth and a concentric outer shell.

Since  $\mathbf{g} = -\nabla\Phi_{gravi}$ , we have  $\oint \mathbf{g} \cdot d\mathbf{s} = \oint d\Phi_{gravi} = 0$  (same starting and end point in a closed contour). Likewise, because we take  $\alpha$  to be constant,  $\oint \alpha \nabla P \cdot d\mathbf{s} = \alpha_o \oint dP = 0$ . If, in addition, we neglect friction, we come to the conclusion that:

$$\left( \frac{D}{Dt} \oint \mathbf{u}_I \cdot d\mathbf{s} \right)_I = 0. \quad (4.59)$$

From Stokes'theorem, this is also,

$$\left( \frac{D}{Dt} \iint (\nabla \times \mathbf{u}_I) \cdot d\mathbf{S} \right)_I = 0. \quad (4.60)$$

where the integral is taken along any surface encircling the material contour. Using (4.56) and (4.50), this can be rewritten as,

$$\left( \frac{D}{Dt} \iint [\zeta + \nabla \times (\Omega \times \mathbf{r})] \cdot d\mathbf{S} \right)_I = 0. \quad (4.61)$$

Coming back to the motion in Fig. 4.5, a convenient choice of surface is clearly a sphere. With this choice, the normal  $d\mathbf{S}$  is in the vertical direction ( $\mathbf{k}$  in Fig. 4.5), and eq. (4.61) can be rewritten as,

$$\left( \frac{D}{Dt} \iint (\zeta + f) dS \right)_I = 0. \quad (4.62)$$

Note that to arrive at this expression, we have used the result (shown in the Appendix) that  $\nabla \times (\Omega \times \mathbf{r}) = 2\Omega$ . We now take the limit in which the horizontal cross section of the column of air in Fig. 4.5 is infinitesimally small. Then  $S \rightarrow dS$  is constant following the flow from the previous arguments, but we now also know, from (4.62), that the product of  $(\zeta + f)S$  must be constant following the flow. Hence we obtain the deceptively simple "vorticity equation":

$$\zeta + f = cst \quad (\text{following the flow}) \quad (4.63)$$

As we illustrate in the following section, this equation provides everything we need to predict the motion in Fig. 4.5.

Although we derived this equation by describing a material circuit in an inertial frame, the end result should be independent of that choice. Indeed, using the fact that  $(DB/Dt)_I = (DB/Dt)_R$  for any scalar  $B$ , we can as well write,

$$\left( \frac{D}{Dt} \iint (\zeta + f) dS \right)_R = 0. \quad (4.64)$$

One could derive this equation by following the same procedure as above in the rotating frame of the Earth, but this would involve the (more mathematically involved) calculation of a "torque" by the Coriolis force.

The variables  $\zeta$  and  $f$  refer to the projection of the vorticity vectors  $\zeta$  and  $2\Omega$  onto the local vertical. There is a more general equation for the absolute vorticity vector  $\zeta_a = 2\Omega + \zeta$  but we will not discuss it in this course (you can see this equation in the picture on the “Welcome to Atmospheric Physics!” page at the beginning of these notes. If you’re interested I have included a derivation in the Appendix).

*NB1\*: In the inertial frame, the local rate of rotation of a fluid parcel is twice the quantity  $\zeta + f$ , which is called the “absolute vorticity” ( $\equiv \zeta_a$ ). It is the sum of the vorticity  $\zeta$  (the “relative vorticity”) due to the relative motion of the parcel with respect to the solid body rotation of the Earth, and that due to the solid body rotation of the parcel around the Earth’s axis ( $f$ , the “planetary vorticity”). As the experiment in the vorticity video showed (specifically, the part showing the vorticity meter in a solid body rotation of a fluid in a tank), in a solid body rotation the fluid locally rotates at the same angular velocity as the tank. The associated vorticity is twice this rate (see technical note in section 4.3.1). In the rotating frame of reference, the local rate of rotation of a fluid parcel is just twice the relative vorticity (the vorticity meter in a pure solid body rotation does not change for an observer rotating itself with the tank).*

*NB2\*: You could take the other limit in which the circuit in the above discussion shrinks (like a the flow in a kitchen sink), i.e.,  $S$  decreases. The prediction from the circulation theorem is that  $(\zeta + f)S$  must remain constant. Hence,  $\zeta + f$  will have to increase. If the circuit shrinks over a limited range of latitude, this requires that the relative vorticity increases. In other words, a cyclone is intensifying. This is a decent model for the growth of hurricanes. There are many other applications of the circulation theorem. An example is given in Q5 (Gulf Stream) of the problem sheet.*

### 4.3.3 Rossby waves

A large class of motions of the atmosphere are loosely defined as being of the “planetary wave” type, to indicate that they are of sufficiently large spatial scale that they are affected by the fact that the Earth rotation vector  $\Omega$  has a projection on the local vertical which varies with latitude. An example is given in Fig. 4.6, showing the height of the 500hPa surface for the Northern Hemisphere on 10 February 2014 –this approximately provides a streamfunction for the flow at mid-tropospheric levels from the discussion in section 4.3.1 and eq. (4.45). A wavenumber 2 structure is clearly apparent in the east-west direction, spreading from the North Pole to 30°N.

500 hPa Geopotential Height and Anomalies 00Z10FEB2014

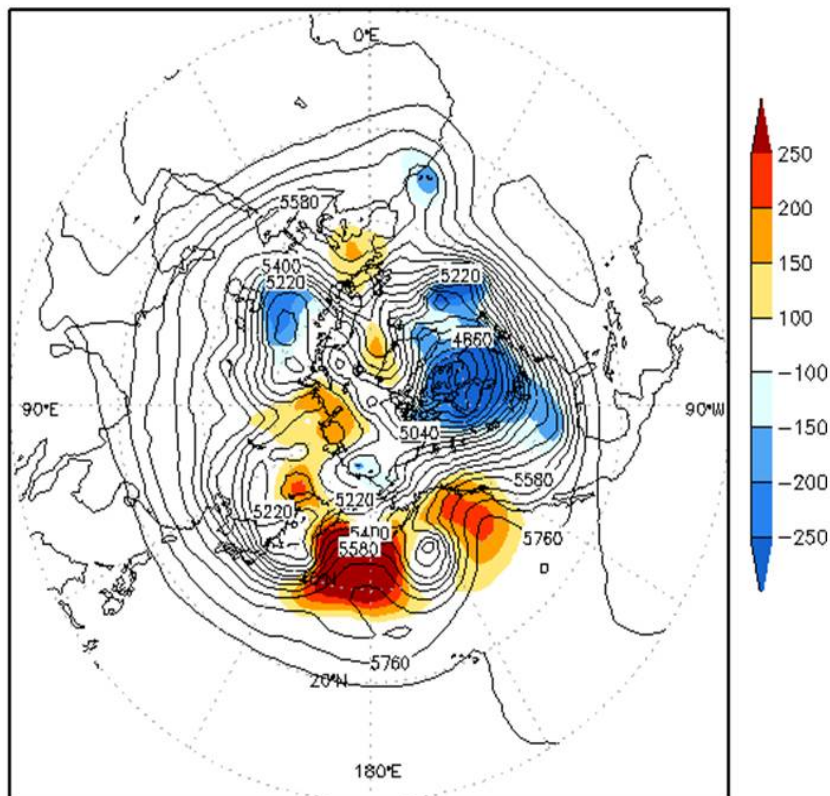


Figure 4.6: The height (in *km*) of the 500*hPa* pressure surface on 10/02/2014. Black contours indicate its absolute values while the colours (in *m*) denote anomalies compared to the long time mean. From <http://www.cpc.ncep.noaa.gov/products/precip/CWlink/MJO/block.shtml>.

The Rossby number for these motions is particularly low  $R_o = U/2\Omega L \approx 10/(2 \times 7.2 \times 10^{-5} \times 14,000 \text{ km}) = 0.005$  (using a wavenumber 2 at  $45^\circ N$ ) so that they satisfy the geostrophic balance and are nearly purely rotational (section 4.3.1). A lot of insight can be gained into these motions by using (4.64), which we express mathematically as:

$$\left( \frac{\partial}{\partial t} + u \frac{\partial}{\partial x} + v \frac{\partial}{\partial y} \right) (f + \zeta) = 0 \quad (4.65)$$

Equation (4.65) states that absolute vorticity “sticks” to air parcels: you can tell the origin of a given air mass from looking at its absolute vorticity (e.g., a low value of  $\zeta_a$  typically originates from low latitudes)! A very powerful tool.

The equation (4.65) supports linear waves called Rossby waves after the Swedish meteorologist Carl Gustav Rossby who highlighted their dynamics in the 1950s. Take the simplest possible case, i.e., linear motion on a state of rest. Then (4.65) can be rewritten as,

$$\frac{\partial \zeta'}{\partial t} + \beta v' = 0 \quad (4.66)$$

in which primes indicate perturbations and

$$\beta \equiv \frac{df}{dy} \quad (4.67)$$

captures the latitudinal variation of the projection of  $\mathbf{\Omega}$  onto the local vertical. This equation can be solved by using the streamfunction  $\psi$  introduced in (4.55) and looking for plane wave solution<sup>2</sup>,

$$\psi' \propto e^{i(kx+ly-\omega t)} \quad (4.68)$$

This provides the dispersion relation,

$$\omega = -\frac{\beta k}{k^2 + l^2} \quad (4.69)$$

and the associated phase velocity  $\mathbf{v}_P$ ,

$$\mathbf{v}_P = -\frac{\beta}{k^2 + l^2} (1, k/l) \quad (4.70)$$

---

<sup>2</sup>The reason a streamfunction can be introduced rigorously here is that we are looking at horizontal motion and have assumed constant density. Using these approximations, the continuity equation (4.26) predicts that the horizontal divergence of the flow has to be zero, i.e.,  $\partial u/\partial x + \partial v/\partial y = 0$ , hence  $u = -\partial\psi/\partial y$  and  $v = \partial\psi/\partial x$ .

The frequency of Rossby waves is typically much lower than that of the weather system we experience nearly daily (the latter were the subject of section 3.6 and, contrary to Rossby waves, the presence of upward and downward motion is crucial for their existence). For example, for the observations in Fig. 4.6, I found  $\omega \approx 2\pi/43\text{days}^{-1}$  (using a wavenumber 2 at  $45^\circ N$  for  $k$  and  $l = 2\pi/3000\text{km}$ ). No wonder why these waves are studied tremendously since, owing to their long timescales, they introduce predictability to our weather.

Rossby waves display a myriad of other interesting features:

- their phase speed is always westward ( $\omega/k < 0$ ). This follows directly from the conservation of vorticity by fluid parcels, as encapsulated in (4.65) and illustrated in Fig. 4.7. The usual way to describe a wave in terms of a restoring force is not useful for Rossby waves since, as emphasized earlier, they are in geostrophic balance and the momentum equation does not say much about time evolution. This is why “vorticity thinking”, as illustrated in Fig. 4.7, brings much more insight into the mechanism of propagation.
- they are associated with a transverse motion of air parcels. This is illustrated in Fig. 4.8, where the velocity vector (blue arrows) is aligned along lines of constant pressure (by geostrophy) while the phase speed (black arrow) is at right angle. This is very different from other types of waves supported by fluids (acoustic, gravity waves, i.e., swell) which involve longitudinal motions. Again, this is a behaviour closer to that of solids (e.g., shearwaves in the solid Earth generated by earthquakes). As you can see, this all has to do with  $\beta \neq 0$ .
- they carry east-west momentum across latitude circles. This property is illustrated in Fig. 4.8. Consider the portion of a latitude circle corresponding to a zonal wavelength (marked by the red  $a$ - $b$ - $c$  line in the figure). At  $a$ , a fluid parcel has  $u' > 0$  and  $v' > 0$ , hence it carries eastward momentum northward. At  $b$ , the parcel goes southward ( $v' < 0$ ) but it has a negative eastward momentum ( $u' < 0$ ), hence again, it carries eastward momentum northward (removing negative eastward momentum from a region is like adding positive eastward momentum to it). At  $c$ , we have the repeat of what occurs at  $a$ . So averaged over a zonal wavelength, there is a net transport of eastward momentum northward. Mathematically this is expressed as a systematic positive correlation between  $u'$  and  $v'$ : averaged over a zonal wavelength (east-west direction), the product  $u'v'$  has a sign proportional to  $-kl$  (simply take  $\psi' \propto \sin(kx+ly-\omega t)$  and check that  $u'v' \propto -kl\cos^2(kx+ly-\omega t)$ ).

The bottom line is that Rossby waves carry zonal momentum with them: this is the mechanism linking trade winds and westerlies that was mentioned in Chapter 1.

## 4.4 References

-Rossby and collaborators, 1939: Relation between variation in the intensity of the zonal circulation of the atmosphere and the displacement of the semi-permanent centers of action, *J. Mar. Res.*, 38-55.

-Taylor, G. I., 1923: Experiments on the motion of solid bodies in rotating fluids, *J. Fluid Mech.*, 104, 213-218.

## 4.5 Problems

**Q1.** A thunderstorm moving in a sheared flow has the following scales:  $L = 10km$ ,  $H = 10km$ ,  $U = 10ms^{-1}$ ,  $W = 1ms^{-1}$ ,  $f = 10^{-4}s^{-1}$ ,  $P' = 10hPa$ . Determine whether the geostrophic and hydrostatic approximations apply to this system.

**Q2.** An aeroplane is due to fly eastward over the ocean at  $45^\circ N$ . At some moment it is at an altitude of  $6000m$  and a pressure altimeter indicates a pressure of  $100hPa$ . The pilot maintains this pressure altitude but notices that after 1 hour the radar altimeter indicates an absolute altitude of  $5750m$ . How far, and in what direction, has the plane drifted off course? Clearly state any assumptions you make. [Hint: this question is more difficult than it looks.]

**Q3.** The derivation of the equation of motion (4.15), and its decomposition into components (4.27), (4.35) and (4.36), was quite mathematical. This question aims at re-deriving those equations from a more intuitive perspective.

- (i) Particle moving purely east-west, i.e.  $\mathbf{u} = (u, 0, 0)$  in the local frame of reference  $(\mathbf{i}, \mathbf{j}, \mathbf{k})$ . By thinking about the particle's circular motion around the Earth at constant latitude  $\phi$ , and its associated centrifugal force, show that it must experience an acceleration  $(\Omega^2 R \cos \phi + u^2/R \cos \phi + 2\Omega u)(\cos \phi \mathbf{k} - \sin \phi \mathbf{j})$ . Identify the corresponding terms in (4.27) and (4.36).

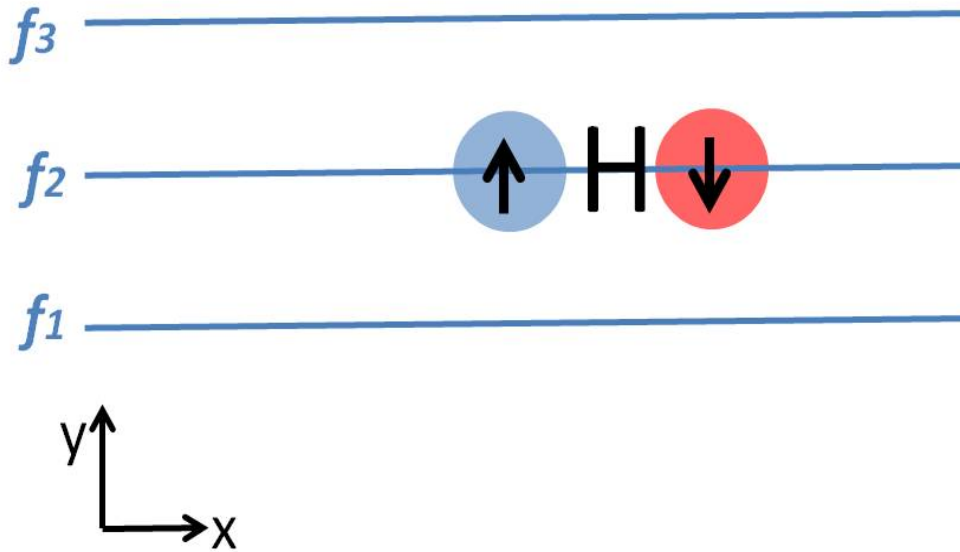


Figure 4.7: Schematic of the propagation mechanism for Rossby waves in the Northern Hemisphere ( $x$ -axis from west to east,  $y$ -axis from south to north). The horizontal line indicates lines of constant planetary vorticity ( $f$ ), increasing towards the  $+y$  direction ( $f_1 < f_2 < f_3$ ). In presence of an anticyclone, these lines are bent and, for the case shown in the figure, low latitudes air parcels move northward to the west of the anticyclone, and high latitudes air parcels move equatorward to the east (black arrows). Assuming that these parcels did not possess significant relative motion before they were disturbed by the anticyclone (i.e., their initial absolute vorticity is simply  $f$ ), the conservation of their absolute vorticity  $\zeta + f$  as they move requires that a region of  $\zeta < 0$  develops to the west of the anticyclone (blue patch), and that a region of  $\zeta > 0$  develops to the east of the anticyclone (red patch). As a result the anticyclone appears to move westward (an anticyclone corresponds to a region of  $\zeta < 0$ ), and creates a cyclone in its lee (a cyclone corresponds to  $\zeta > 0$ ). You can easily see from there why a wave of anticyclone/cyclones would naturally propagate westward.

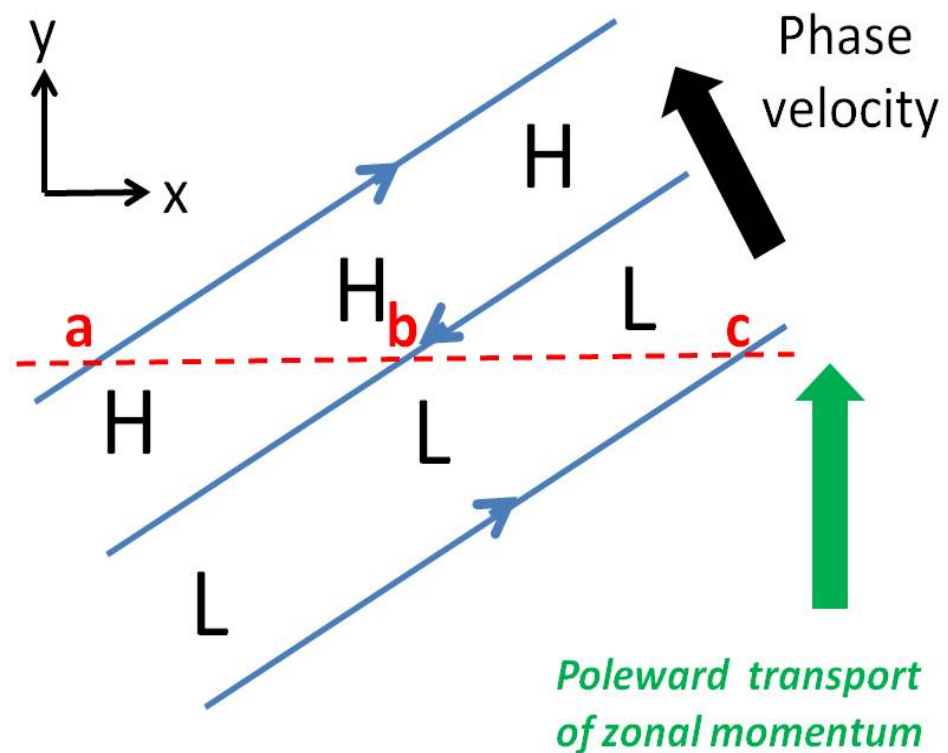


Figure 4.8: Schematic of the phase lines (blue) for a Rossby wave with  $k > 0, l < 0$  in the Northern Hemisphere (same axes as in previous figure). The flow (blue arrows) is clockwise around the high pressure (H) and anti-clockwise around the low pressure (L). The phase velocity (black arrow) is perpendicular to these motions. For the case considered here, the transport of east-west momentum is to the North (green upward arrow).

- (ii) Particle moving purely north-south, i.e.  $\mathbf{u} = (0, v, 0)$ .
- A particle of unit mass is stationary on the Earth's surface at latitude  $\phi$ . Show that its angular momentum is  $\Omega R^2 \cos^2 \phi$ .
  - Suppose this particle is subject to an impulsive force which sets it moving northward, staying on the surface. It has experienced no torque so its angular momentum must be conserved; why does this imply that it must develop an eastward velocity component?
  - If in a time  $\delta t$  the particle has reached latitude  $\phi + \delta\phi$  and acquired an eastward velocity component  $\delta u$ , show that its angular momentum is now  $[\Omega + \delta u/R \cos(\phi + \delta\phi)]R^2 \cos^2(\phi + \delta\phi)$ .
  - Using conservation of angular momentum, expanding  $\cos(\phi + \delta\phi)$  and neglecting 2nd order terms in small quantities, show that  $\delta u = 2\Omega R \delta\phi \sin \phi$  and hence that  $\delta u/\delta t = 2\Omega v \sin \phi$ . Identify this term in (4.35).
- (iii) Particle moving purely upward,  $\mathbf{u} = (0, 0, w)$ . Repeat part (ii) but consider a particle impelled vertically upwards with speed  $w$ .

**Q4.** The schematic below (Fig. 4.9) represents a front between two air masses at different temperatures. We suppose that the temperature difference is 6 K at all levels, that the front extends over a horizontal distance of 300 km and from the surface ( $P_2 = 1000hPa$ ) to a level of  $P_1 = 200hPa$ . We wish to estimate the wind at  $200hPa$  at the center of the front.

- (i) By using eqs. (4.47) and (4.49), show that the changes in zonal (east-west) wind with height can be approximated as,

$$u_2 - u_1 \approx \frac{R_d}{f} \left( \ln \frac{P_2}{P_1} \right) \frac{\partial \bar{T}}{\partial y} \quad (4.71)$$

where  $\bar{T}$  is the averaged temperature over the  $1000 - 200hPa$  layer.

- (ii) Assuming that the mean latitude of the front is  $45^\circ N$ , estimate the wind at its center at  $200hPa$ . State any assumptions made.

**Q5\*** In this question, we apply the concept of vorticity to ocean currents making up the great "subtropical gyres" (Fig. 4.10, red loop). We accept that the impact of the wind on the ocean, within the  $10^\circ - 50^\circ N$  band of latitude where the gyres are found, is to drive an equatorward flow in its

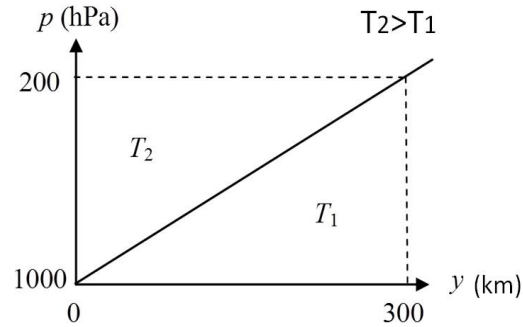


Figure 4.9: Schematics of temperature variations at a front.

upper ( $0 - 1000m$ ) layers. As water parcels flow equatorward, their absolute vorticity  $\zeta + f$  is accordingly changed. Note that throughout this question absolute vorticity is not conserved, either because of the effect of the winds, or because of the effect of frictional forces near the continental shelves.

- (i) Show that since the equatorward current is on the order of a few  $cm/s$  and its horizontal scale is that of the North Atlantic basin, the absolute vorticity of water parcel in the equatorward flow is approximately  $f$ . Determine the resulting loss of absolute vorticity along the equatorward flow.
- (ii) To close the mass budget, a “return” current must occur in the poleward direction. In the North Atlantic, this current is called the Gulf Stream. Considering that the latter has a magnitude of a few  $m/s$  and an horizontal extent of a few tens of  $km$ , do you think the approximation  $\zeta_a \approx f$  is still valid in the Gulf Stream?
- (iii) Based on your answer to the previous question, and thinking of the behaviour of absolute vorticity within a closed loop around the subtropical gyre, determine whether water parcels must gain or loose absolute vorticity in the Gulf Stream.
- (iv) By thinking about the effect of horizontal friction on vorticity explain why the Gulf Stream is found on the east coast of the US and not on the west coast of Portugal.



Figure 4.10: Schematics of the ocean circulation in the North Atlantic. The subtropical gyre is highlighted as the red “loop”. Image courtesy of the SEOS project.

**Q6.** One sometimes reads or hears that, by analogy with atmospheric low pressure systems, the flow in a bath tube which is being emptied circulates in opposite direction in the Northern and Southern Hemisphere. Give at least two reasons why this is bonkers.

**Q7.** Past Exam Question (2003 no.4).

- (i) What is vorticity and why is it useful for understanding the weather?
- (ii) Consider a long-wave pattern at the level of non-divergence in a zonal current of uniform constant velocity,  $U$ . From the principle of conservation of absolute vorticity and making the assumption that the total velocities are independent of latitude show the Rossby wave equation can be written as:

$$(U - c) \frac{\partial^2 v'}{\partial x^2} + \beta v' = 0 \quad (4.72)$$

where  $c$  is the wave velocity,  $v'$  the meridional velocity perturbation and  $\beta$  the meridional rate of change of the Coriolis parameter. Find an expression for  $c$  in terms of the wavelength and  $\beta$ .

- (iii) Calculate the wavelength of the Rossby wave if it appears stationary at  $50^\circ N$  when the zonal wind is  $50 \text{ms}^{-1}$ . For the same zonal wind, what would happen to a wave of the same wavelength at lower latitudes? (The radius of the Earth is 6371 km).

# Chapter 5

## Climate change

We defined climate in Chapter 1 as the state of the atmosphere averaged over a sufficiently long time. What that time averaging period needs to be is not clear for several reasons. First, the atmosphere on its own is capable of fluctuations of its statistics over timescales of decades. The MIT meteorologist Ed Lorenz (the one who is now associated with the “Butterfly effect”) talked about the atmosphere being an “almost intransitive system”, i.e., a system whose statistics can vary significantly over time (Lorenz, 1968). Second, the atmosphere interacts with other systems and this also leads to changes on a very wide range of timescales:

- seasonal to interannual, due to changes in sea surface temperature
- multidecadal to multi-centennial due to changes in the state of the oceans (temperature *and* circulation).
- centennial to millennial due to changes in the state of the ice sheets
- millions of years due to the motion of continental plates (tectonics)

In addition, the natural variability of solar activity, as well as the geometry of the Earth’s orbit around the Sun, and of its own axis of rotation, also introduces changes in the amount of solar energy reaching the top-of-the-atmosphere. These occur on timescales on the order of decades for the so-called “11-yr” solar cycle, and several tens of thousands of years to several hundred of thousand years for the Milankovitch cycles (see the fascinating account of their history in Imbrie and Imbrie, 1979).

We focus in this chapter on a very special type of climate change: the one caused by perturbations of the composition of the atmosphere as a result of human activities, with a particular emphasis on the burning of fossil fuel (increase in carbon dioxide concentration). Only the physical aspects are

discussed, with a focus on the ocean-atmosphere system. For a more holistic view of the problem, I highly recommend the short book by Prof D. Archer (2009).

## 5.1 Anthropogenic radiative forcing

As discussed in Chapter 2, carbon dioxide is a greenhouse gas owing to its tri-atomic structure. The major absorption band of the  $CO_2$  molecule is centered near  $15\mu m$ , which happens to be in the spectral region where the atmosphere emits most intensely infrared radiation (Fig. 1.6). Thus it is no surprise that the accumulation of carbon dioxide in the atmosphere is perturbing the heat balance of the Earth.

Figure 5.1 quantifies the magnitude of the change in downward radiation at the tropopause with respect to pre-industrial times. Carbon dioxide is seen to dominate the anthropogenic forcing, with an anomalous downward energy flux (infrared) on the order of  $1.5Wm^{-2}$ . Methane comes second with a forcing on the order of  $1Wm^{-2}$  (as you can see in the plot this number involves not only the direct effect of methane on radiation but its knock-on effect on other greenhouse gases through chemical reactions). Note that some of the anthropogenic forcings act to cool the planet, for example aerosols, because they increase the reflection of solar radiation. This effect is both direct (aerosols reflecting directly the sunlight back to space) and indirect (by promoting the formation of clouds with smaller water drops and higher albedo). Aerosols also have a warming effect by absorbing and re-emitting infrared radiation which cancel partly the previous two. The net is estimated to be a cooling on the order of  $\approx 0.25 + 0.55 = 0.8Wm^{-2}$  in Fig. 5.1.

## 5.2 Response of the atmosphere to a sudden doubling of $CO_2$

We focus here on the  $CO_2$  impact only (infrared), and consider the “thought experiment” of what would happen to the atmosphere if we were to suddenly multiply its  $CO_2$  concentration by a factor of two. Even when restricting attention to the atmosphere-ocean system only, as we’ll do, there are several timescales involved in this process:

- The first (fast, on the order of a few days to weeks) is that in which the temperature field simply reflects the local change in radiative heating induced by doubling  $CO_2$  concentrations (i.e., increases where there is

5.2. RESPONSE OF THE ATMOSPHERE TO A SUDDEN DOUBLING OF CO<sub>2</sub> 113

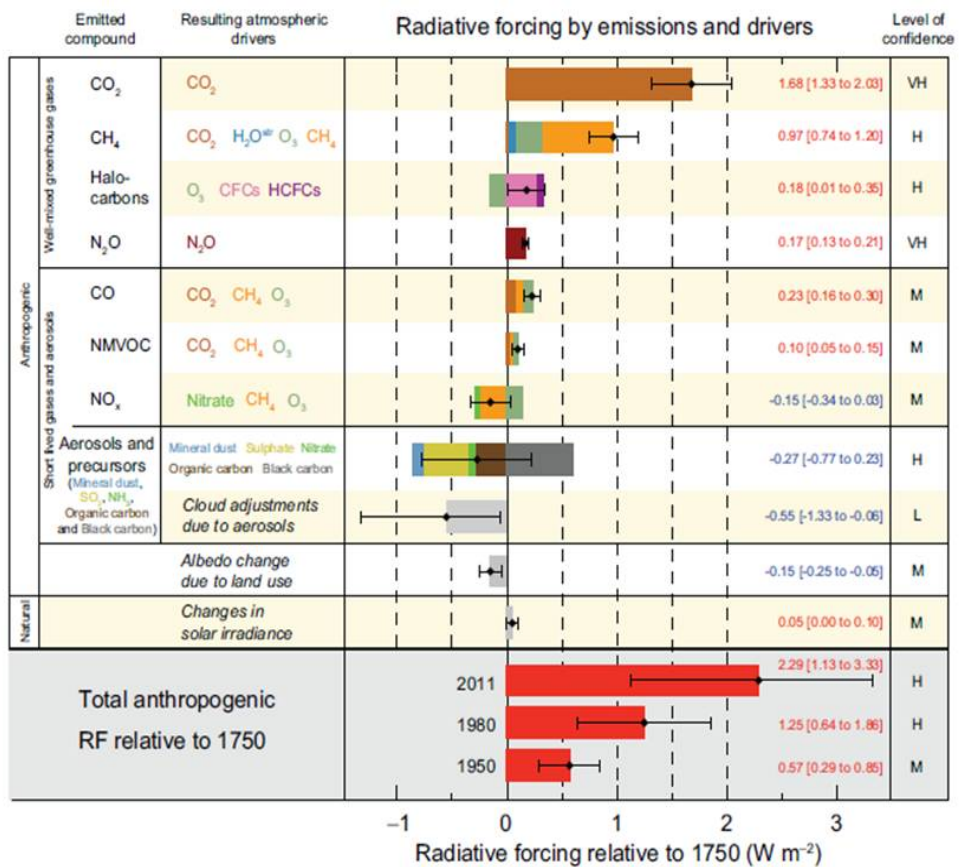


Figure 5.1: Anomalous (i.e., 2011 vs 1750) downward radiative flux at the tropopause in  $Wm^{-2}$ . The radiative forcing of various constituents is listed. Figure taken from the 5th assessment report of the IPCC.

more heating, decreases where there is less heating or more radiative cooling). This effect must also account for the interaction of these changes with convection, as discussed in Chapter 3.

- The second timescale is on the order of a few years and corresponds to a warming of the upper ocean. This warming feeds back on atmospheric temperature profiles through radiation and convection.
- Finally, on timescales of years to decades and longer, the ocean circulation moves the excess heat both laterally and vertically until a final equilibrium is reached.

### 5.2.1 Fast response: atmospheric processes only

Figure 5.2 shows the change in upward (blue) and downward (red) longwave fluxes (i.e., integrated over wavelengths greater than  $4\mu m$ ) for a doubling of  $CO_2$  concentrations from  $368ppm$  to  $736ppm$ . This calculation is the same than the one used in Chapter 2 (Fig. 2.16) for the reference case of  $CO_2$  concentrations at  $368ppm$ . Note that in this calculation, neither the temperature or the moisture profiles of the atmosphere are changed, just the amount of  $CO_2$ .

The 1st thing to notice is that there is a decrease in the upward flux (the blue curve is negative) and an increase in the downward flux (the red curve is positive). The decrease in upward flux is readily understood as an increase in the optical thickness of the atmosphere in the infrared when  $CO_2$  is doubled. Likewise, the increase in downward flux reflects the greater emissivity (Kirchoff's law) of the atmosphere as a result of the  $CO_2$  doubling. One can actually obtain a qualitative explanation for the “bell shape” structure seen in this figure using the simple calculation in Chapter 2 (section 2.4.3, isothermal atmosphere). For the case of the downward irradiance for example (red curve in Fig. 5.2), the absence of change at the TOA simply reflects the boundary condition of no downward irradiance there. The fact that the change decreases close to the Earth's surface reflects that, irrespective of the amount of  $CO_2$ , the downward irradiance ultimately converges to the “saturated value” ( $B_o$  in section 2.4.3). The maximum change seen in between reflects the greater optical depth of the atmosphere in the longwave when  $CO_2$  is added and so the fact that “saturation” is reached faster. Similar arguments can be made for the change in upward irradiance, as discussed in the Lecture.

To estimate the effect of these fluxes on the temperature, we compute the associated change in heating rate  $\Delta Q_{rad} = Q_{rad}(736ppm) - Q_{rad}(368ppm)$ ,

5.2. RESPONSE OF THE ATMOSPHERE TO A SUDDEN DOUBLING OF  $CO_2$  115

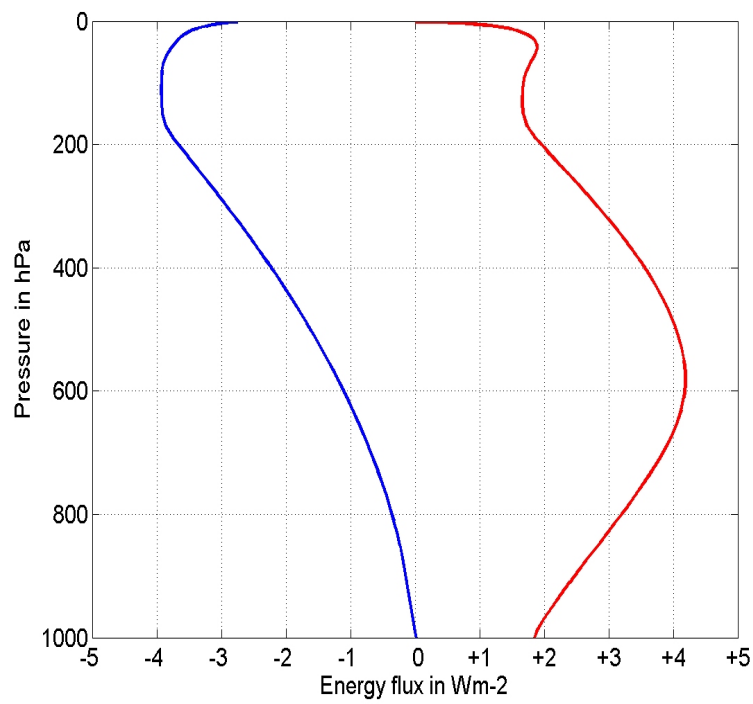


Figure 5.2: Changes in upward (blue) and downward (red) infrared fluxes (in  $Wm^{-2}$ ) as a result of a doubling of atmospheric concentrations of carbon dioxide. The changes are shown as a function of pressure.

with

$$\Delta Q_{rad} = \frac{d}{dz}(\Delta F^\downarrow - \Delta F^\uparrow) \quad (5.1)$$

using the definitions and notations in Chapter 2. The calculation in Fig. 5.2 was carried out in pressure coordinates rather than height  $z$ , so we must first re-express the previous equation in pressure coordinates. To do so we use the hydrostatic equation, yielding,

$$\Delta Q_{rad} = -\rho g \frac{d}{dP}(\Delta F^\downarrow - \Delta F^\uparrow) \quad (5.2)$$

The unit of  $Q_{rad}$  is  $Wm^{-3}$  which is not particularly helpful. It is more intuitive to convert this heating rate in units of  $K/day$  and this can be done by simply dividing by  $\rho c_p$ . (Note that  $c_p$  and not  $c_v$  is used because we focus on an infinitesimal layer between  $P$  and  $P + dP$ , i.e., a layer of constant pressure). The result is shown in Fig. 5.3. One observes anomalous heating of the troposphere, on the order of  $0.1K/day$  and a larger cooling of the upper stratosphere and mesosphere (this increase in the magnitude mostly reflects the little amount of mass at these high altitudes).

One can qualitatively understand these contrasting responses. The tropospheric warming results both from more absorption of the radiation emitted by the ground (same  $T$  but greater optical depth), and more infrared radiation emitted by the stratosphere. The stratospheric cooling is perhaps more surprising but can be understood in the following way. First, the stratosphere emits more infrared both downward and upward, which tends to cool it. In addition, it also receives less upward infrared radiation from the troposphere, which also cools it. This effect is partly opposed by the increased opacity of the stratosphere with more  $CO_2$ , i.e., more absorption of infrared radiation in the stratosphere, but the net is overwhelmingly a cooling.

The size of the anomalous heating is such that it would take about  $10days$  to reach a typical change of  $1K$  in the troposphere. In a globally averaged sense, the atmosphere sees mostly ocean as its lower boundary. Because of the latter's large thermal inertia, the surface temperature would change by much less in  $10days$ . Thus the troposphere warms up but its lower layers remain "climatological". The atmospheric lapse-rate then decreases which makes the atmosphere more stable to displacements of air parcels from low levels (Chapter 3) –note that the vertical structure in the anomalous heating in Fig. 5.3 adds further to this "boundary effect". This is reflected in weaker updrafts/downdrafts and a general weakening of the atmospheric circulation. You'll be pleased to learn that this effect was only emphasized recently in the journal *Nature Geosciences* (Bony et al., 2013).

5.2. RESPONSE OF THE ATMOSPHERE TO A SUDDEN DOUBLING OF  $CO_2$  117

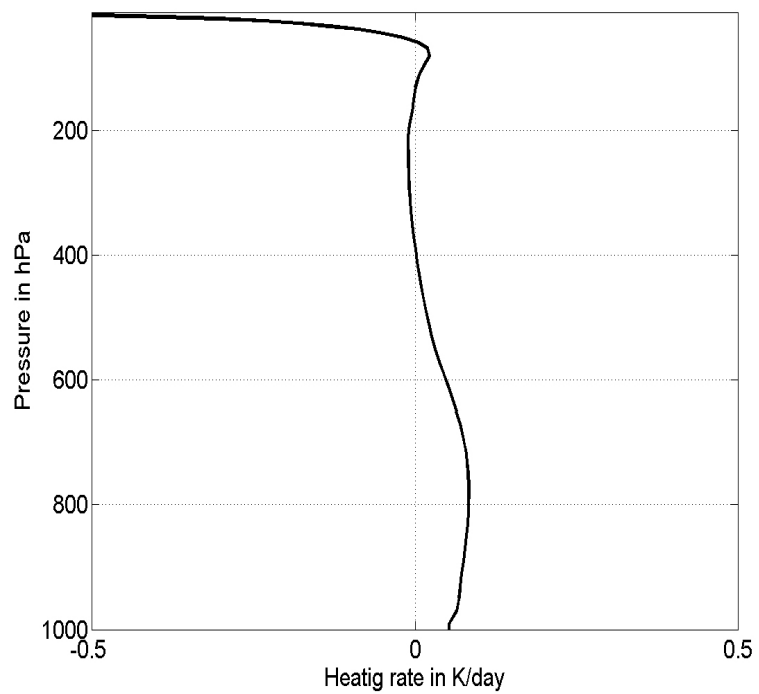


Figure 5.3: Same as Fig.5.2 but for the heating rate, expressed in  $K/day$ .

The same calculations can be carried out latitude by latitude, the result being that the tropospheric heating is more pronounced at the equator (Fig. 5.4). This can be understood from Beer's law, the reduction in upward infrared radiation at the tropopause being proportional to the amount of radiation emitted by the air column, which is greater in the Tropics. Interestingly, this tropical enhancement is opposed by a larger downward radiative flux from the stratosphere at high latitudes (this simply reflects that the tropopause is lower down at the poles than at the equator, i.e., that there is more "stratospheric mass" at the poles than at the equator). As can be seen in Fig. 5.4 though, the tropospheric effect dominates and the Tropics gain more energy than the poles when doubling  $CO_2$  concentrations.

The tropical amplification of the heating mimics the situation in the time mean, whereby the Earth experiences an energy deficit at the poles and an energy gain at the equator. Interestingly, this excess heating is truly realized in the atmosphere (infrared heating), rather than mostly absorbed at the sea surface as is the case for the time mean (see Chapter 1). In other words there is more available potential energy within the atmosphere to power the storms (Chapter 3). Assuming that conversion rates of this energy into kinetic energy of storms is unchanged, the sudden doubling of  $CO_2$  will lead to a change in the distribution of storms: either the same number but with higher winds, or less weak storms, and / or more strong storms.

### 5.2.2 Slow response: the atmosphere interacts with the upper ocean

Figure 5.2 indicates that there is a net anomalous downward radiative flux at the Earth's surface, with a magnitude  $\simeq 2Wm^{-2}$ . The upper ocean is well mixed over a layer of depth  $h \approx 100m$ , and its heat capacity per unit area is  $\rho_o c_o$  (density  $\rho_o = 1025kgm^{-3}$  and heat capacity of seawater  $c_o = 4000Jkg^{-1}K^{-1}$ , respectively) so it would take a time  $\Delta t$  to generate a change of  $1K$ , where

$$\Delta t = \rho_o c_o h \frac{1K}{2Wm^{-2}} = 6.5years \quad (5.3)$$

This rough estimate shows that the interaction with the ocean is important in setting the response of the atmosphere to a  $CO_2$  change on timescales beyond a few years.

This upper ocean warming perturbs the radiative - convective equilibrium at fixed surface temperature response discussed in the previous subsection. A new type of equilibrium must be reached, in which a warmer ocean leads to more destabilization of the atmosphere. An illustration of this effect is

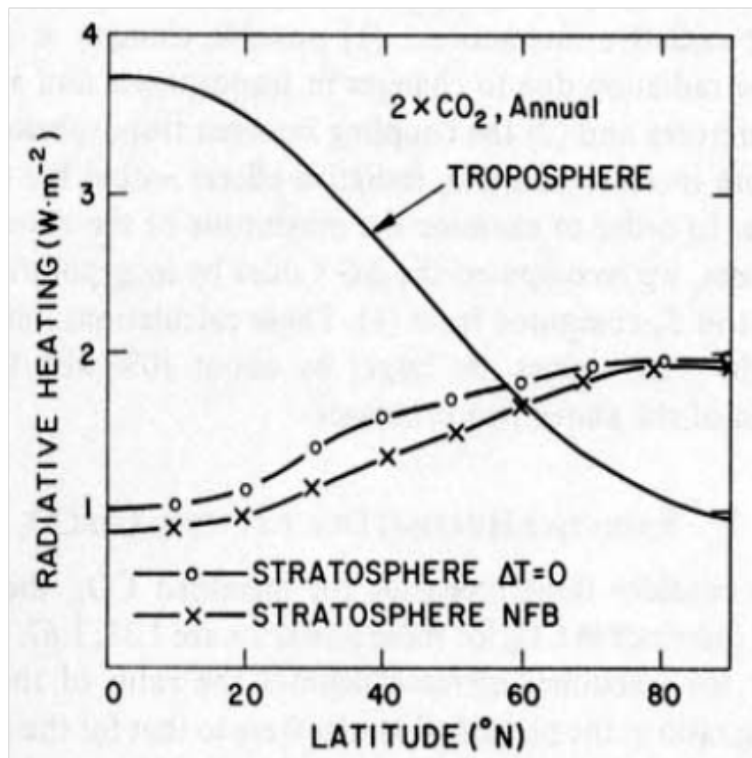


Figure 5.4: Gain in energy (in  $Wm^{-2}$ ) of the troposphere as a result of doubling  $CO_2$  concentrations. The contribution from the troposphere (continuous curve) and the stratosphere (curves with circles and crosses) to this gain (=the sum of the two) are shown. The two curves for the latter reflect different assumptions made regarding the adjustment of stratospheric temperatures. The troposphere contribution equals the reduction in the upward radiative flux at the tropopause. The stratospheric contribution equals the increase in the downward radiative flux from the stratosphere. From Ramanathan et al. (1979).

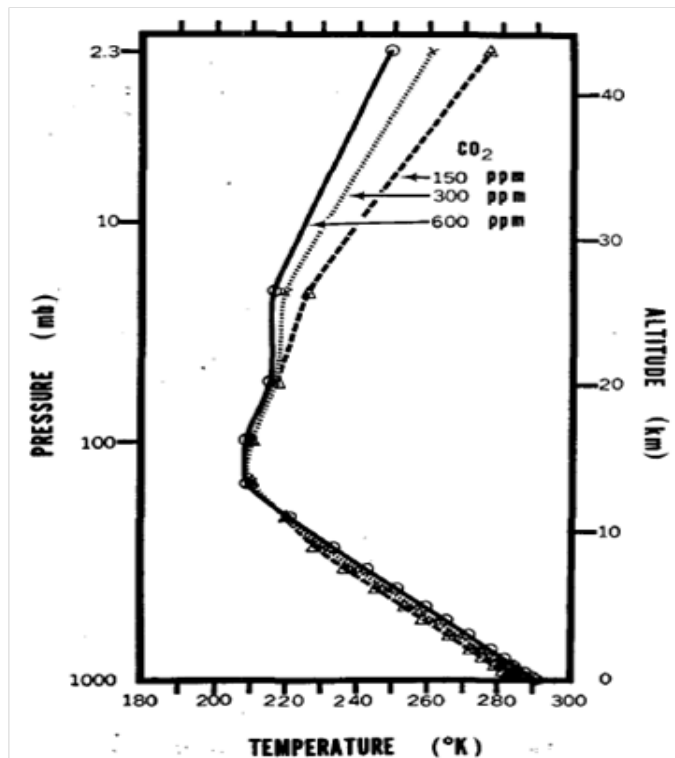


Figure 5.5: Equilibrium temperature profiles as a function of height for different carbon dioxide concentrations (and fixed relative humidity). This calculation does not include changes in ocean circulation, solely the thermal interaction of the ocean and atmosphere. From Manabe and Whetherald (1967).

provided in Fig. 5.5, based on the radiative-convective equilibrium calculations discussed in Chapter 3. Qualitatively, the response is similar to that expected from Fig.5.3, i.e., a warming of the troposphere and a cooling of the stratosphere. The main difference is that now the whole lower troposphere is warmer, as a result of the warmer sea surface temperature.

Two further important effects are introduced by the increase in sea surface temperature:

- First, because the atmosphere warms as a whole, its equilibrium vapour pressure increases. When condensation will occur, there will thus be more water falling as rain. This is the argument sometimes made regarding increased chances of flooding and rain related damages as a result of anthropogenic forcing.
- Second, since water vapour is the main greenhouse gas, its increas-

ing concentration in the atmosphere triggers a positive feedback loop: more water vapour leads to greater surface warming, which leads to greater surface evaporation and (assuming rainfall does not entirely compensate), more water vapour in the atmosphere.

### 5.2.3 Very slow response: the atmosphere interacts with the ocean circulation

Both the changes in atmospheric heating rates and sea surface temperature discussed in the previous two subsections will lead to changes in atmospheric circulation patterns (either shift or intensification, or both). These in turn will alter ocean currents and the capacity of the ocean to transport heat laterally and vertically. The associated timescales can be as fast as a decade and as long as a millenium.

Figure 5.6 (right panel) illustrates the change in ocean heat content through time in response to a sudden doubling of atmospheric  $CO_2$  in the Environmental Physics climate model (*EPcm*), a simple climate model coded in MATLAB (linked on Blackboard). One observes a rapid adjustment of tropical and high latitude upper ocean temperatures (red and blue curves), but it takes much longer to adjust the subsurface ocean temperatures (tropical in magenta, high-latitudes in cyan). This longer adjustment corresponds to the time it takes to circulate waters through the different layers in the model. If the ocean circulates water between upper and deeper layers with an intensity  $\Psi$  (in  $m^3s^{-1}$ ) and if the deep layer volume is  $V$ , then it will take a time,

$$\Delta t = V/\Psi \approx \frac{1000m \times (2.5 \times 10^{14}m^2)}{10 \times 10^6m^3s^{-1}} \approx 1,000years \quad (5.4)$$

to do so. To obtain this number, a thickness of  $1000m$  was used for the deep layer, a surface area equal to that of one hemisphere (*EPcm* covers only one such hemisphere) and a value of  $10^7m^3s^{-1}$  was used for  $\Psi$  (this is about ten times the volume flux of all the rivers of the world).

The timescale in (5.4) is clearly reflected in the top-of-the-atmosphere net radiative flux (left panel) which, after a sudden increase to  $\simeq 4Wm^{-2}$  associated with the initial  $CO_2$  doubling, only very slowly goes back to zero (the new equilibrium)<sup>1</sup>.

---

<sup>1</sup>*EPcm* also displays the fast (weeks) and slow (years) response discussed in the previous subsections. You can very easily convince yourself of this by running the model over one month, over one year, etc, to see the rich behaviour of atmospheric responses to a doubling of  $CO_2$ .

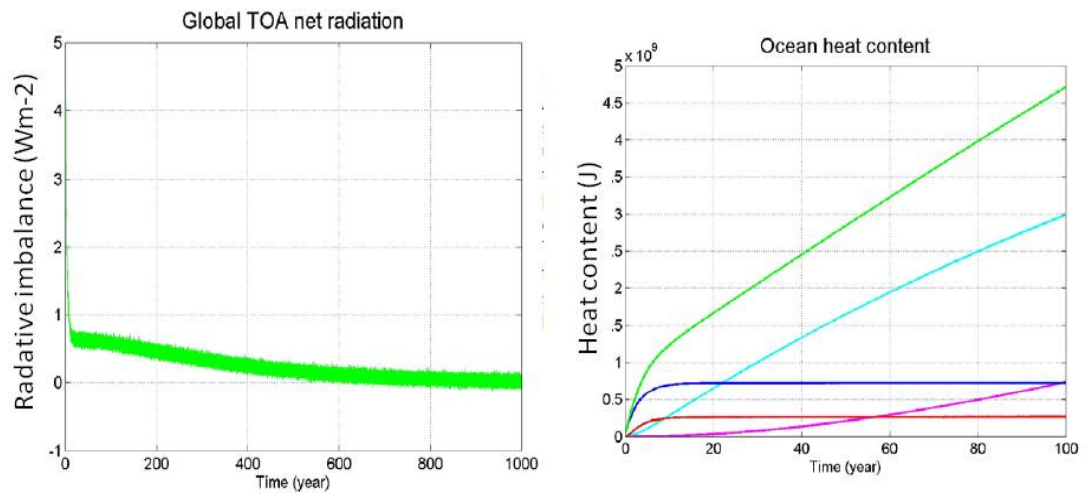


Figure 5.6: Changes in (right) heat content (in  $J$ ) and (left) top-of-the-atmosphere net radiative flux (in  $Wm^{-2}$ ) in response to a sudden doubling of atmospheric  $CO_2$  concentrations in  $EPcm$ . The different colors in the right panel correspond to different oceanic layers (red=upper tropics, blue=upper high latitudes, magenta=deep tropics, cyan=deep high latitudes).

The link between TOA radiative imbalance and ocean heat storage simply reflects conservation of energy (Chapter 1):

$$\iint \Delta F_{TOA} dx dy = \frac{\partial}{\partial t} \iiint \rho_o c_o \Delta T_o dx dy dz + \dots \quad (5.5)$$

in which  $\Delta F_{TOA}$  is the net radiative imbalance at the TOA and  $\Delta T_o$  is the change in ocean temperature caused by doubling atmospheric  $CO_2$  concentrations. Terms not explicitly written in this equation are the melting of the cryosphere, and the weak storage of heat in the atmosphere and land.

## 5.3 Climate change in realistic models and observations

This section very briefly summarises the slides discussed in the last lecture. Regarding climate models:

- Climate models are numerical machines solving a large set of coupled, non linear, ordinary differential equations. Their main issue is the difficult parameterization of processes occurring on a spatial scale smaller than their grid size (clouds, convection, ocean turbulence, etc).
- In response to an increase in atmospheric  $CO_2$  concentration (and all other forcings discussed in Fig. 1), the models show an increase in global averaged surface temperature through time. The models all capture the “troposphere warms / stratosphere cools” signature. Ocean warming is sluggish and probably more diffusive in the models than in the real world.

Concerning the observations:

- Observations do show the expected opposite temperature trends in the troposphere and the stratosphere. The global averaged surface temperature has also increased since the beginning of the instrumental record (early 20th century), with pronounced decadal timescale fluctuations.
- Top-of-the-atmosphere net radiative fluxes show an imbalance on the order of  $+0.5 W m^{-2}$  since 2001 (net heating). This is, as expected, smaller than accounted for by anthropogenic forcing (Fig. 5.1) since this must account for the extra emission of infrared radiation by the ocean+atmosphere (“the response” to anthropogenic forcing). Observations of global ocean heat content agree with the TOA imbalance qualitatively and quantitatively.

If you are interested to read more about the role of ocean heat uptake in this problem, a recent and non technical summary is provided in Whitmarsh et al. (2015).

Predictions of the 21st century climate rely entirely on climate models and as such can be debated and criticized at will because of the many imperfections of the models. Likewise, all attempts to “prove” climate change through analysis of existing timeseries of surface temperature (and other relevant climatic timeseries) are endlessly subject to criticisms on statistical grounds. My personal take is that we can say something from first principles about the timescales response to, and the magnitude of the forcing associated with anthropogenic accumulation of atmospheric carbon dioxide. The timescales are mesmerizing: as we’ve seen in section 5.2, the interaction between the atmosphere and the ocean leads, at fixed atmospheric  $CO_2$  concentration, to adjustment times of several centuries; Earth system models with interactive  $CO_2$  suggest adjustment times of several tens of thousands of years (Archer, 2009). Thus it is not simply the climate we or our children live in which we are affecting. Overall, we should keep alive the “back-of-the-envelope” spirit: it shows that the current rate of accumulation of  $CO_2$  in the atmosphere is a major forcing in terms of rising sea level, melting of the cryosphere, etc (Czaja, 2012).

## 5.4 References

-Archer, D., 2009: “The Long Thaw: how humans are changing the next 100,000 years of Earth’s climate”, Princeton University Press, 180pp.

-Bony et al., 2013: Robust direct effect of carbon dioxide on tropical circulation and regional precipitation, *Nature Geoscience*, 6, 447-451.

-Czaja, 2012: A consideration of the forcings of climate change using simple physics, Discussion paper 2 of the Grantham Institute for Climate Change.

-Imbrie and Imbrie, 1979: “Ice ages, solving the mystery”, Harvard University Press, 224 p.

-IPCC Fifth Assessment Report, 2013: please see Blackboard for a web link to the various sections. If you have the stamina, this is an excellent source of information / figures for issues related to climate change.

-Lorenz, E. N., 1968: Climatic Determinism, AMS monograph, 8, 30, 1-3.

-Whitmarsh, et al., 2015: Ocean heat uptake and the global temperature record, Grantham Institute briefing paper No 14.

## 5.5 Problems

**Q1. Sea ice melting.** Satellite observations suggest that the Earth has been gaining  $0.5Wm^{-2}$  of energy at the top-of-the-atmosphere since the early 2000s. Estimate how long it would take to (i) melt Arctic sea ice (ii) increase the temperature of the global ocean by  $0.1K$ , were all this energy available to do so. [Data: latent heat of fusion  $l_f = 3 \times 10^5 Jkg^{-1}$ , ice density  $\rho_i = 916kgm^{-3}$ , ice thickness  $h_i = 2m$ , ocean heat capacity  $c_o = 4000Jkg^{-1}K^{-1}$ , ocean density  $\rho_o = 1025kgm^{-3}$ , average depth of the oceans  $h_o = 3800m$ .]

**Q2. Emission level.** One way to think about the response of tropospheric temperature to a sudden increase in  $CO_2$  concentration is illustrated in Fig. 1. Before the increase, the atmosphere effectively emits at a height  $z_e$ , defined so that the total outgoing longwave radiation by the Earth (OLR) equals  $\sigma T(z_e)^4$  in which  $\sigma$  is Stefan-Boltzmann constant.

- (i) Compute the emission level of the Earth, making a reasonable assumption regarding surface temperature and lapse-rate.
- (ii) Explain why, as the  $CO_2$  concentration is suddenly doubled, the emission level must increase.
- (iii) Estimate this increase if, at equilibrium, the troposphere and the Earth's surface warm by  $3K$ , assuming no change in lapse-rate.
- (iv) The lapse-rate is empirically found to decrease with surface warming in climate models. Would this tend to amplify the surface temperature change or to reduce it?

**Q3. Clausius-Clapeyron scaling.** From Thermodynamics (Year 2), the pressure of water vapour at equilibrium (denoted here by the symbol  $e_{eq}$ ) with liquid water satisfies, at a given temperature  $T$ ,

$$\frac{de_{eq}}{dT} = \frac{s_v - s_l}{v_v - v_l} \quad (5.6)$$

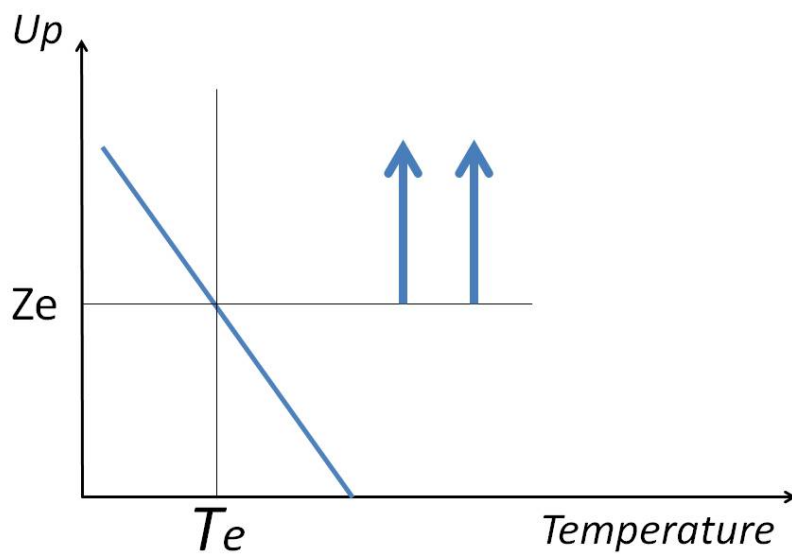


Figure 5.7: Schematic of temperature as a function of height, indicating the emission temperature and emission level. The outgoing longwave radiation (blue arrows) can be thought of originating from this level.

in which  $s$  is the specific entropy,  $v$  the specific volume and the subscripts  $l$  and  $v$  refer to liquid and gas phases, respectively.

- (i) Show that this can be rewritten as

$$\frac{de_{eq}}{dT} \simeq \frac{l_v}{Tv_v} \quad (5.7)$$

stating any assumptions made.

- (ii) Show that after using the ideal gas law this can be further rewritten as,

$$\frac{de_{eq}}{dT} \simeq \frac{e_{eq}l_v}{R_vT^2} \quad (5.8)$$

in which  $R_v = k_B/m_v$ ,  $m_v$  being the mass of a water molecule.

- (iii) Use this expression to prove that equilibrium vapour pressure increases by 7 % for every degree kelvin increase in temperature. [Data:  $l_v = 2.5 \cdot 10^6 \text{ Jkg}^{-1}$ ,  $R_v = 461 \text{ Jkg}^{-1} \text{ K}^{-1}$ ].

**Q4.** Using the formula in **Q3** from Chapter 4, discuss whether you agree with the following statement taken from a popular science article about the very anomalous 2013-2014 winter weather in the Northern Hemisphere:

“The Jet Stream is driven in part by the temperature difference between cold Arctic air and the warmer air of the middle latitudes. Because the Arctic is warming more rapidly than the rest of the planet, that difference is shrinking. This ought to produce a less potent Jet Stream.”

[Info: the polar warming amplification ( $\approx 1K$ ) is restricted to a surface layer extending roughly from  $1000hPa$  to  $600hPa$ .]

**Q5. Ocean heat uptake.** We consider a “box-model” of the climate system to predict changes in top-of-the-atmosphere net radiative flux in response to a sudden increase in atmospheric  $CO_2$  concentrations. The ocean is decomposed into an upper (thickness  $h = 50m$ ) and a deep layer (thickness  $H = 2000m$ ). The density and specific heat of seawater are denoted by  $\rho_o = 1025 \text{ kgm}^{-3}$  and  $c_o = 4100 \text{ Jkg}^{-1} \text{ K}^{-1}$ , respectively. At the top-of-the-atmosphere, the perturbation in the net radiative flux (positive downwards) is written as  $N' = F' - \alpha T'$  in which  $F' = 4 \text{ Wm}^{-2}$  for  $t > 0$  (and  $F' = 0$  for  $t < 0$ ) is the anthropogenic forcing,  $T'$  is the global surface temperature anomaly, and  $\alpha = 1.6 \text{ Wm}^{-2} \text{ K}^{-1}$  is the climate feedback parameter.

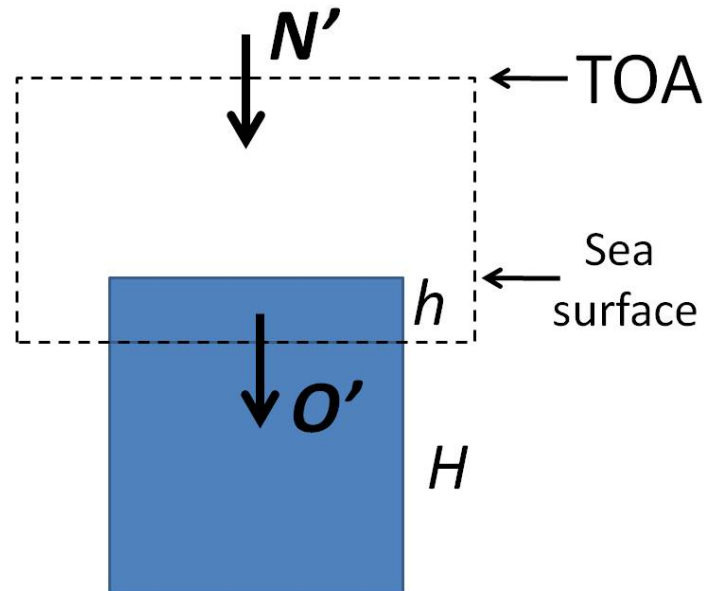


Figure 5.8: Schematic of a box-model for ocean heat uptake  $O'$ .

- (i) Find the timescale  $t_u$  beyond which one can neglect the heat capacity of the upper ocean layer. Likewise, until which timescales  $t_d$  is the deep ocean acting like a heat reservoir?
- (ii) Discuss qualitatively and quantitatively the TOA radiative imbalance on short timescales ( $\ll t_u$ ).
- (iii) Climate models suggest that on intermediate timescales ( $\gg t_u$  but  $\ll t_d$ ), the ocean heat uptake can be reasonably well modeled as  $O' \approx \kappa T'$  where  $\kappa = 0.5 \text{ W m}^{-2} \text{ K}^{-1}$  is an “heat uptake efficiency”. Discuss qualitatively and quantitatively the radiative imbalance at the TOA on these timescales.
- (iii) Discuss qualitatively and quantitatively the equilibrium state of the model.

# Chapter 6

## Appendices

### 6.1 Radiative transfer

#### 6.1.1 Radiation pencils vs. photon showers

You might have been wondering how to relate the concept of radiation intensity with the quantum physics ideas you've been learning so far. To do so, consider an horizontal plane and focus on computing the monochromatic irradiance across a surface area  $A$  (Fig. 6.1). In Chapter 2, we have been writing this as the integral of the radiation intensity  $I_\lambda$  over solid angle:

$$F_\lambda = \int I_\lambda \cos \theta d\Omega \quad (6.1)$$

A more intuitive view is to count photons with energy  $E$  such that  $hc/\lambda \leq E \leq hc/\lambda + dE$  crossing the horizontal surface  $A$  per unit time. In the direction making an angle  $\theta$  with the vertical, these occupy the volume of the parallelepiped of (slanted) side  $cdt$ . This volume is simply  $dV = Acdt \cos \theta$ . If  $n_E dE$  denotes the number density of photons with the required energy, the number of photons contained in this volume is  $dN_1$ :

$$dN_1 = (Acdt \cos \theta)n_E dE \quad (6.2)$$

Now, all the photons in this volume do not travel towards the surface in the direction  $\theta$ . If we were in 1D, we would simply introduce a factor  $1/2$  at this stage, to represent photons travelling upward or downward. In 3D, we use the solid angle and write that in that volume  $dV$  only a fraction  $\chi d\Omega/4\pi$  travel towards the surface along the direction  $\theta$  (if the radiation were isotropic we would have  $\chi = 1$ ; if the radiation were entirely coming from the direction  $\theta$ , we would have  $\chi d\Omega/4\pi = \delta(\theta' - \theta)$  where the latter symbol reflects the

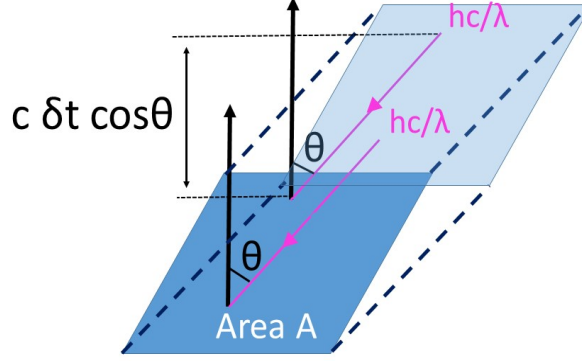


Figure 6.1: Calculation of the irradiance as a result of photons with energy  $E = hc/\lambda$  travelling from a given direction at speed  $c$  towards the surface  $A$ . This “photon shower” view contrasts with that of the “radiation pencil” illustrated in Fig. 2.4 in Chapter 2.

Dirac symbol). The number of photons travelling towards the surface along the direction  $\theta$  and contained within the parallelepiped is thus  $dN_2$ :

$$dN_2 = dN_1 \chi d\Omega / 4\pi = (A c dt \cos \theta) n_E dE \chi d\Omega / 4\pi \quad (6.3)$$

Since these all carry approximately the energy  $E = hc/\lambda$ , the amount of radiation energy through  $A$  per unit time, per unit energy interval is obtained by summing over all parallelepipeds. Let’s call this  $dF_E$ :

$$dF_E = \sum dN_2 E / (A dt) = \int c E n_E dE \chi \cos \theta d\Omega / 4\pi \quad (6.4)$$

Physically,  $dF_E$  represents exactly the same quantity as  $F_\lambda d\lambda$ . Thus,

$$\left( \int c E n_E \chi \cos \theta d\Omega / 4\pi \right) dE = \left( \int I_\lambda \cos \theta d\Omega \right) d\lambda \quad (6.5)$$

Using the fact that  $|dE| = hc d\lambda / \lambda^2$ , this suggests the following formula for the intensity of radiation,

$$I_\lambda = \frac{\chi}{4\pi} \times (c n_E \frac{hc}{\lambda^2}) \times \frac{hc}{\lambda} \quad (6.6)$$

I’ve written it as the product of three terms, to reflect more clearly its meaning. The first term is a geometric factor reflecting the geometry of the radiation. The second is the expected “transport” term considering that photons

travel at speed  $c$  and accounting for the conversion “per unit energy interval” to “per unit wavelength interval”. The last term is simply the energy of the photons associated with the monochromatic radiation at wavelength  $\lambda$ .

### 6.1.2 Conservation of intensity

An interesting use of (6.6) is that the three terms identified on its right hand side are conserved if photons do not interact with matter (scattering, absorption). This is so because photons do not interact with each other so that their statistics are unchanged in absence of scattering or absorption. This provides a straightforward explanation why  $I_\lambda$  is conserved in absence of scattering or absorption.

### 6.1.3 Application to blackbody radiation

For this special case, we can use  $\chi = 1$  (isotropic) and also the result from Quantum Physics (Year 2):

$$n_E = \frac{8\pi E^2}{c^3 h^3} \times \frac{1}{e^{E/k_B T} - 1} \quad (6.7)$$

Inserting this equation into (6.6), we recover eq. (2.1) in Chapter 2.

## 6.2 Thermodynamics of moist air

### 6.2.1 Entropy of cloudy air

We consider a sample of air in which vapour and liquid phases are assumed to be in equilibrium, i.e.,  $e = e_{eq}(T)$  ( $RH = 1$ , see Fig. ??). If  $m$  denotes the total mass of this sample, its specific entropy  $s$  satisfies,

$$ms = m_d s_d + m_v s_v + m_l s_l \quad (6.8)$$

in which  $s_d, s_v$  and  $s_l$  are the specific entropies for dry air, vapour and liquid water, respectively. These are known functions of temperature and pressure:

$$s_d = s_{d,ref} + c_{p,d} \ln \frac{T}{T_{ref}} - R_d \ln \frac{P_d}{P_{ref}} \quad (6.9)$$

$$s_v = s_{v,ref} + c_{p,v} \ln \frac{T}{T_{ref}} - R_v \ln \frac{e}{P_{ref}} \quad (6.10)$$

and

$$s_l = s_{l,ref} + c_l \ln \frac{T}{T_{ref}} \quad (6.11)$$

(The constants  $T_{ref}$  and  $P_{ref}$  are arbitrary values where we assume we know the entropies).

Using the fact that on the vapour - liquid phase boundary  $s_v - s_l = l_v/T$  where  $l_v$  is the latent heat of vaporization, we have,

$$s = (1 - q_t)s_d + q_v\left(\frac{l_v}{T} + s_l\right) + q_l s_l \quad (6.12)$$

in which we have introduced the specific humidity  $q_v$ , specific content of liquid water  $q_l$  and total specific content of water  $q_t = q_v + q_l$ . Rearranging,

$$s = (1 - q_t)s_d + \frac{l_v q_v}{T} + q_t s_l \quad (6.13)$$

After using the formulas for  $s_d$  and  $s_l$ , this can be rewritten as,

$$s = s_{ref} + [(1 - q_t)c_{p,d} + q_t c_l] \ln \frac{T}{T_{ref}} - (1 - q_t)R_d \ln \frac{P_d}{P_{ref}} + \frac{l_v q_v}{T} \quad (6.14)$$

in which  $s_{ref} = (1 - q_t)s_{d,ref} + q_t s_{l,ref}$ . Considering that  $q_t \ll 1$ , this formula can be approximated as,

$$s \approx s_{ref} + c_{p,d} \ln \frac{T}{T_{ref}} - R_d \ln \frac{P_d}{P_{ref}} + \frac{l_v q_v}{T} \quad (6.15)$$

which is the form used in Chapter 3.

### 6.2.2 A general formula for the Brunt-Vaisala frequency\*

We will start from (3.5) and, to simplify this expression further, we use the fact that  $\alpha$  is a state function, i.e., a mathematical function of any two thermodynamic variables (this is only true because of our assumption of thermodynamic equilibrium). Because of the additional assumption of isentropic ascent, entropy  $s$  is a natural choice. We'll take pressure  $P$  (the total pressure,  $P = P_d + e$ ) as the other variable,

$$\alpha = \alpha(P, s) \quad (6.16)$$

As a result, and assuming small perturbations,

$$\alpha_e - \alpha_p \approx \left( \frac{\partial \alpha}{\partial s} \right)_P (s_e - s_p) \quad (6.17)$$

(the term involving pressure changes drops because of our assumption that the environment and the parcel are at the same pressure). Using one of Maxwell's relations, this can be rewritten as,

$$\alpha_e - \alpha_p \approx \left( \frac{\partial T}{\partial P} \right)_s (s_e - s_p) \quad (6.18)$$

At this stage we haven't actually used that  $s_p = cst$ . Following the same procedure used in the dry case when we considered how  $\theta$  is conserved by a parcel moving upwards or downwards, we write,

$$s_e - s_p \approx \frac{ds_e}{dz} (z_p - z_o) \quad (6.19)$$

As a result, the parcel's motion obeys,

$$\frac{d^2 z_p}{dt^2} = -\frac{g}{\alpha_e} \left( \frac{\partial T}{\partial P} \right)_s \frac{ds_e}{dz} (z_p - z_o) \quad (6.20)$$

showing that the Brunt-Vaisala frequency is,

$$N^2 = \frac{g}{\alpha_e} \left( \frac{\partial T}{\partial P} \right)_s \frac{ds_e}{dz} \quad (6.21)$$

Stepping back from all this Thermodynamic, we realize that we have actually not explicitly introduced moisture here –the above derivation is entirely general. For example, in the case of pure dry air ( $P = P_d$ ), we recover (3.13) by using  $s = c_{p,d} \log \theta$ , and  $(\partial T / \partial P)_{s_d} = \alpha_d / c_{p,d}$  (since for dry air,  $ds = c_{p,d} dT / T - R_d dP / P$  and  $P_d \alpha_d = R_d T$  from the ideal gas law).

Acknowledging that at constant entropy, temperature always increases with pressure ( $(\partial T / \partial P)_s > 0$ ), (6.21) provides a fairly simple rule to test the stability of a temperature profile (for the case of either pure dry air, or cloudy air in thermodynamic equilibrium): the profile is stable only if the entropy increases with height.

## 6.3 Dynamics of rotating fluids

### 6.3.1 Formula for $D/Dt$ in a change of frame of reference

Consider any vector  $\mathbf{A}$ , which can be written in either an inertial frame with orthonormal axes  $(\mathbf{i}_I, \mathbf{j}_I, \mathbf{k}_I)$ , or in a rotating frame with orthonormal axes  $(\mathbf{i}_R, \mathbf{j}_R, \mathbf{k}_R)$ ,

$$\mathbf{A} = A_{x,I} \mathbf{i}_I + A_{y,I} \mathbf{j}_I + A_{z,I} \mathbf{k}_I = A_{x,R} \mathbf{i}_R + A_{y,R} \mathbf{j}_R + A_{z,R} \mathbf{k}_R \quad (6.22)$$

Taking the  $(D/Dt)_I$  of this equation, that is the rate of change of vector  $\mathbf{A}$  in the inertial frame, we have,

$$\left(\frac{D\mathbf{A}}{Dt}\right)_I = \left(\frac{DA_{x,I}}{Dt}\right)_I \mathbf{i}_I + \left(\frac{DA_{y,I}}{Dt}\right)_I \mathbf{j}_I + \left(\frac{DA_{z,I}}{Dt}\right)_I \mathbf{k}_I \quad (6.23)$$

[NB: were we to take  $(D\mathbf{A}/Dt)_R$  we would obtain  $(D\mathbf{A}/Dt)_R = (DA_{x,R}/Dt)_R \mathbf{i}_R + (DA_{y,R}/Dt)_R \mathbf{j}_R + (DA_{z,R}/Dt)_R \mathbf{k}_R$  since the axes  $(\mathbf{i}_R, \mathbf{j}_R, \mathbf{k}_R)$  do not move in the rotating frame.]

Equation (6.23) is also,

$$\left(\frac{D\mathbf{A}}{Dt}\right)_I = \left(\frac{DA_{x,R} \mathbf{i}_R}{Dt}\right)_I + \left(\frac{DA_{y,R} \mathbf{j}_R}{Dt}\right)_I + \left(\frac{DA_{z,R} \mathbf{k}_R}{Dt}\right)_I \quad (6.24)$$

The r.h.s can be further expanded using the product rule, for example for the 1st term:

$$\left(\frac{DA_{x,R} \mathbf{i}_R}{Dt}\right)_I = A_{x,R} \left(\frac{D\mathbf{i}_R}{Dt}\right)_I + \left(\frac{DA_{x,R}}{Dt}\right)_I \mathbf{i}_R \quad (6.25)$$

Using (4.10), this is also,

$$\left(\frac{DA_{x,R} \mathbf{i}_R}{Dt}\right)_I = A_{x,R} \left(\frac{D\mathbf{i}_R}{Dt}\right)_I + \left(\frac{DA_{x,R}}{Dt}\right)_R \mathbf{i}_R \quad (6.26)$$

hence:

$$\left(\frac{D\mathbf{A}}{Dt}\right)_I = \left(\frac{D\mathbf{A}}{Dt}\right)_R + A_{x,R} \left(\frac{D\mathbf{i}_R}{Dt}\right)_I + A_{y,R} \left(\frac{D\mathbf{j}_R}{Dt}\right)_I + A_{z,R} \left(\frac{D\mathbf{k}_R}{Dt}\right)_I \quad (6.27)$$

For the choice of a rotating frame centred at the Earth's core, with  $\mathbf{k}_R = \mathbf{k}_I$  (parallel to the axis of rotation of the Earth) and  $(\mathbf{i}_R, \mathbf{j}_R)$  rotating at the angular velocity of the Earth  $\Omega = 2\pi/1day$ , we obtain,

$$\left(\frac{D\mathbf{A}}{Dt}\right)_I = \left(\frac{D\mathbf{A}}{Dt}\right)_R + \boldsymbol{\Omega} \times \mathbf{A} \quad (6.28)$$

since  $(D\mathbf{i}_R/Dt)_I = \boldsymbol{\Omega} \times \mathbf{i}_R$ ,  $(D\mathbf{j}_R/Dt)_I = \boldsymbol{\Omega} \times \mathbf{j}_R$  and  $(D\mathbf{k}_R/Dt)_I = \mathbf{0}$ .

### 6.3.2 Kelvin's identity

The rate of change of the contribution  $\mathbf{u}_I \cdot d\mathbf{s}$  of a small part of the circuit in eq. (4.57) can be written as,

$$\frac{D}{Dt}(u\delta x + v\delta y + w\delta z) = \frac{Du}{Dt}\delta x + \frac{Dv}{Dt}\delta y + \frac{Dw}{Dt}\delta z + u\delta u + v\delta v + w\delta w \quad (6.29)$$

in which, in this section only, we denote by  $u, v, w$  the velocities in the inertial frame and  $x, y, z$  the associated coordinates. It follows that for any segment of the circuit,

$$\left( \frac{D}{Dt} \int \mathbf{u}_I \cdot d\mathbf{s} \right)_I = \int \left( \frac{D\mathbf{u}_I}{Dt} \right)_I \cdot d\mathbf{s} + \left[ \frac{1}{2} \mathbf{u}_I^2 \right], \quad (6.30)$$

where the last term is the difference in the values between the end points. For a closed circuit this term vanishes, leading to eq. (4.57).

### 6.3.3 The vorticity equation\*

To obtain an equation for the vorticity vector  $\boldsymbol{\zeta}$  (all components, not only its vertical component), “all you need” is to take the curl of (4.15), and use vector identities. In practice though, it is pretty tedious and so, to do this in an efficient way though we need to a little bit of preparatory work. First, we rewrite (4.15) as,

$$\frac{\partial \mathbf{u}_R}{\partial t} + (\mathbf{u}_R \cdot \nabla) \mathbf{u}_R = -\nabla \Phi - \alpha \nabla P - 2\boldsymbol{\Omega} \times \mathbf{u}_R + \mathbf{F}_{fric} \quad (6.31)$$

Then we use the following vector identity,

$$\nabla(\mathbf{A} \cdot \mathbf{B}) = (\mathbf{A} \cdot \nabla) \mathbf{B} + (\mathbf{B} \cdot \nabla) \mathbf{A} + \mathbf{A} \times (\nabla \times \mathbf{B}) + \mathbf{B} \times (\nabla \times \mathbf{A}) \quad (6.32)$$

to obtain,

$$\frac{\partial \mathbf{u}_R}{\partial t} + (2\boldsymbol{\Omega} + \boldsymbol{\zeta}) \times \mathbf{u}_R = -\nabla(\Phi + \mathbf{u}_R^2/2) - \alpha \nabla P + \mathbf{F}_{fric} \quad (6.33)$$

The quantity  $2\boldsymbol{\Omega} + \boldsymbol{\zeta}$  that appears in this equation requires a physical interpretation. It is the sum of the vorticity of the relative flow ( $\boldsymbol{\zeta}$ ) and the vorticity of the solid body rotation at angular velocity  $\boldsymbol{\Omega}$ . We will call it from now on the absolute vorticity,

$$\boldsymbol{\zeta}_a \equiv 2\boldsymbol{\Omega} + \boldsymbol{\zeta} \quad (6.34)$$

and measures the total local spin (planetary + relative) of a fluid parcel – see the discussion in Section 1.3.2. Typically in a cyclone, the relative and planetary vorticity add up, so the total spin can be quite large. They tend to cancel each other in anticyclones.

To see where the  $2\boldsymbol{\Omega}$  comes from, acknowledge that the velocity of the Earth’s solid body rotation is  $\boldsymbol{\Omega} \times \mathbf{r} = \Omega r \cos \phi \mathbf{i}$ , so that it is a function of latitude and radius  $r = R + z$ . As discussed in the lecture, the gradient

(or shear) in velocity associated with the variations with latitude ( $\phi$ ) adds up to the shear introduced by the variations with  $r$  to produce a planetary vorticity vector always parallel to  $\boldsymbol{\Omega}$ . To be more quantitative one needs to do the math properly. A simple derivation is to compute  $\nabla \times (\boldsymbol{\Omega} \times \mathbf{r})$  in a Cartesian coordinate system centred at the Earth's core (since the curl of a vector must be independent of the coordinate system used to compute it, we might as well use the simplest coordinate system –we'll denote it by  $\mathbf{i}', \mathbf{j}', \mathbf{k}'$ , the latter being parallel to  $\boldsymbol{\Omega}$ ). Using the vector identity,

$$\nabla \times (\mathbf{A} \times \mathbf{B}) = \mathbf{A}(\nabla \cdot \mathbf{B}) - \mathbf{B}(\nabla \cdot \mathbf{A}) + (\mathbf{B} \cdot \nabla)\mathbf{A} - (\mathbf{A} \cdot \nabla)\mathbf{B} \quad (6.35)$$

this becomes  $\nabla \times (\boldsymbol{\Omega} \times \mathbf{r}) = \boldsymbol{\Omega}(\nabla \cdot \mathbf{r}) - \mathbf{r}(\nabla \cdot \boldsymbol{\Omega}) + (\mathbf{r} \cdot \nabla)\boldsymbol{\Omega} - (\boldsymbol{\Omega} \cdot \nabla)\mathbf{r}$ . The second and third terms are zero because  $\boldsymbol{\Omega}$  is a constant vector. Since  $\nabla \cdot \mathbf{r} = 3$  and  $(\boldsymbol{\Omega} \cdot \nabla)\mathbf{r} = \boldsymbol{\Omega}\partial(z\mathbf{k}')/\partial z = \boldsymbol{\Omega}$ , we get  $\nabla \times (\boldsymbol{\Omega} \times \mathbf{r}) = 3\boldsymbol{\Omega} - \boldsymbol{\Omega} = 2\boldsymbol{\Omega}$ .

We are now ready to take the curl of (6.33). Note first that the first term on the r.h.s. of (6.33) will not contribute since  $\nabla \times \nabla = \mathbf{0}$ . So we simply have,

$$\frac{\partial \boldsymbol{\zeta}_a}{\partial t} + \nabla \times (\boldsymbol{\zeta}_a \times \mathbf{u}_R) = \nabla \times (-\alpha \nabla P + \mathbf{F}_{fric}) \quad (6.36)$$

where we have also used  $\partial \boldsymbol{\zeta}_a / \partial t = \partial \boldsymbol{\zeta} / \partial t$ . This can be simplified further by using (6.35) to produce,

$$\left( \frac{D\boldsymbol{\zeta}_a}{Dt} \right)_R + \boldsymbol{\zeta}_a(\nabla \cdot \mathbf{u}_R) - (\boldsymbol{\zeta}_a \cdot \nabla)\mathbf{u}_R = \nabla \times (-\alpha \nabla P + \mathbf{F}_{fric}) \quad (6.37)$$

At first sight this looks more complicated, but using the continuity equation (4.26), the first two terms on the l.h.s combine to produce,

$$\left( \frac{D}{Dt} \left( \frac{\boldsymbol{\zeta}_a}{\rho} \right) \right)_R - \left( \frac{\boldsymbol{\zeta}_a}{\rho} \cdot \nabla \right) \mathbf{u}_R = \alpha \nabla \times (-\alpha \nabla P + \mathbf{F}_{fric}) \quad (6.38)$$

The first term on the r.h.s can also be simplified by using the vector identity,

$$\nabla \times (A \nabla B) = \nabla A \times \nabla B \quad (6.39)$$

to produce,

$$\left( \frac{D}{Dt} \left( \frac{\boldsymbol{\zeta}_a}{\rho} \right) \right)_R = \left( \frac{\boldsymbol{\zeta}_a}{\rho} \cdot \nabla \right) \mathbf{u}_R - \frac{\nabla \alpha \times \nabla P}{\rho} + \frac{\nabla \times \mathbf{F}_{fric}}{\rho} \quad (6.40)$$

or, after multiplication by  $\rho$ :

$$\rho \left( \frac{D}{Dt} (\alpha \boldsymbol{\zeta}_a) \right)_R = (\boldsymbol{\zeta}_a \cdot \nabla) \mathbf{u}_R - \nabla \alpha \times \nabla P + \nabla \times \mathbf{F}_{fric} \quad (6.41)$$